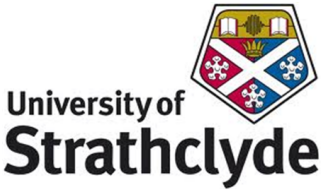

Design and Implementation of an Efficient Solar Powered Irrigation Management System for Drip Irrigated Maize Field

Million Trocco Mafuta

A thesis submitted for the Degree of

Master of Philosophy

Institute for Energy and Environment

Department of Electronic and Electrical Engineering

University of Strathclyde, Glasgow

November 2014

Declaration of Authenticity and Author's Rights

This thesis is the result of the author's original research. It has been composed by the author and has not been previously submitted for examination which has led to the award of a degree.

Signed: 

Date: 23rd November, 2014

Dedication

To my beloved daughters, **Takondwa** and **Idnas.**

Previously Published Work

[1] **Mafuta, M.**, Zennaro, M., Bagula, A., Ault, G., Gombachika, H., & Chadza, T. (2013). Successful Deployment of a Wireless Sensor Network for Precision Agriculture in Malawi. *International Journal of Distributed Sensor Networks, 2013,* 1–13. URL `http://www.hindawi.com/journals/ijdsn/2013/150703`

[2] Dauenhauer, P., Frame, D., Strachan, S., Dolan, M., **Mafuta, M.**, Chakraverty, D., & Henrikson, J. (2013). Remote Monitoring of Off-Grid Renewable Energy: Case Studies in rural Malawi, Zambia, and Gambia. In *IEEE 2013 Global Humanitarian Technology Conference,* California, USA.

[3] **Mafuta, M.**, Chadza, T., Gombachika, H., Ault, G., Frame, D., & Banda, E. (2012). Remote Monitoring for Wireless Sensor based Irrigation System in Malawi. In *National Commission for Science and Technology (NCST) - National Research Dissemination,* Lilongwe, Malawi.

[4] **Mafuta, M.** (2011). *Adaptive Solar Powered Irrigation System Controller for Maize Yield and Irrigation Water Optimization in Malawi*. [Poster] Glasgow: University of Strathclyde.

I declare that my contribution to the above published papers where I was the main author was over 86%, while the one where I was a co-author had about 13% of my contribution.

Signed: 

Date: 23rd November, 2014

Abstract

Purpose - The thesis investigates effects of automatic variation of the deficit irrigation level with the growth stage of drip irrigated maize on grain yield and crop Water Use Efficiency (WUE). It further examines the impact of water-efficient irrigation controllers on the solar Photovoltaic energy level requirements for water pumping systems.

Methodology - A Wireless Sensor and Actuator Network was deployed to monitor field conditions and actuate irrigation valves according to whether the level of moisture was within the set points. A Control Treatment (CT) field was fully irrigated using constant moisture threshold levels, while an Experimental Treatment (ExT) field had the highest level of deficit irrigation at the early and later growth stages. Full irrigation was applied at the middle growth stage. Irrigation depths and grain yields were measured, while WUE and the solar energy required by the water pumping system were calculated.

Findings - The findings show that 880 mm and 560 mm of water were applied to CT and ExT fields, respectively. This represents a 36% water saving and a corresponding water pumping energy saving of 36% in the ExT field. The grain yields were 0.752 kg/m^2 and 0.812 kg/m^2 for CT and ExT fields, respectively. This shows that, despite applying a lower amount of water, the ExT improved the grain yield by 7.4%. Furthermore, the results show an increase in WUE from 0.86 kg/m^3 for the CT field to 1.45 kg/m^3 for the ExT field, representing a 69% improvement.

Research limitations/implications - This study focused on the maize production under Malawi's weather conditions. However, the concept would easily be replicated in other crops and in other parts of the world with two modifications: firstly, sensor calibration must be done on-site; and secondly, the specific crop coefficient pattern must be used to develop the irrigation scheduling strategy.

Acknowledgments and Disclaimer

Acknowledgments

I would like to thank my supervisor, Professor Graham Ault for his insights, guidance and advice that lead to the successful completion of this study. The support he offered was extraordinary. Thanks are also due to my local supervisor, Mr. E. Banda who was very instrumental in the implementation phase of the project. His guidance was very crucial. Many thanks should also go to Mr. D. Frame for his guidance and advice during my study. He also contributed extensively to the development of this thesis.

I sincerely thank Dr. H. Gombachika for his data analysis expertise. His critiques and insights were very critical to the development of this thesis. He also contributed extensively to the editing of this thesis. I was also profoundly overwhelmed by the support I received from Mr. T. Chadza. He was very instrumental in many aspects ranging from physical work to technical expertise. His able hands were always itching for help and he contributed significantly to this study. Ms. E. Phiri also deserves a part on her back for her skills in editing, without which, this thesis would have not been as it is.

Let me also thank the following people for various roles they played: Dr. M. Zennaro, Dr. A. Bagula, Dr. C. Booth, Dr. L. Stankovic, Mr. W. Maruwo, Mr. W. Kuotcha, Dr. A. Madhlopa, Mr. K. Tembo, and Mr. R. Bakolo. A special thank you goes to Mr. M. Munthali of Bvumbwe Agricultural Research Station for his agricultural expertise, without which, the growing of maize would not have succeeded. I also thank Jane, Takondwa and Idnas for their patience, support and encouragement they provided. I was unavailable to them when they needed me most. I sincerely thank them for their understanding.

Lastly, but not least, I would like to thank the Community Rural Electrification and Development Project funded by the Scottish Government through the University of Strathclyde for funding my studies and for providing the equipment deployed in this study.

Disclaimer

The choice of all the products and equipment used in this research was solely on a professional basis. There was no direct financial relation with the trademarks mentioned in this thesis that might lead to a conflict of interest. However, mention of a trade name or a proprietary product is for the convenience of the reader and does not imply a guarantee or warranty neither by the University of Strathclyde nor by the author of this thesis.

Table of Contents

List of Figures

List of Tables

List of Abbreviations and Acronyms

APL Application Layer

ASW Available Soil Water

CT Control Treatment

ET Evapotranspiration

ExT Experimental Treatment

FAO Food and Agriculture Organization

FC Field Capacity

GMS Granular Matrix Sensor

GoM Government of Malawi

GPRS General Packet Radio Service

HTML HyperText Markup Language

IMS Irrigation Management System

IS Irrigation Station

ISM Industrial, Scientific and Medical

LGPL Lesser General Public License

MAC Media Access Control

MAD Management Allowable Depletion

MCU Microcontroller Unit

MPP Maximum Power Point

MPPT Maximum Power Point Tracking

NWK Network Layer

OSI Open Standard for Interconnection

PAN Personal Area Network

PE Polyethylene

PGF PV Generation Factor

PHP Hypertext Preprocessor

PHY Physical Layer

PSWC Percentage Soil Water Content

PV Photovoltaic

PVC Polyvinyl chloride

PWP Permanent Wilting Point

RAW Readily Available Water

RMS Remote Monitoring Station

RSSI Received Signal Strength Indicator

RTC Real Time Clock

S-MS Soil-Moisture Sensor

SD Secure Digital

SMP Soil Moisture Potential

SMS Short Message Service

SPVWP Solar Photovoltaic Water Pumping

TAW Total Available Water

TDH Total Dynamic Head

WAMP Windows Apache MySQL Package

WEU Water Energy Use

wfv water fraction by volume

WSAN Wireless Sensor and Actuator Network

WSN Wireless Sensor Network

WUE Water Use Efficiency

ZC ZigBee Coordinator

ZED ZigBee End Device

ZR ZigBee Router

Chapter 1

Introduction

1.1 Problem Definition

According to the 2008 Population and Housing census conducted by the Government of Malawi (GoM) through the National Statistical Office, Malawi has a population of 13 million that is progressively growing at the rate of 2.8 percent per annum. Eighty-three percent (83%) of which live in rural areas and heavily rely on agriculture for their livelihood (GoM, 2008). Although Malawi is endowed with several surface lakes, many areas are chronically water deficient especially during the dry seasons and drought periods. Mostly, this is due to sporadic rainfall and high levels of evapotranspiration associated with the possible impact of climate change and indeed high temperatures of the Sub-Saharan region where Malawi is situated. Sporadic rainfall, the continued population growth and the consequential chronic food shortages have compelled the GoM to promote irrigation farming as a means of achieving food self-sufficiency. This is made clear in the newly launched Malawi Green Belt Initiative that seeks to reduce dependency on rain-fed agriculture (Mpaka, 2010).

An integral part of sustainable development of irrigation farming is the availability of water resource. Unfortunately, studies have shown that this resource is becoming scarce as it faces high demand from agricultural, industrial, commercial and domestic

use. A report by Comprehensive Assessment Secretariat (2006) presented at World Water Week Conference in Stockholm found that one-third of the world's population is presently plagued by water scarcity. Ironically, the United Nations had initially forecast this startling figure to take place in 2025.

In order to alleviate the water scarcity problem, national and international laws are being put in place to save and renew this commodity as observed by Ghinassi (2006). Agriculture is likely to suffer more from water shortages than any other water user (Ghinassi, 2006). This poses a serious threat to food security. It is therefore imperative that Malawi should develop and implement sustainable water management system strategies that emphasize water use efficiency and conservation. One such, and most effective strategy, is to improve irrigation efficiency. With the Green Belt Initiative recently launched, Malawi needs to adopt irrigation schemes that put water use efficiency as a priority while optimizing crop yield in irrigated agriculture. One plausible solution is the proper irrigation scheduling.

The main objective of proper irrigation scheduling is to provide knowledge about how much water is to be applied and when. This does not only avoid over-irrigation which wastes water and energy but also avoids under-irrigation which reduces crop yield. Several methods for scheduling irrigation exist including: intuition (grower experience); calendar days since the last rainfall or irrigation; crop evapotranspiration; and soil water measurement (Shock, 2006). Nonetheless, many researchers (Dukes *et al.*, 2008; Grabow *et al.*, 2008; Nautiyal *et al.*, 2010; Shock, 2006) have demonstrated that the most effective indicator of irrigation scheduling is the soil moisture status. Based on this indicator Dukes *et al.* (2008) reported water saving in irrigating turf grass ranging from 28% to 83% and 69% to 92% in dry and wet weather conditions, respectively.

With the recent advent of effective Soil-Moisture Sensors (S-MSs), numerous 'smart' irrigation controllers have been designed based on feedback from soil moisture status. However, since these controllers use constant moisture threshold levels (without further user input) they are mostly suitable for turf grass which requires, virtually, a constant level of moisture throughout its growth stages. By contrast, maize requires more water in its root zone during its middle growth stage only. Stressing the crop (through

insufficient water application) during this critical growth stage lowers its yield substantially. This entails that user intervention is high if current irrigation controllers are to yield better results in terms of optimizing crop yield and reducing water use in maize irrigation or indeed any other crop having similar water requirements to maize.

1.2 Key Research Hypothesis

Current irrigation controllers use constant preset threshold levels when scheduling irrigation. An advanced On-demand S-MS controller which researchers consider as the most effective controller uses two threshold levels (upper and lower) and maintains soil moisture within these fixed levels unless there is user involvement to vary the thresholds. The reasonable inference drawn from this is that, on average, the crop receives a constant level of available soil moisture throughout its growth stages. Since maize crop requires more water only at middle stage of its growing period, it is being profligate to apply more water when it is not needed. Moreover, research has shown that the variation of available soil moisture and/or depletion level of available water at various growth stages of maize has momentous effects on its yield (Ali, 1976; Kalippa *et al*., 1974; Nadanam & Morachan, 1974) as cited in Tariq *et al.* (2003).

The hypothesis for this study then is as follows:

> *Designing and implementing a fully automated irrigation controller that uses the crop coefficient pattern to adjust moisture threshold levels when scheduling irrigation can improve crop water use efficiency and hence solar Photovoltaic (PV) energy used in water pumping and can optimise crop yield.*

It is envisaged that the implementation of such an efficient irrigation system in Malawi will help in uplifting the living standards of poor people. Farmers will also have enough time to do other development activities rather than devoting their time to monitoring and adjusting moisture threshold levels for the irrigation system. Since the automated

irrigation system will be powered by solar PV energy which is environmental friendly as opposed to fossil fuels, then it will go a long way to guarding against the possible impact of climate change.

Finally, the water saved through the use of the proposed efficient irrigation system can be channelled to other activities. Conversely, automated irrigation systems would be implemented where initially it was impossible due to limited water and power supplies. Moreover, prior to this research, there has been no publication of S-MS based irrigation systems suitable for weather conditions for Malawi apart from Fandika (2006) who explored the use of evapotranspiration (ET) based controller for maize irrigation using water budget scheduling strategy.

1.3 Research Objectives

The intent of this research was to develop and implement an adaptive and low-cost on-demand S-MS irrigation controller that seeks to schedule irrigation efficiently to suit the geographic location and weather conditions for Malawi. This approach will not only optimise solar energy use but also manage scarce water resources more effectively, enhance crop yield, and reduce labor by minimizing subsequent user input. Accordingly, the specific objectives of the study were as follows:

(a) to develop an advanced and efficient irrigation scheduling strategy;

(b) to develop hardware and software for an irrigation system controller based on the developed efficient scheduling strategy;

(c) to design a drip irrigation system suitable for maize cropping;

(d) to design a remote monitoring mechanism for the irrigation system;

(e) to conduct field tests using the developed irrigation system controller; and

(f) to analyse data obtained from field tests to attest the hypothesis.

1.4 Scope

This study was conducted in the city of Blantyre, southern part of Malawi in which maize was planted and irrigated between late July and mid November 2012. One field was irrigated based on constant preset moisture thresholds throughout the growing period of the maize, while the other used variable thresholds to mimic the crop coefficient pattern of the water requirements by the maize crop. Soil moisture sensors were calibrated based on the soils at this site. Although the study was limited to the geographic location of Blantyre, the system could easily be reconfigured/recalibrated for other crop types in other regions and climates.

Since this research focused on the development of the Wireless Sensor and Actuator Network (WSAN) based irrigation controller, all advanced agricultural technicalities were sought from the agricultural experts particularly from Bvumbwe Agricultural Research Station. It is therefore assumed that any potential user of the system developed through this research will follow all basic and good farming practices such as salinity, organic manure and fertilizer combinations and application time to mention but a few.

1.5 Chapter Summary and Thesis Outline

In this chapter, the problem which was being addressed has been described. Both overall and specific objectives have been articulated. Finally, the chapter has described the scope within which the developed system was defined.

The remainder of this thesis is organized as follows: Chapter 2 reviews literature on irrigation controllers and gives a background to irrigation scheduling concepts for maize production; Chapter 3 specifies the Irrigation Management System (IMS) by defining and developing its functional components; chapter 4 develops an adaptive and efficient irrigation scheduling strategy upon which the IMS is based; the remote monitoring system which is also an integral part of the IMS is presented in chapter 5; results and discussions are presented in chapter 6; and finally conclusions and recommendations are outlined in chapter 7.

Chapter 2

Literature Review and Background

2.1 Overview

The proposed work in this research is an extension of tremendous contributions that researchers have demonstrated in the recent past especially with the advent of S-MSs and Wireless Sensor Networks (WSNs) . Most of these researchers have shown that some irrigation controllers have a potential of saving water and energy used in pumping but at the expense of high costs and user intervention while others exacerbate the water scarcity problem than the traditional farming practices. In irrigated cropping, water conservation and crop yield optimization goals can be achieved by strictly following proper irrigation scheduling strategy. This ensures that crop yields are improved despite water stresses from droughts. Although water in some cases may be in abundance, the application of excess water may result in ground water pollution, loss of nutrients due to leaching, soil erosion due to surface run-off and loss of energy used in pumping.

2.2 Irrigation Scheduling

In irrigated cropping water conservation and crop yield optimization goals can be achieved by strictly following proper irrigation scheduling strategy. With proper irrigation scheduling, crop yield can be improved while reducing water use, saving energy

used in pumping and minimizing loss of soil nutrients due to leaching, needless to say the reduction of the negative environmental impacts that come with soil erosion as a result of over-irrigation. Efficient irrigation scheduling attempts to answer the following two questions:

(a) *How much water should be applied to the field?*
(b) *When should the water be applied?*

In essence, according to Ellis and Merry (2007), the objective of proper irrigation scheduling is to provide knowledge on crop water requirements (for its optimum growth) at a particular point in time and determining the timing of water application to avoid crop and soil damage. Among several techniques of answering the first question, soil moisture measurements and evaluation of ET using meteorological data score highly in literature (Shock, 2006). In the former case, moisture sensors are used to sense the available soil moisture and compare it with a preset (required) level, and the difference is the amount of water that must be applied; whereas the latter uses weather data to directly evaluate the ET loss which is the amount of water that must be applied. The other techniques used are intuition (grower experience) and calendar days since the last rainfall or irrigation (Shock, 2006). The second question can be answered by setting up a minimum level of moisture required by crops and when the level of moisture in the soil reaches that threshold, irrigation has to be initiated.

To effectively ascertain proper irrigation scheduling, a sound knowledge is required on crop physical characteristics, crop-water requirements, and soil-water characteristics. The rest of this section discusses these concepts briefly.

2.2.1 Maize Crop Physical Characteristics

Maize (Zea mays L.), also known as corn, is a cereal crop that falls into grass category of plants. It is cultivated in most parts of the world and it is used for human and animal consumption worldwide. Maize is the number one staple food in Malawi and accounts for 70% of the cultivated land. It grows well in almost all soil types across

Malawi apart from too sandy and waterlogged soils where, otherwise, strict and very good farming practices (e.g. soil drainage and application of organic and inorganic matter) need to be followed. Maize is a tall (may grow up to 3 m) and deep rooted crop which sees its roots going as deep as 200 cm in less restrictive soils, but most of water uptake activity is within 80 cm to 100 cm of the surface when the crop is fully grown (FAO, 2010). Whereas for medium to shallow soils vigorous water uptake activities take place within the top 60 cm hence irrigation must be as deep as this. Table 2.1 shows rooting depths of some crops adapted from Texas Water Development Board (2004).

Table 2.1: *Approximate rooting depths of some crops (Texas Water Development Board, 2004).*

Crop	Approximate rooting depth (cm)	Crop	Approximate rooting depth (cm)
Alfalfa	120-180	Peanuts	0-75
Citrus	60-150	Potatoes	60-90
Cabbage	45-120	Sorghum	60-90
Corn	75-120	Soybeans	60-90
Cotton	90-120	Sugar beet	60-120
Grass	0-120	Sugar cane	60-180
Melons	0-90	Tomatoes	60-120
Oats	0-150	Turf grass	15-75
Onions	45	Wheat	90-120

Belfield and Brown (2008) observed that, as a tropical grass, maize requires relatively higher levels of insolation and suitable air temperature averaging between 18 ºC and 32 ºC while soil temperature in excess of 12 ^{o}C is optimal for germination and early seedling growth. However, according to Belfield and Brown (2008), maize can adapt to many climates with an effect of having variable maturity periods ranging from 70 to 210 days. Specifically, maturity period for most varieties of maize in Malawi where mean temperature exceeds 20 ^{o}C ranges from 90 to 120 days. The maize variety used in this study was a hybrid SC 403 (Seed Co Malawi Ltd) with a maturity period of 90 to 100 days.

2.2.2 Maize Crop Water Requirements

Maize water requirements vary depending upon a wide range of factors including climate, soil type (influencing water-holding capacity) and growing period. With regards to climate and growing period, FAO (2010) reported maize crop water requirements of between 500 mm and 800 mm for medium maturity, while Doorenbos and Pruitt (cited in Tariq *et al.*, 2003 p.2) observed water use of between 430 mm and 490 mm. Belfield and Brown (2008) cited 300 mm as a potential water requirement by maize crop depending on water-holding capacity of soil, otherwise they reported 500 mm to 1200 mm as optimal water requirement. This simply shows how tedious it is to determine the total amount of water needed by maize crop per growing season. Moreover, even if it was possible, the water use by the crop is not evenly distributed. It depends on the daily weather conditions as well as growth stage. In terms of growth stage, FAO (2010) showed that water requirements by maize is lower at early and later stages of maize growth but more water is used up at its middle stage. This is characterized by the crop coefficient (K_c) which peaks at tasseling and cob development stages as shown in Fig. 2.1.

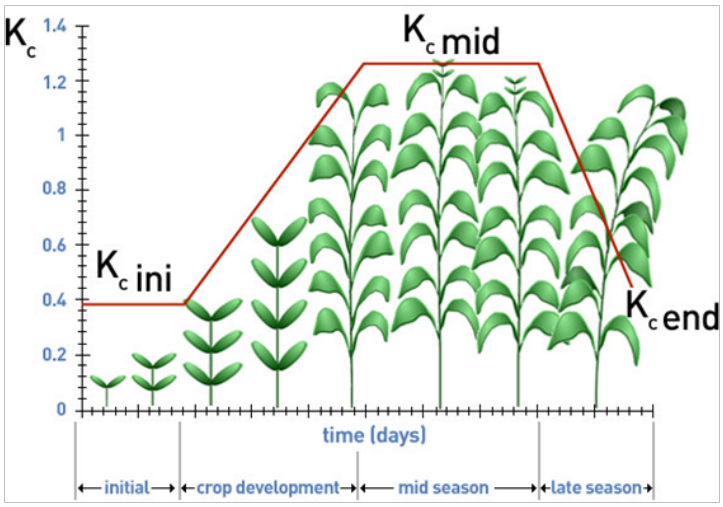

Fig. 2.1: *Typical crop coefficient curve for maize (FAO, 2010)*

2.2.3 Soil Water Characteristics

Knowledge of soil water dynamics is very crucial when practicing irrigation farming regardless of which scheduling technique is exercised. Water retention capability of the soil determines how much pressure the crop roots must exert in order to suck it up. The level of retention mainly depends on the textural composition of the soil.

2.2.3.1 Field Capacity, Permanent Wilting Point and Available Soil Water

When excess water is applied and diffuses into the soil (assuming run-off is avoided), the soil is said to have been saturated and gravitational drainage (deep percolation) ensues. Just after this drainage process ceases, water is retained by the soil and it is called Field Capacity (FC). This is a measure of water-holding capacity of the soil and the level varies for different soil types. Table 2.2 shows that clay and silty clay have a potential to hold more water than the rest of the soils. The least amount of water is held within large pore spaces of sand soil. It is this water that plants use for their metabolic processes and part of it is evaporated. As ET continues, there will be a point when the little water remaining in the soil will no longer be extracted by plants as it will be firmly held between soil particles (Bernier, 2008). If water is not replenished before this stage, then crops wilt beyond recovery. As such, the remaining water at this stage is called Permanent Wilting Point (PWP). PWP is also a soil-texture dependent parameter as depicted in table 2.2.

Available Soil Water (ASW), also known as Available Water Storage Capacity of the soil, is the difference between FC and PWP (refer to Fig. 2.2). Just like FC and PWP, ASW varies with soil texture (see table 2.2). To avoid stressing crops by reaching PWP, ASW should not be depleted completely. This is done by observing Management Allowable Depletion (MAD) for a particular crop and at a particular growth stage as discussed in the next section.

Table 2.2: *Volumetric soil moisture content at field capacity, permanent wilting point and available soil water for various soil textures (Bernier, 2008).*

Soil texture	Field Capacity (FC)	Permanent Wilting Point (PWP)	Available Soil Water Content (ASW)
	mm of water per m of soil		
Sand	100	40	60
Loamy Sand	160	70	90
Sandy Loam	210	90	120
Loam	270	120	150
Silt Loam	300	150	150
Sandy Clay Loam	360	200	160
Sandy Clay	320	180	140
Clay Loam	290	180	110
Silty Clay Loam	280	150	130
Silty Clay	400	200	200
Clay	400	220	180

2.2.3.2 Management Allowable Depletion

As stated earlier on, ASW is depleted from the soil through ET. As ASW is getting depleted, crops find it harder and harder to absorb water from the soil until at such a point that crop-stress signs (e.g. curling of leaves) appear. The level at which ASW can be depleted without stressing crops is known as Management Allowable Depletion (MAD). Abubaker (2009) claimed that many crops have a MAD of 50%. That is, water needs to be added to the soil when half of ASW is depleted. Nevertheless, Bernier (2008) noted that for water stress sensitive crops the recommended MAD depends on "crop grown, development stage and irrigation system used" (p. 23). As such, it is recommended that MAD be varied with crop growth stage if crop yield is to be optimized while avoiding unnecessary irrigation events.

2.2.3.3 Readily Available Water and Total Available Water

Readily Available Water (RAW) is a fraction of ASW that can safely be depleted from the soil by crops to satisfy ET potential of the atmosphere. The fraction is determined

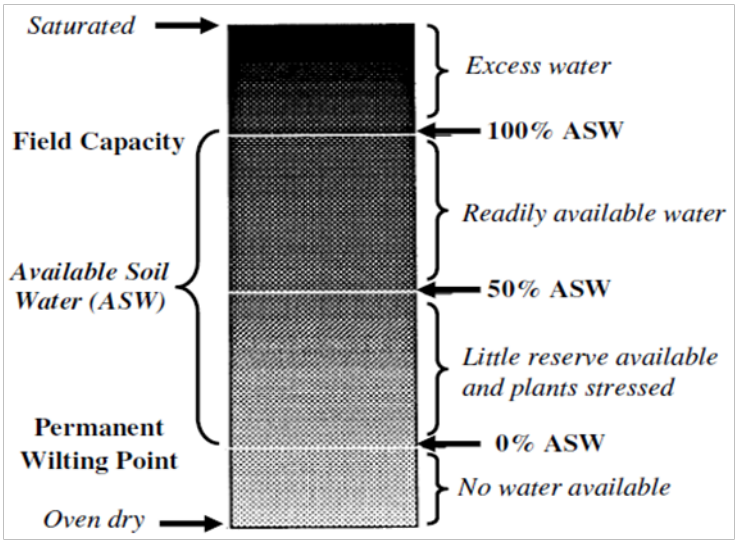

Fig. 2.2: *Soil moisture profile for a typical soil (Bernier, 2008)*

by the MAD. Mathematically, RAW can be expressed by equation 2.1.

$$RAW = ASW * MAD \tag{2.1}$$

RAW is the water that crops actually use (see Fig. 2.2). Of course part of it still evaporates. However, since this measurement is given per unit depth of soil (see table 2.2), the actual water available in the root zone of the crop depends on the actual root depth of the plant. This water is called Total Available Water (TAW) and is given as the product of RAW and root depth (Rd) as shown in equation 2.2.

$$TAW = RAW * Rd \tag{2.2}$$

Rd varies with the growth stage of the plant; hence RAW is a plant-growth-stage dependent parameter.

2.3 Review of Current Irrigation Controllers

An irrigation controller is an electronic or electro-mechanical device that helps farmers to schedule irrigation; It determines when and how much water to apply to the field. Several strategies and tools have been proposed in literature and are available

to farmers allowing them to schedule irrigation efficiently. These tools include evapotranspiration based controllers, irrigation timers (clocks), and on-demand S-MS based controllers. These controllers are reviewed in sections 2.3.1 through 2.3.3

2.3.1 Evapotranspiration Based Irrigation Controllers

A large body of literature describes evapotranspiration (also known as Weather) based controllers. These controllers estimate the ET for a particular crop (ET_c) which, according to Irmak and Harman (2003), is the loss of soil moisture through a combined process of plant transpiration and evaporation that occurs from the soil and plant surfaces. ET_c is evaluated by multiplying the crop coefficient (K_c) with the reference crop evapotranspiration (ET_o). Abubaker (2009) and Davis *et al.* (2007) observed that K_c is a crop dependent parameter which varies with the type of the crop, production environment and the growth stage of the crop. As such, the controller needs to be fed with the appropriate values of the K_c for a particular crop at a specific growth stage of the crop. After computing K_c the controller has to evaluate ET_o which is a climate dependent parameter and can be computed from weather data. The minimum weather data needed for computing ET_o using the recommended ASCE standardized reference ET equation includes air temperature, solar radiation, relative humidity, and wind speed (Allen *et al.*, 2005). Davis *et al.* (2007) observed that the external data can be collected either from on-field weather stations or from remote weather stations. Once the ET_c is established then using water-budget scheduling technique, water is applied to replenish the one taken up from the soil through ET. Fig. 2.3 shows a photo of three brands of ET controllers undergoing testing at the University of Florida, Agricultural and Biological Engineering Department (Davis, cited by Dukes, 2012).

The major advantage of the ET method of scheduling irrigation is in the reduction of user intervention when weather data is fed in automatically. Once the installation and initial settings have been done properly, further user input is not required. Grabow *et al.* (2008) argued that as long as the controller receives weather information, it automatically adjusts irrigation cycles to accommodate varying weather conditions and

Fig. 2.3: *Photos of three brands of ET controllers (Dukes, 2012)*

growth stage of the crop. However, since the weather data is collected through on-field weather stations or from remote weather stations which requires complex data acquisition mechanisms that may include communication with satellites, this method is very expensive and not economical or convenient for small-scale farmers. In addition, whichever way is used in data collection for establishing ET, many researchers (Nautiyal *et al.*, 2010; Dukes *et al.*, 2008; Grabow *et al.*, 2008; Shock, 2006) have argued that ET is usually overestimated and consequently, there is less water saving than in S-MS based irrigation systems. Worse still, ET based controllers fail to account for capillary rise where, if water table rises, roots may be able to take up the ground water for the crop's metabolic process. This is the reason why Abubaker (2009) concluded his thesis by recommending periodic soil moisture monitoring where ET estimations are used to schedule irrigation.

2.3.2 Irrigation Timers

Dukes *et al.* (2009) described timers (irrigation clocks) which have extensively been used to schedule irrigation especially for landscapes. These open-loop control systems are based on S-MS and operate in a "bypass" mode where information from soil moisture sensors is used to either allow or bypass scheduled irrigation. Fig. 2.4 shows how a commercial RS500 S-MS controller manufactured by Acclima, Inc. (Meridian, ID, USA) can be arranged to bypass a scheduled irrigation event.

According to Dukes *et al.* (2009) the controller has an adjustable moisture threshold setting which is chosen by the user. The scheduled irrigation is bypassed when soil

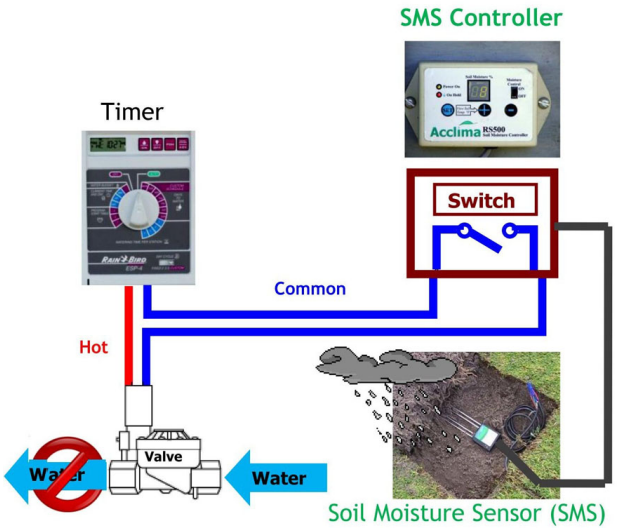

Fig. 2.4: *Simplified diagram showing how a soil moisture sensor is typically connected to an automated irrigation system (Dukes* et al.*, 2009)*

moisture exceeds this setting. Some timers incorporate rain sensors which enable them to bypass or interrupt the preset irrigation event when a specific amount of rainfall has been recorded (Tichenor *et al.*, 2004). Consequently, these controllers save more water than the basic irrigation timers. Following this, a law was enacted in Florida to enforce the incorporation of rain sensors into basic irrigation timers (Tichenor *et al.*, 2004).

The strength of the irrigation timers is that they are simple and cheap since they do not require complicated scheduling strategies. Additionally, they are readily available and user friendly in terms of choosing appropriate scheduling programs. However, the main drawback of these controllers is the extensive involvement of the user due to the failure of the system to automatically schedule irrigation depending upon conditions in the environment which change throughout the growing season. This is cumbersome and prone to errors. The user has to select a program, one that would apply a specific amount of water at a specific time. For example the user may time the controller to apply 0.2 m^3 of water every two days. If the moisture in the soil goes just above the set value, then irrigation cannot be initiated until the second day which can result in stressing the crop if the next day experiences high ET levels due to varying weather conditions.

Dukes *et al.* (2009) further stressed that these controllers require the user to change

the program depending upon the actual moisture condition of the soil as one way of accommodating varying weather conditions which change throughout the growing season. This is prone to errors as it depends on the experience of the user. Moreover, with the set-and-forget mentality it is more likely that users choose to water often as it is easier to notice signs of stressed turf than those from over-irrigation to a small extent. It is for this reason that Dukes *et al.* (2009) observed that 47% more water in Florida is applied using this scheduling technique than home owners without automated systems.

2.3.3 On-demand S-MS Based Controllers

Dukes (2012) presented a detailed description of how on-demand S-MS based controllers operate. Just like irrigation timers, these controllers are based on S-MS, in which case the information about the soil moisture status is used to determine crop water needs. They have two threshold levels within which the soil moisture is maintained. The controller irrigates when soil moisture reaches the lower threshold and stops irrigating when a high moisture threshold is read by the sensor. Unlike the irrigation timers which only allow or bypass a pre-programmed irrigation event, the on-demand S-MS controllers initiate and terminate irrigation events.

Although Dukes (2012) reported great water savings by these technologies (30-40% and 70-90% during dry and wet conditions, respectively), just like ET controllers and irrigation timers, on-demand S-MS controllers are labour intensive because they require user intervention to re-adjust the threshold levels. This is so because water demand by crops varies not only with weather conditions but also with growth stage. Otherwise, users tend to set high threshold levels (close to field capacity) thereby over-irrigating unnecessarily when crop water demand is low. This is evident from the controller that Miranda *et al.* (2005) designed which was able to "autonomously control the soil water potential (SWP) in the crop root zone between field capacity (FC) and management allowed deficit (MAD) set by the user" (p. 185).

Notably, applying large amounts of water (close to FC) when crop water need is low (e.g. at early and later growth stage of maize crop) does not necessarily mean that the

excess water will remain in the soil for a very long time waiting for the crop to absorb it. Biran *et al*., as cited in Cardenas-Lailhacar and Dukes (2007), observed that ET (dominated by evaporation) is encouraged when there is more water in the soil than necessary.

2.4 Wireless Sensor Network

One of the objectives of this study was to develop an inexpensive but robust and reliable controller. This was going to accelerate its adoption in Malawi as it would meet smallholders' socioeconomic preferences. Current advanced and commercial irrigation controllers use wired infrastructure to collect data from in-field sensors to a central decision making node that schedules irrigation events. In addition to being prohibitively expensive, wired infrastructure limits farmers' movements in the field and in some situations it may be impractical to run wires.

The rapid increase in WSNs deployment in industrial, agricultural and environmental monitoring applications is as a result of being a low power and low data rate, hence energy efficient technology. It also offers mobility and flexibility in connectivity which promotes network expansion when needed. As noted by Balendonck *et al.* (2008) and Fazackerley and Lawrence (2009), this has opened a new chapter in how precision agriculture can cost-effectively be implemented. In particular, Fazackerley and Lawrence (2009) showed that WSNs can tremendously reduce the cost of on-demand S-MS controllers from $3000 to $100 per completed node excluding the cost of the soil moisture sensor. Ali *et al.* (2010) developed a prototype of irrigation controller based on WSN whose main objective was to distribute water properly and evenly; and noted that ZigBee technology scores highly on low-cost, reasonable range, average data rate and low power requirements as compared to Bluetooth, Wi-Fi, and Wibree.

However, Balendonck *et al.* (2008) noted that WSNs are still under development stage; as such, they are at times unreliable, power hungry, fragile and can easily lose communication especially when they are deployed in a harsh environment. It is therefore

necessary to remotely monitor the status of the WSN when the deployment is a remote site where frequent physical visits may become inevitable but costly and time consuming. To this end, Kalpana *et al.* (2011) deployed a WSN for remote monitoring of a crop field. They designed and implemented a WSN that could monitor the air temperature, humidity, light intensity both from a crop field and remote places. Their system comprised nodes equipped with small size application specific sensors and radio frequency modules. Sensor data were transmitted via radio frequency link to a centrally localized computer terminal for data logging and analysis. However, they employed a computer on site for data logging and analysis which is costly and, hence, not suitable for smallholder farmers.

2.4.1 ZigBee Network Protocol

ZigBee is a networking standard for Personal Area Network (PAN) which is based on the Media Access Control (MAC) and Physical (PHY) layers of the IEEE 802.15.4 standard (see Fig. 2.5). The PHY and the MAC layers have the same functionality of providing RF and communication components as in the IEEE 802.15.4 protocol. This means that the PHY layer of ZigBee operates in the unlicensed Industrial, Scientific and Medical (ISM) radio bands of 868 MHz, 915 MHz and 2.4 GHz depending on the region; the ISM band in Malawi is 2.4 GHz.

The ZigBee protocol operates in a layered structure similar to the Open Standard for Interconnection (OSI) network model. Since ZigBee standard sits on top of the IEEE 802.15.4 standard, the ZigBee stack has two of its four layers - PHY layer and Data Link layer (MAC) defined in the IEEE 802.15.4 standard. The other two top layers are the Network (NWK) layer and the Application layer (APL) (refer to Fig. 2.5). The NWK layer is responsible (if the device is a coordinator) for the formation of a network among the devices. That is, it is responsible for routing management, network management, security management and message broker. The functionality of the device is defined by the applications that run on the device. The applications may include issues like measuring soil moisture and temperature and sending such data to a coordinator.

The APL houses such applications for the device and may have the following objects: application support sub-layer, application framework and ZigBee object as illustrated in Fig. 2.5.

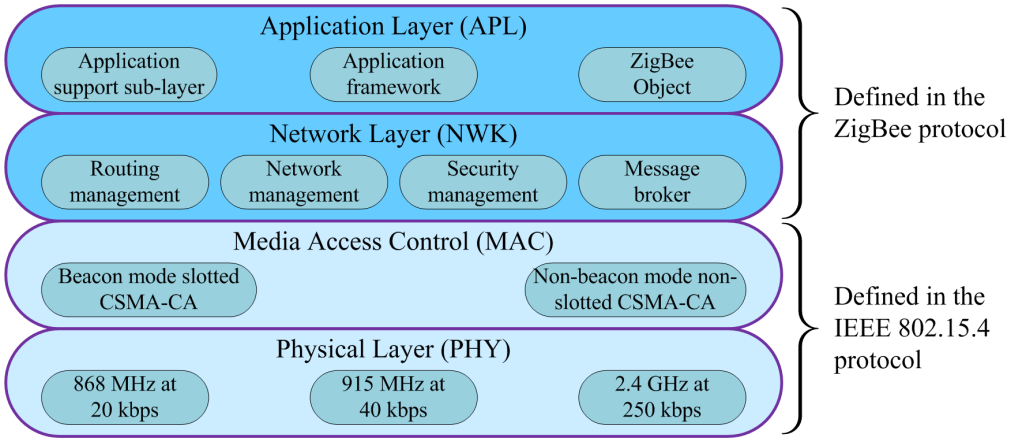

Fig. 2.5: *ZigBee stack*

The ZigBee protocol mainly focuses on low cost and low power consumption. The low power consumption characteristic is really appealing since sensors are usually placed at a remote location where battery power supply is the only option and needs to be sustained. In order to attain a low power consumption characteristic, the ZigBee protocol operates at low data rates (250 kbps at 2.4 GHz). Nonetheless, this imposes its limitation where high data transmission applications are required. Such applications may use other IEEE standards for instance Bluetooth (802.15.1) and Wi-Fi (802.11) which offer high data rates of 1 Mbps and 54 Mbps, respectively, but at the expense of battery power. Nevertheless, in precision agriculture, sensor data do not require wide bandwidth since it is not necessary to continuously monitor soil moisture and temperature as there could be no significant changes in these parameters in a short period. Hence, ZigBee is well suited for precision agriculture in remote areas where high battery performance may be required.

2.4.1.1 Device Types

The ZigBee standard classifies network devices/nodes into three categories: ZigBee Coordinator (ZC) , ZigBee Router (ZR) and ZigBee End Device (ZED) . As the heart of

the network, ZC permits and sanctions all ZRs and ZEDs that are in quest of connecting to its network. This is the most capable node in the network as it is responsible for network formation (allocating addresses and ensuring security). As such, there must be one (and only) ZC per any given ZigBee network. ZigBee stack allows any ZR to assume the responsibility of a coordinator if ZC is removed from the network.

ZR extends the network by relaying information between two devices. This means that it acts as a link in the network which can have up to 30 hops. Each ZR can have its own children to which it allocates addresses. For a small ZigBee network a ZR device may be less compelling.

Unlike ZC and ZR, ZED spends most of the time asleep only waking up when it is required to perform its intended function thereby saving battery power. This is the case because ZED operates as a termination of the network. It is limited in its functionality since it does not participate in routing. This makes it capable of carrying out its duties and communicating with its parent device only. A ZED can physically move around the network as a mobile device and freely associate itself with a new parent device.

2.4.1.2 Network Topology

Depending on the situation and environment ZigBee networks can take three forms of topologies: Star, Cluster-Tree and Mesh.

A star topology comprises one coordinator and several other end devices. No ZigBee router is required in this topology. The coordinator communicates with all end devices, and there is no direct messaging between end devices (refer to Fig. 2.6 a). Synchronisation may or may not be enforced by enabling or disabling beacon mode accordingly.

A cluster-tree topology is made up of one coordinator and several child nodes which are routers and end devices (Prince-Pike, 2009). Apart from communicating with its parent node a router may as well have its own child nodes, but there is only one path between any pair of devices in this network (refer to Fig. 2.6 b) and therefore tree

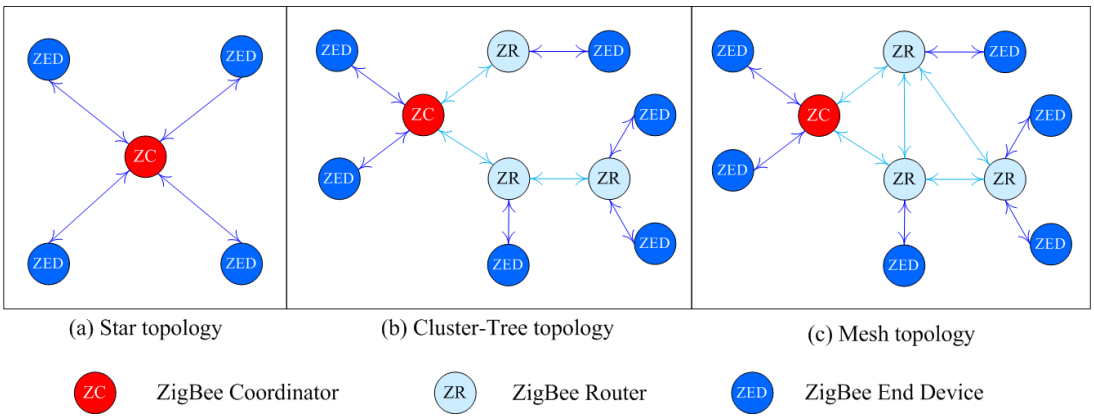

Fig. 2.6: *Network topologies for the ZigBee protocol*

routing algorithm is requested. Distributed synchronisation mechanism which enables guaranteed bandwidth is used and achieved by enabling beacon mode.

A slight modification to the cluster-tree topology is required to yield a mesh network. This is done by allowing devices to communicate with each other using multiple routes (refer to Fig. 2.6 c). Consequently, devices are able to send and receive messages reliably even when their preferred path is down or congested. This reliability is the major advantage of a ZigBee mesh network over star and cluster-tree networks. However, mesh network has no guarantee of bandwidth since no synchronisation is used which requires disabling of beacon mode.

2.5 Solar Photovoltaic Water Pumping System

Although Malawi is making strides towards rural electrification, implementation of grid power to the remotest areas where farming is practiced still remains a challenge because of high installation costs of new transmission lines and transformers as well as not being feasible due to a poor road network. To effectively achieve socioeconomic preferences of smallholder farmers who live in rural areas and constitute 83% of Malawi's population (GoM, 2008), it is judicious to implement efficient irrigation schemes that use Solar Photovoltaic Water Pumping (SPVWP) technology. Moreover, Malawi being in a tropical region is well endowed with large amounts of solar radiation amounting to 3000 hours per year (GoM, 2003), which translates to over 8 hours

per day. It is also reported (GoM, 2003) that SPVWP systems have to a small extent been implemented in Malawi; but, despite these systems having good characteristics such as environmental friendliness, good reliability, ease of installation and long life, the challenge is high initial installation cost which impedes their diffusion into rural areas.

Furthermore, research indicates that SPVWP systems have not yet diffused into remote areas of developing countries where the priority is given to drinking water. As such, it is not feasible as it cannot meet operational and maintenance costs according to (Meah *et al.*, 2008) and Malawi is no exception to this observation. However, with the Government of Malawi's promotion of irrigation farming, it is clear that implementation of SPVWP systems will receive more interest as the irrigation-water versus drinking-water equation gradually balances up. With relatively high initial cost, it is worthwhile to install and use a PV system for an income generating activity in addition to drinking water.

In addition, a group of individuals (typical of a community set up) can shoulder the cost for the PV system with an aim to use the system for income generating activities including charging mobile phones and growing of cash crops. The income generated from these activities can be used to offset and meet installation and maintenance costs in the long run. This venture also creates jobs in remote areas, thereby improving socioeconomic status of the rural community.

A typical SPVWP system consists of a PV Array, a controller, a motor, a pump and may or may not include a storage tank. The controller may comprise charge controller, battery bank and an inverter. A careful selection of these components does not only have a bearing on system capacity but also determines the initial and installation costs as well as its robustness, efficiency and hence reliability. Sections 2.5.1 through 2.5.3 examine how high water pumping capacity, low cost and high efficiency requirements may be achieved. This may accelerate the diffusion rate of PV installations in rural areas of Malawi where a large percentage of the population lives below the poverty line.

2.5.1 Photovoltaic Energy and Storage Requirements

A Photovoltaic (PV) cell is a semiconductor material specially doped to convert solar energy directly into electricity. An interconnection of many PV cells is required to form a PV module (array) that provides a desired amount of DC power. A PV array is a highly reliable assembly that can last over 20 years without need for maintenance apart from general cleaning; and hence, even though its initial cost is high, it has the lowest life-cycle cost where less than 10 kW applications are required but either there is no grid power or operation and maintenance cost of the internal-combustion engines is high (Thomson, 2003).

Clearly, PV energy which is required to drive the motor-pump set is directly related to solar radiation. This energy is not available at night or during cloudy days. To satisfy a high water demand with minimum system power design (which cuts system cost substantially), it is necessary to store energy when it is available. Two strategies are used to store PV energy in SPVWP systems: a battery bank and a water tank.

Although battery bank installation looks simpler than constructing a water tank, many researchers have pointed out the disadvantages of this strategy. It is observed that the lead-acid, deep-cycle batteries which are suitable for PV systems are not only prohibitively expensive but also not readily available on the market (Oi, 2005). Oi (2005) further observed that batteries require persistent maintenance as they degrade rapidly when the electrolyte is not checked and replenished regularly. Of course nowadays there are maintenance-free batteries on the market, but their price tag is very high for the poor masses in the developing countries to acquire.

Thomson (2003) bemoaned short battery lifetime which ranges typically from 3 to 8 years in cool climates and reduces to typically 2 to 6 years in hot climates due to increased rate of internal corrosion as a result of high ambient temperatures. In addition, the charging and discharging process can further reduce battery lifetime if it is not controlled properly. This attracts another cost for the need of sophisticated charge controllers.

Another challenge of the use of batteries according to Thomson (2003) is power conversion efficiency which is typically 85% and it may be as low as 75% in hot climates. This means that, to effectively drive a motor-pump set with specified power rating, a PV array has to be oversized by at least 25% and hence faces an increased capital cost.

On the other hand, a water tank to exploit the PV produced energy immediately without battery storage may also reduce efficiency of the SPVWP system through loss of water as a result of evaporation if the tank is open. Closed tanks tend to be expensive to build but the loss of stored water is reduced. Nevertheless, the best option for energy storage in SPVWP systems is a water tank since once it is constructed it requires minimal maintenance over time. Moreover, the cost for building a tank is much lower than battery bank installation; as such only about 5% of SPVWP systems employ battery banks (Oi, 2005).

2.5.2 Motor-Pump Set and Inverter

There are three categories of pumps used in SPVWP systems according to their applications: submersible; surface; and floating pumps (Meah *et al.*, 2008). Unlike submersible pumps which are used to draw water from deep wells (boreholes), surface water pumps draw water from shallow wells, rivers, and ponds; whereas floating pumps are used where the water sources have variable heads (Meah *et al.*, 2008). These pumps can also be classified according to their principles of operation as centrifugal and displacement pumps. Similarly, motors used in SPVWP systems can be classified by various domains as either DC or AC, synchronous or asynchronous, brushed or brushless.

Proper selection of the motor-pump combination is critical as it depends on the site, durability, availability, head of water, maintainability, quality of water, and overall system cost. Oi (2005) noted that centrifugal pumps are relatively expensive but have high efficiency and high water volume pumping capability than displacement pumps which also require regular maintenance; and that an AC induction motor is cheaper than brushless DC motor but both have maintenance-free operation than a brushed

motor. Although a submersible centrifugal pump coupled to an AC Induction motor looks attractive, it requires an expensive inverter for converting DC power from PV array to AC. According to Andrada and Castro (2007), such a system is not ideal for rural communities in developing countries.

Eliminating the inverter from this SPVWP system gives room for direct coupling of PV array to the motor-pump set which reduces initial system cost substantially. Such a system was once tested and analyzed by Mokeddem *et al.* (2007) where a PV array was directly coupled to a low cost brushed DC motor and a centrifugal pump. After four-month performance tests they found that the system was ideal for low delivery flow rate applications and they recommended its use for irrigation in remote areas.

However, the major drawback of the direct coupling design is the use of brushed DC motor which requires periodic replacement of brushes, typically every two years (Oi, 2005). This is not ideal for remote areas of developing countries where it is not easy to access repairs and spares. Direct coupling of PV array to a brushless DC motor with centrifugal pump and a water tank is a more interesting configuration since it promises the achievement of a low cost, reliable and low maintenance SPVWP system installation suitable for irrigation in remote areas. Moreover, there is a growing trend of manufacturers for submersible pumps to use brushless motors and assemble them as a unit which lowers its cost substantially.

2.5.3 Efficiency Improvement through Maximum Power Point Tracking

For efficient operation of the load (motor-pump set) in this system, the PV power supply needs to be optimized. Since power drawn from a PV array fluctuates widely with cell temperature and insolation throughout the day, it is important to match the operating characteristics of the load and the PV array. The load must operate at the knee (refer to Fig. 2.7) of the current-voltage (I-V) curve for the PV array. This knee point is called *Maximum Power Point* (MPP) because it is the point where the product of I and V is a maximum. However, as the insolation and cell temperature fluctuate

throughout the day MPP also changes. When this happens, the load forces the PV to operate outside the MPP, and the PV array responds by delivering little power to the load.

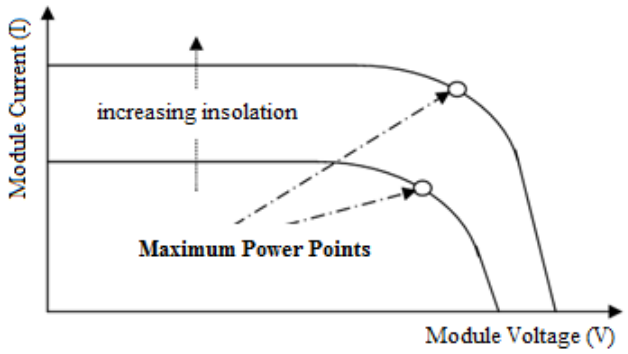

Fig. 2.7: *Typical I-V curves of a PV module with varying insolation*

A control mechanism known as *Maximum Power Point Tracking* (MPPT) is used to vary the current or voltage so as to maintain the system operation close to MPP (Thomson, 2003). Thomson (2003) also observed that advanced DC-AC inverters incorporate MPPT, but they are expensive and limited in control strategy flexibility. Alternatively, a low cost standalone (specialized) control unit is used as a MPPT. Interestingly, the cost of the control unit can be offset by slightly reducing the number of the PV panels; that is, fewer PV panels which are optimized may provide desired or even more output power than many panels which are inefficient.

The controller does not only optimize the operation of the PV, but also eases motor starting and allows the motor-pump set to operate effectively over a wide range of solar radiation, flow rates and water heads (India Electric Market , 2000). This means that with the MPPT controller water pumping can start early in the morning and stop late in the evening thereby producing high water volume per day.

However, being an electronic device, in addition to consuming 4-7% of PV output power (India Electric Market , 2000) the MPPT controller has high probability of failure especially when it is operated in a harsh environment (e.g. humid and high ambient temperature). This poses threats on the system availability which according to Short and Mueller (2002) is a major concern in PV systems installed in remote areas of developing countries where it is difficult to access repairs and spare parts. Irrigation in

particular cannot afford to lose a water pumping system even just for a week, otherwise crops will wilt. This is why Short and Mueller (2002) reported that whenever any form of electronic controller (including inverter and MPPT) is used in SPVWP systems such a controller "must be inherently extremely reliable or easily reparable/replaceable at local level" (p. 281).

Based on the above discussion, this study proposes direct coupling (between motor-pump set and array) for remote SPVWP systems in developing countries. The elimination of electronic controllers and batteries in SPVWP systems offers high availability, low cost and maintenance-free operation. The form of energy storage in this case is a big capacity water tank. Fig. 2.8 shows the proposed SPVWP system suitable for developing countries.

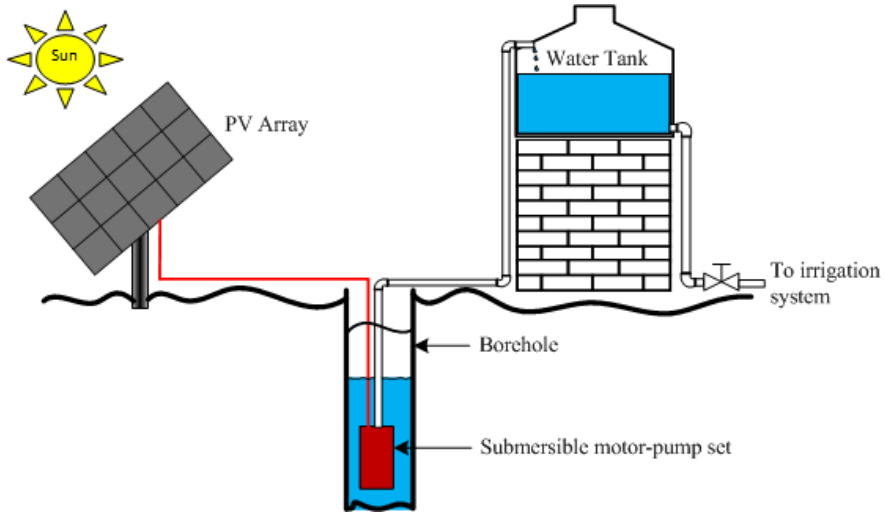

Fig. 2.8: *Low cost PV water pumping system*

2.6 Soil Moisture Monitoring Technology

The process of determining moisture status in the soil can take two basic forms: water potential and water content. Soil water potential, also known as soil tension, is the amount of force needed to extract water from the soil. Water potential describes how hard it is for plant roots to absorb water from the soil, and the higher the potential the drier the soil and the harder the roots must work to get water. On the other hand, soil

water content is the amount of water per given volume of undisturbed soil or weight of dry soil. It can also be expressed in relative depth as millimeter of water per meter of soil. Specific soil characteristic curves are used to relate water potential to water content.

There are three major forms of devices used to measure soil moisture based on the above two strategies and these are: *tensiometers, electrical resistance sensors* and *dielectric sensors*. The suitability of each of the sensors depends on the cost, reliability, ease of interfacing to the controller, accuracy and soil texture.

2.6.1 Tensiometers

A tensiometer is a sealed, degassed-water-filled shaft fitted with a porous ceramic tip on the lower end that is buried in the soil to a desired depth and a protruding vacuum gauge on the upper end (Morris, 2006). Since the tensiometer measures soil water potential or tension, the vacuum gauge is calibrated in either *centibars (cb)* or *kilopascals (kPa)* which are equivalent units (i.e. 1 cb = 1 kPa). The device, while fixed into the ground, can be connected to a data-logger, hand-held meter or to an irrigation controller through a pressure transducer (Pardossi *et al.*, 2009) or electric switch. While pressure transducers are expensive, the switching tensiometers are traditionally suitable for a bypass-mode S-MS controller which requires fixing of a threshold level below which irrigation must be initiated.

Tensiometers are easy to install and are available in different lengths. For example, Irrometer Company produces several tensiometer models with shaft lengths ranging from 15.2 to 152 cm. The length of the shaft partly dictates the price for the tensiometers. For example, Morris (2006) reported a price range of $45 to $80 with tensiometer lengths ranging from 15 to 122 cm. However long the shaft may be, the zone of influence is the ceramic tip which must be buried within the active root zone of the plant and ensuring that it makes a good contact with the soil substrate. This requirement may be difficult to achieve in swelling soils when dry conditions are inevitable, and the sensor may need to be re-installed.

To accommodate moisture variability in the deep rooted plants, one short shafted tensiometer may be buried in the top soil and a long tensiometer buried further deep into the soil as shown in Fig. 2.9. This arrangement can also be used in on-demand irrigation controllers where the upper threshold, which is used to stop irrigation, is set by the deeper tensiometer and the shallow tensiometer is used as the lower threshold which is used to initiate irrigation.

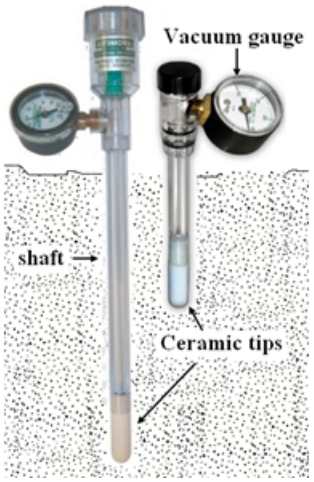

Fig. 2.9: *Tensiometers placed at different depths in the root zone (Photos courtesy - Irrometer Co.)*

The main advantage of tensiometers is their high accuracy (typically, +/-3% of span) regardless of varying temperatures and soil osmotic potential. However, they are fragile and need regular maintenance as they require water refilling in the tube (Pardossi *et al.*, 2009). Nevertheless, they are low cost and have long life span if properly installed and maintained. The major bottleneck of tensiometers is that, typically, they work best in the range of 0 to 80 kPa which makes them suitable for course textured soils only, because fine textured soils still contain more water at a tension reading of 80 kPa (Morris, 2006).

2.6.2 Electrical Resistance Sensors

The principle behind electrical resistance sensors is to measure the resistance of the water in the soil. Since water conducts electricity, the resistance of the soil decreases

with an increase in the amount of water in it. These sensors have electrodes embedded in a porous material that absorbs water to establish equilibrium. As the soil dries up the water is released from the porous material and the resistance measured between the electrodes increases accordingly. Resistance sensors measure water potential, but unlike tensiometers they have a wider range of measurement.

Gypsum blocks and *Granular Matrix Sensor (GMS)* are two types of electrical resistance sensors with gypsum blocks being the oldest and simplest sensors costing $5 to $15 while GMS are new and less degradation-susceptible sensors costing $25 to $35 a piece (Morris, 2006). While a gypsum block has smaller pores in its matrix – making it sensitive to moisture in fine textured soils only, GMS has larger pores which improves its sensitivity in coarse textured soils and in very wet conditions (Pardossi *et al.*, 2009). Typical examples of GMS sensors are Watermark 200SS and Watermark 200SS-V (both from Irrometer Company, Inc.) which measure soil moisture in the range of 0 to 200 kPa and 0 to 239 kPa, respectively.

The resistance from the electrical-resistance sensors cannot, however, be measured with a DC meter. DC current polarizes the soil sample and produces readings that fluctuate wildly (Morris, 2006). Special interfaces are needed for meters or data loggers that are incapable of exciting the sensor with an AC signal. One such interface is SMX module (EME systems Co.) which produces voltage that can be measured by an ordinary meter. Watermark 200SS-V has a built-in interface with a price tag of $88 compared to $53 for the ordinary Watermark 200SS. Fig. 2.10 shows photos of the two versions of the Watermark sensors.

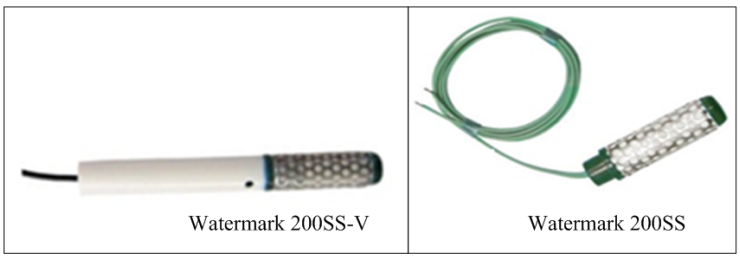

Fig. 2.10: *Versions of Watermark sensors (Photos courtesy - Irrometer Co.)*

Besides wider measuring range, low cost and maintenance-free operation, the other advantages of GMS include durability and accuracy especially in wet conditions. How-

ever, besides having low resolution and slow reaction time – making them unsuitable for high-infiltration-rate soils (e.g. sand), GMS sensors are also temperature-dependent; hence demanding temperature sensors for compensation when connecting to data loggers (Muñoz-Carpena, 2009).

The installation procedure is similar to that of tensiometers. They are buried into the soil to a desired depth within the root zone of the plant, and ensuring that it makes good contact with the soil. Just like tensiometers, GMS sensors are problematic in dry-swelling soils as they lose contact with the surrounding soil and may need to be re-installed.

2.6.3 Dielectric Sensors

Unlike the two previously discussed sensors which measure water tension, dielectric sensors measure water content. They estimate soil water content by inducing an alternating electric field into the soil and evaluating the speed of the wave which is then related to the bulk permittivity of the soil. The speed of the wave in the soil increases when the soil dries – thereby reducing bulk permittivity. This is so because water is the major contributor of the bulk permittivity of the soil than air and soil minerals (Muñoz-Carpena, 2009); hence, water content in the soil is correctly estimated from the computed bulk permittivity.

Depending on the nature of the output signal, dielectric sensors can be classified into several categories including *Time Domain Reflectometry*; *Frequency Domain: Capacitance and Frequency Domain Reflectometry*; *Amplitude Domain Reflectometry: Impedance*; *Phase Transmission*; and *Time Domain Transmission*. A comprehensive analysis of these sensors can be found from Muñoz-Carpena (2009).

Nevertheless, all these sensors become accurate after soil- specific calibration. They also require good contact with the surrounding soil, and the bigger the sensing sphere of influence the larger the sensing soil volume. Large sensing volume helps to curb problems in non-heterogeneous soils where it is difficult to get an average reading of

a large volume of soil using one representative sensor (Pardossi *et al.*, 2009). This is a major drawback for these sensors because as one thinks of a bigger-sensing-sphere sensor they must think about the price for such a sensor.

Some companies produce three-prong versions of dielectric sensors which have capabilities of sensing soil temperature and electrical conductivity in addition to sensing water content. Examples of these versions are: EC-TE and EC-TM (both from Decagon Devices, Inc.). Another new and research-grade dielectric sensor which measures temperature as well is SM300 (Delta-T Devices Ltd). This has an accuracy of as high as ± 2.5% and produces an output voltage ranging between 0 and 1V which can directly be read by meters or data loggers. However, as Morris (2006) reported, these devices are very expensive with the cost ranging from $500 to $4,400. Fig. 2.11 shows photos of some dielectric sensors available on the market.

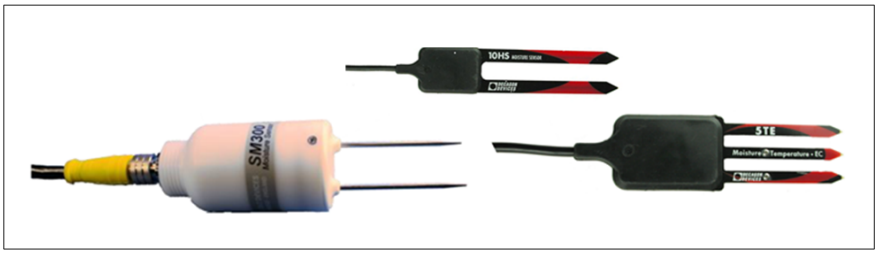

Fig. 2.11: *Examples of dielectric sensors (Photos courtesy - Decagon Devices, Inc. and Delta-T Devices Ltd.)*

2.7 Chapter Summary

This chapter, has introduced basic irrigation scheduling concepts. Additionally, it has reviewed current irrigation controllers by discussing how they operate, analysing their comparative merits and demerits, and providing insights of how they can better service water scarcity problem and solar PV energy conservation. It has also discussed WSANs as an option over wired infrastructure in order to develop an inexpensive and power-efficient solution for effective irrigation scheduling. The chapter further examined how high water pumping capacity, low cost and high efficiency requirements

of SPVWP systems may be achieved. Finally, the chapter has discussed merits and demerits of various technologies used in soil moisture sensing.

The next chapter specifies an irrigation management system by firstly giving its overview and outlining the experimental field design. Secondly, it discusses two functional components of the irrigation management system: the irrigation station and the remote monitoring station. Finally, the chapter develops the components of the irrigation station.

Chapter 3

Specifying the Irrigation Management System

3.1 Overview

This study was conducted at a site in Blantyre, southern part of Malawi. The site is 1045 m above sea level and its coordinates are: latitude 15º 48' 28.41" S; and longitude 35º 00' 24.04" E. There are two distinct seasons in this area; the rainy season is from November to April with an average annual rainfall of 1,127 mm, and the dry season is from May to October. The average minimum annual temperature ranges from 13 °C to 24 °C during the cold season (May to July) while the maximum annual temperature ranges from 21 °C to 32 °C during the hot season (September to November). Watermark 200SS moisture sensors were calibrated based on the soil and climatic conditions of this site.

Two plots were planted to maize and irrigated during the dry season between late July and mid November 2012. One field was used as a Control Treatment (CT) and was irrigated based on constant preset moisture thresholds throughout the growing period of the maize. The lower threshold was set at 50% MAD while the upper was set at 10% MAD.

The field under Experimental Treatment (ExT) used variable thresholds following the crop coefficient pattern of the water requirements by maize crop. Initially the lower and the upper threshold levels were set at 70% MAD and 40% MAD, respectively, then the controller automatically increased the respective levels to 50% MAD and 10% MAD at the middle growth stage of maize plants. The controller automatically then reduced the levels back to 70% MAD and 40% MAD at the later stage of maize crop development.

Finally, in order to avoid over-irrigation, both CT and ExT controllers used water-budget analysis (the way ET controllers work) to calculate time required to refill the water and compute the application efficiency by measuring, after some blackout time, the actual moisture and comparing it with what was required. The blackout time was necessary to allow water diffusion into the soil. However, the controllers were configured to interrupt an irrigation event when an unexpected moisture pattern was reported by sensors.

3.2 Experimental Field Layout

Earlier research studies conducted in Malawi (Waddington *et al.*, 1990; Benson, 1999; Chilimba, 1999) revealed that the minimum recommended plot size for field trials is four ridges, 6 metres long and 90 cm apart. This translates into an effective field size of approximately 17.4 m^2 (2.9 m by 6 m). With tall varieties of maize the planting stations have to be 90 cm apart with three seeds per station, otherwise 75 cm is ideal for most varieties (Benson, 1999).

Considering the specified minimum parameters above, two plots of 11 m by 4.4 m each were selected for this study. This resulted into an effective field size of 48.4 m^2 having 6 ridges each. The ridges were spaced at 80 cm and the planting stations were set at 21.5 cm. One seed was planted per station. A 1.2 m gap between the two plots was necessary so that the applied water in one field could not diffuse into the other. Furthermore, each plot was levelled to allow even distribution of water in the field. Fig. 3.1 shows the experimental field layout as specified above.

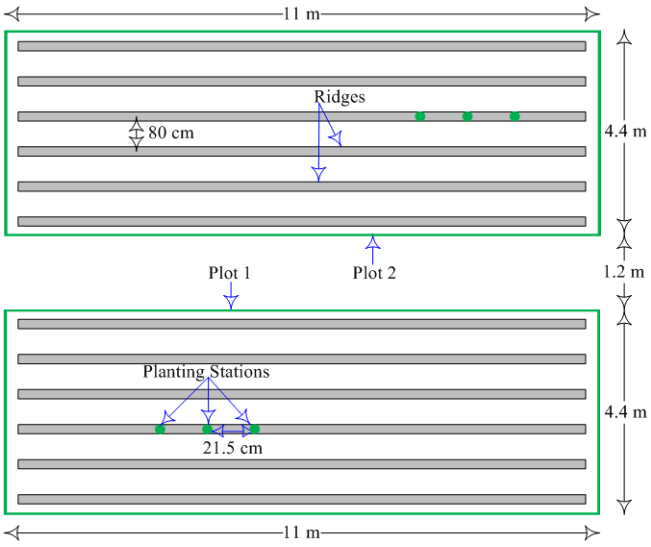

Fig. 3.1: *Experimental field layout*

3.3 Functional Components of the Irrigation Management System

The purpose of the Irrigation Management System (IMS) was to automate an irrigation process. Specifically, the interest was in studying fluctuations in soil moisture in an agricultural field. Accordingly, sensor data were automatically gathered at intervals of 1 minute or 15 minutes depending on whether the irrigation was in progress or not. The data were retrieved at the end of the observation period. Based on the results, the irrigation system switched on valves and finally irrigated the field.

The general work-flow of the system consists of (1) taking soil moisture and temperature samples at predefined time intervals, (2) sending and storing sampled data in a coordinator node, (3) sending the data from the coordinator to a gateway node for forwarding to a Remote Monitoring Station (RMS) through a cellular network, (4) going to sleep, and (5) waking up and repeating the previous steps. Depending on the values stored in the coordinator node, the irrigation valves had to be opened or closed.

In order to realize these functional requirements, the IMS was divided into two major sections: Irrigation Station (IS) and RMS. These two sections were linked via a cellular network as shown in Fig. 3.2. The RMS was used to capture performance parameters

of the IS at a remote site. The parameters included soil moisture level, soil temperature, battery voltage levels of sensor nodes, quality of wireless links, valve status and sensor board temperature. The idea was to get timely information without visiting the site physically, consequently, saving time and money. The rest of this chapter develops the IS, while the RMS is developed later in chapter 5

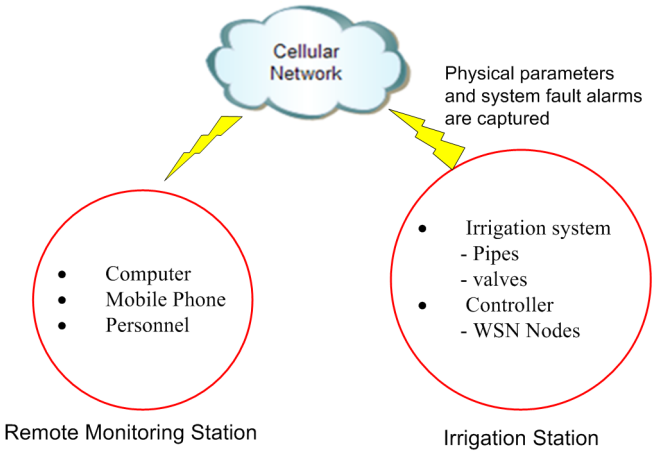

Fig. 3.2: *The architecture of the Irrigation Management System*

3.4 Irrigation Station (IS)

The work-flow of the IS can be mapped into a five-component system architecture depicted by Fig. 3.3 which includes (1) soil moisture and temperature sensor; (2) sensor node; (3) coordinator node; (4) gateway node; and (5) irrigation system. Based on this architecture, the irrigation controller comprises the sensor node, the coordinator node, and the gateway node. The soil moisture and temperature sensor component of the IS is developed in section 4.2 of chapter 4; the three components of the irrigation controller are discussed in sections 3.4.2 through 3.4.4; after which the irrigation system is developed in section 3.4.5. Since the three components of the irrigation controller were based on WSN, then section 3.4.1 first discusses the WSN protocol, topology and devices used.

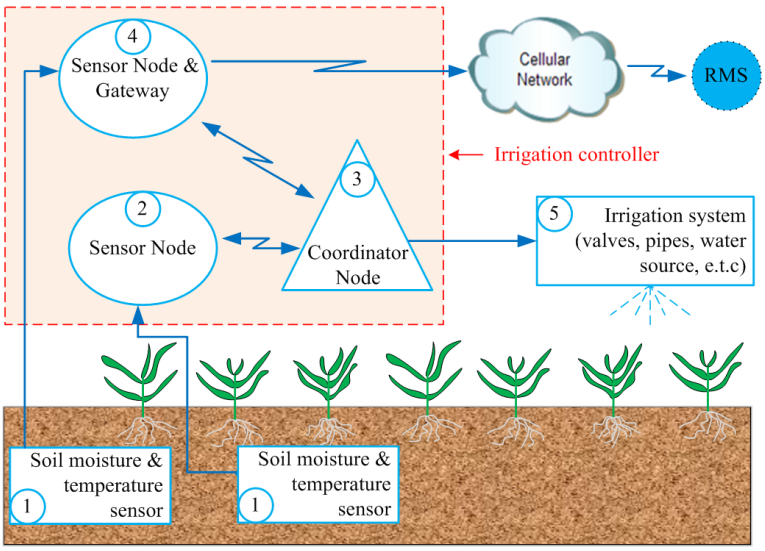

Fig. 3.3: *The architecture of the Irrigation Station showing the irrigation controller and other components*

3.4.1 WSN Protocol, Topology and Devices Used

The WSN deployed in this study used ZigBee, an IEEE 802.15.4 networking standard for Personal Area Networks (PANs). A detailed description of this protocol was discussed in literature review chapter (Section 2.4.1). The major advantages of this protocol include the following: (1) use of unlicensed frequency band - 2.4 GHz in Malawi; (2) low cost - hence suitable for developing countries; (3) low power consumption - hence suitable for deployment in remote location where battery power supply is the only option and needs to be sustained; and (4) flexibility in terms of network topology.

In this study an Open WSN node was used as a sensor node. The advantage of the Open Source model when applied to WSNs is relevant in terms of cost, personalisation and independence from a single entity as compared to proprietary solutions. In particular, the Waspmote node by *Libelium* was selected. Waspmotes are built around XBee transceivers which provide flexibility in terms of multiplicity of operating power, protocols, and operating frequencies. According to Libelium (2010), other Waspmote characteristics include (1) minimum power consumption of the order of 0.7 mA in the hibernation mode; (2) flexible architecture allowing extra sensors to be easily installed in a modular way; (3) the provision of Global Positioning System, General Packet Radio Service (GPRS) and Secure Digital (SD) card on board; and (4) the provision of a

Real Time Clock (RTC) . Furthermore, Waspmotes are powered with a lithium battery which can be recharged through a special socket dedicated for the solar panel; this option is quite beneficial for deployments in developing countries where power supply is either scarce or unstable.

As discussed in section 2.4.1, ZigBee networks can take three forms of topologies: Star; Cluster-Tree; and Mesh. However, this study adopted a star topology for the advantages it offers. With this topology, there is a potential of battery life saving since all ZigBee End Devices (ZEDs) spend most of their time asleep, only waking up to measure and send the data to the ZigBee Coordinator (ZC). Otherwise, as the case with cluster tree and mesh, ZigBee Routers (ZRs) need to be awake since they provide paths for other devices to the ZC thereby wasting battery power in the process.

This study deployed five ZigBee devices, four of which were placed in the field and one centrally placed. All the four in-field sensor nodes were configured as ZEDs and were used to capture soil moisture and temperature levels in the field, and then send the information to a central processing node. The central node was configured to be a ZC so as to form a star topology with the four in-field nodes as shown in Fig. 3.4. These configurations and updating of the firmware for the WSN devices were done using X-CTU, a Windows-based configuration tool developed by *Digi International, Inc*.

Note that the positions of the in-field nodes coincided with those of the moisture sensors as discussed earlier in section 4.2.2.

A PAN was created by uploading appropriate software programs (see Appendix B) into the in-field and the central nodes. The ZC program allowed this node to: (1) select a 16 bit PAN ID that uniquely identifies the network; (2) select the channel for the network - within 2.4 GHz ISM band; (3) assign network addresses to joining ZEDs; and (4) enable network security. On the other hand, the ZED program allowed such devices to accept configuration parameters as assigned by the ZC.

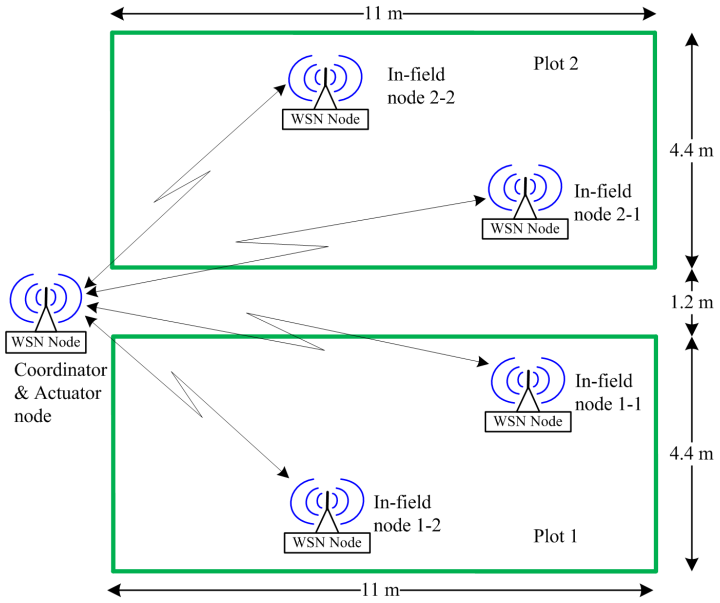

Fig. 3.4: *Location of wireless sensor nodes in the field - forming a star network topology*

3.4.2 Sensor Node

As shown in Fig. 3.4 there were four in-field sensor nodes; two in each of the two plots. The hardware design is based on a modular architecture as shown in Fig. 3.5 allowing the integration of only those modules that are needed in each device. Consequently, one of the four in-field sensor nodes (node 2-2) was assigned additional responsibility of a gateway to relay field data to a remote station for diagnostic purposes by the management personnel.

The Waspmote sensor board is centered around ATmega1281MCU which is a high-performance, low-power processing unit having 128 kB of programmable flash memory. In addition, it has 7 analog and 8 digital Input/Output (I/O) pins which allow several external devices and sensors to easily connect simultaneously.

The agriculture board was used as an interface between the sensors and the Waspmote sensor board. This board has Analog to Digital and Digital to Analog Converters (ADC & DAC) and many other specialized interfacing circuits for several sensors. Specifically, the board has an interfacing circuit for Watermark sensor which makes it possible for measuring AC resistance from the sensor.

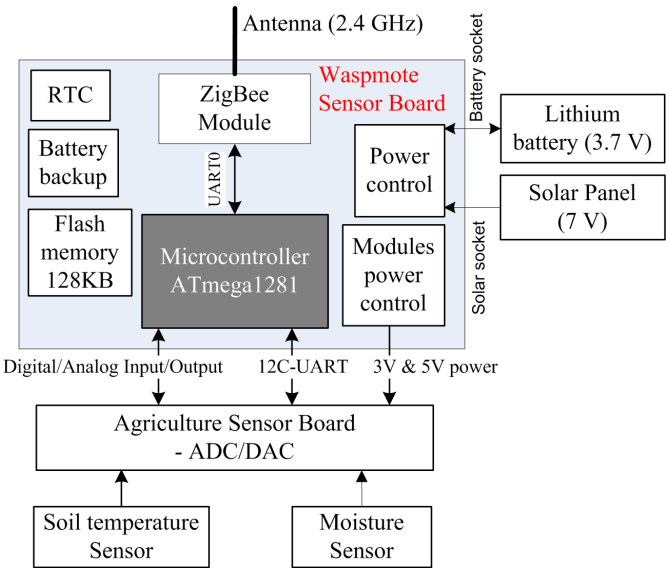

Fig. 3.5: *Architecture of an in-field wireless sensor node*

The in-field sensor node was equipped with a wireless communication model which was used to send sensor data to a Coordinator node described later in section 3.4.3. The communication model comprised an XBee transceiver (ZigBee) module, with a sensitivity of -96 dBm, and a 2 dBi antenna.

Powering requirements for all the four in-field sensor nodes were satisfied by 2.5 W solar panels and 1,150 mAh rechargeable lithium batteries. It must be noted that these power ratings were suitable for the in-field sensor nodes since these nodes were using deep sleeping mode as a way of conserving energy.

The main function of the in-field sensor nodes was to capture and send field and diagnostic data to the coordinator node. In order to achieve this functional requirement a software program was developed and uploaded into the sensor nodes to allow them measure soil moisture, soil temperature, their battery levels, and board temperature (for diagnostic purposes) at time intervals of 15 minutes when the system was idle and 1 minute when irrigation was taking place. The rest of the time sensor nodes were in a deep sleep mode to conserve battery power. Once the measurements were completed, the nodes relayed the data through the XBee transceivers to the coordinator node for processing.

A 15 minute sampling interval was considered long enough to preserve battery power

for the nodes on one hand, and short enough to fully monitor the soil moisture trends. In other words, as it is generally expected that, increasing the sampling interval can save a substantial amount of battery power for the sensor nodes at the expense of information. However, in order to avoid over-irrigation as a result of late termination of the irrigation event, the study reduced the sampling interval from 15 minutes to 1 minute when the irrigation was in session. This permitted prompt termination of the irrigation event.

The flow chart in Appendix C shows the software architecture for three of the in-field sensor nodes. One of these nodes was used as a gateway for sending a Short Message Service (SMS) to RMS and hence it had slightly different hardware and software architectures.

3.4.3 Coordinator and Actuator Node

The Coordinator and Actuator Node component was the heart of the irrigation controller and had several crucial roles to perform. Firstly, as the most capable node in the network, it permitted and sanctioned all ZEDs that were in quest of connecting to its network. That is, it was responsible for network formation by assigning addresses to all joining nodes and ensuring security for the network. As such, the node was equipped with a ZigBee module which was configured at software level as a ZC.

Secondly, the coordinator node was used to receive and aggregate data from the four in-field sensor nodes discussed earlier in section 3.4.2. The received sensor data included the Watermark frequency and the soil temperature which were used to derive Soil Moisture Potential (SMP) . When receiving data from the sensor nodes the coordinator also captured the Received Signal Strength Indicator (RSSI) of every packet received. This is a measure of the quality of the link between itself and a particular in-field sensor node.

Thirdly, this node was used to relay data to a gateway node for forwarding to RMS. The SMP, battery level, soil temperature, board temperature and RSSI from all four

sensor nodes together with its own battery level, board temperature and system running time were aggregated and prepared suitable for SMS transmission system. Thereafter, the SMS data were relayed to the gateway for forwarding to RMS every 30 minutes regardless of whether irrigation was in session or not. Before transmitting data to the gateway node, the coordinator had to save a copy to an SD card.

Fourthly, the coordinator node was used as an actuator, in which case four of the I/O pins of its Microcontroller Unit (MCU) were connected to a latching circuit and were used to initiate or halt the irrigation by sending corresponding short pulses to the pins. Specifically, two pins were dedicated for each of the two solenoid valves; in which case when initiating irrigation the coordinator had to send a HIGH pulse lasting 1 second to the latching circuit through one pin. The latching circuit had to hold this state until the coordinator sent another HIGH pulse to the other pin indicating completion of irrigation and, hence, valves should close. Consequently, coordinator battery power was saved unlike when it was going to hold the pulse for the entire irrigation duration.

Fig. 3.6 illustrates the hardware architecture of the coordinator and actuator node that permitted it to carry out the above stated functions. In addition, in order to make the controller more robust in terms of powering requirements, the capacity of both solar panel and battery was increased from 7 V, 2.5 W to 12 V, 14 W for the case of the solar panel and from 1,150 mAh to 7,000 mAh for the battery. Notably, the high capacity power option provided to the coordinator node was tapped from the valves' power supply unit as shown in Fig 3.6.

Finally, the software configuration of the coordinator node permitted it to operate as a control element for the irrigation system, in which case it had to make a decision on whether to irrigate or not depending on the level of the SMP. A software program was developed and uploaded onto this node to allow independent and effective control of irrigation events in the two plots based on their respective scheduling strategies developed under section 4.5. In addition to facilitating the process of reporting valve status change, the software permitted the coordinator node to assess the status of all the other in-field nodes and report any mishaps to the gateway. The detailed structure of the program is depicted by the flow chart shown in Appendix D.

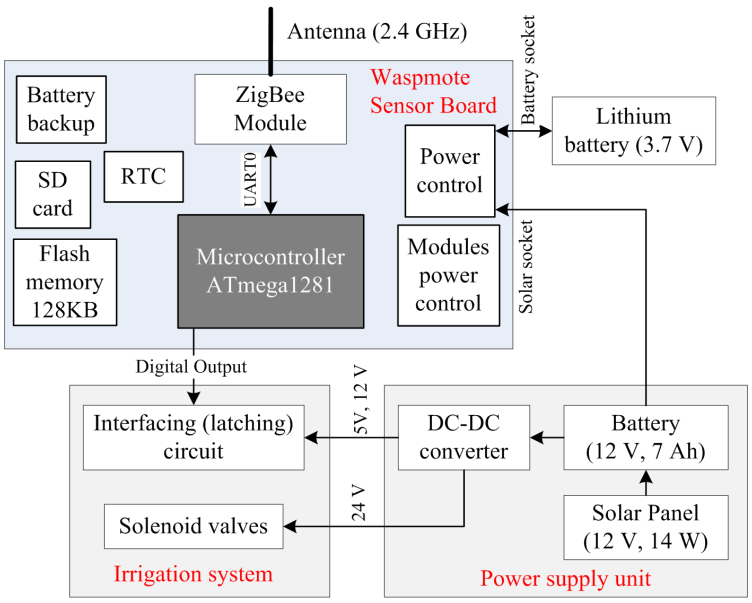

Fig. 3.6: *Coordinator and actuator node architecture also showing connections to irrigation system and power supply unit*

3.4.4 Gateway Node

One of the four in-field sensor nodes discussed in section 3.4.2 assumed the role of a gateway used to send data to the RMS through a cellular network. In addition to a ZigBee module, this particular node was equipped with a GPRS module (refer to Fig. 3.7). Just like any other wireless sensor node in this experiment, it was capturing Watermark frequency, soil temperature and its board temperature and battery level. The sensed data were sent to a coordinator for processing and aggregating with the other sensor nodes' data. Afterwards, the coordinator sent the aggregated data back to the gateway every 30 minutes. The GPRS module residing on top of the gateway node was then used to communicate with the cellular network to forward the SMS data to the RMS for remote system diagnosis.

Despite gathering sensor data at intervals of 1 minute or 15 minutes depending on whether the irrigation was in progress or not, this study opted for sending the data to the RMS at intervals of 30 minutes. This arrangement reduced considerably the cost of the remote monitoring system by decreasing the number of SMSs sent.

Although the coordinator node could be used to send data directly to a remote server by equipping it with a GPRS module, it was compelling to use a separate node as

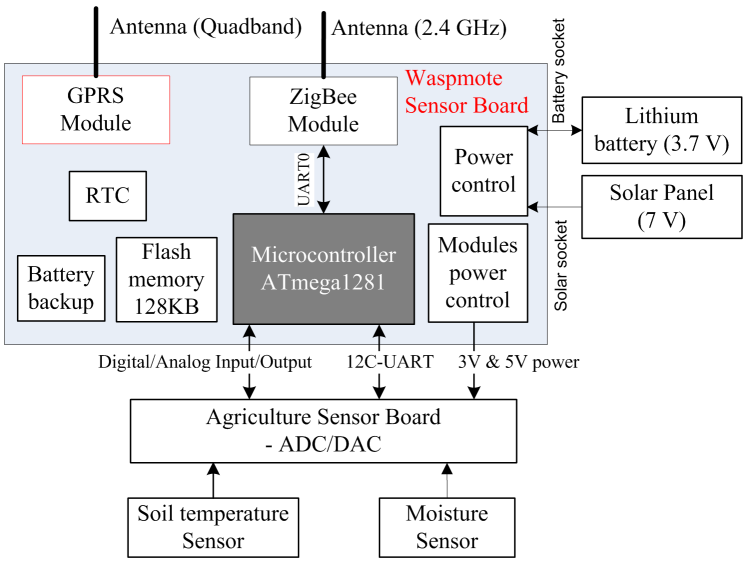

Fig. 3.7: *Architecture of a gateway wireless sensor node*

a gateway because of the following confounding issues: Firstly, the coordinator was configured to be a non-sleeping device because it was responsible for network set-up and maintenance. It was also responsible for actuating solenoid valves in addition to receiving sensor data from all other nodes in the network. As such, it was the busiest node in the network, consequently, its battery was being depleted extensively. It was therefore necessary to delegate SMS sending duties to a gateway node which, otherwise, was less loaded. Note that sending the same amount of data through ZigBee module consumes less power (2 mW) than sending through GPRS to the cellular network (1,000 - 2,000 mW) (Libelium, 2010).

Secondly, since the coordinator node was the heart of the whole system, its failure was very critical and constituted a single-point-of-failure phenomenon. On a regular basis, the gateway was checking the status of the coordinator and reporting any hitches directly to the personal mobile number of the management personnel. This allowed the personnel to quickly fix the problem.

The flow chart shown in Appendix E shows how the gateway node was configured to carry out the necessary duties as described above. The flow chart also shows how most of system fault alarms were captured and reported to the management personnel with assistance from the coordinator node.

3.4.5 Irrigation System

This chapter develops an irrigation system which is one of the major components of the IS as depicted by Fig. 3.3. Upon receipt of the command from the irrigation controller the irrigation system opened valves to water the field.

There are numerous types of irrigation systems including drip, furrow and sprinkler. The suitability of each type depends on the cost, water application efficiency and topology of the field among other things. Accordingly, this study opted for a drip irrigation system for the advantages it offers. Unlike sprinkler system which sprinkles water all over the field, drip irrigation, also known as trickle irrigation is a type of irrigation system that applies water slowly and directly into the root zone of plants. In this case scarce water resources are conserved since there is little or no chance for water to evaporate before seeping into the ground. Besides, Humphreys *et al.* (2005) found that drip was 33% higher in water productivity than both sprinkler and furrow. However, the biggest challenge of drip irrigation is its high installation cost especially for a large field where a great deal of pipes, drippers, valves and other accessories has to be deployed throughout the field.

As shown in Fig. 3.8, there are basically five major components in a drip irrigation system: (1) drippers (emitters); (2) water pipes (lines); (3) valves and other accessories; (4) water tank; and (5) water source and pumping system.

3.4.5.1 Drippers (Emitters)

Since the intent of drip irrigation is to apply water where it is needed most, then it suffices to say that drippers have to coincide with planting stations. However, with one plant per station having a space of 21.5 cm between stations, a great deal of drippers is required. This can obviously inflate the cost of the system. It is therefore prudent to install drippers between every other two planting stations as shown in Fig. 3.8. A ridge of 11 m in length can accommodate 52 planting stations spaced at 21.5 cm (i.e. 1100/21.5+1). This requires 26 drippers. Since there are 6 ridges on each plot, then the total number of drippers needed per plot is 156 (i.e. 26*6).

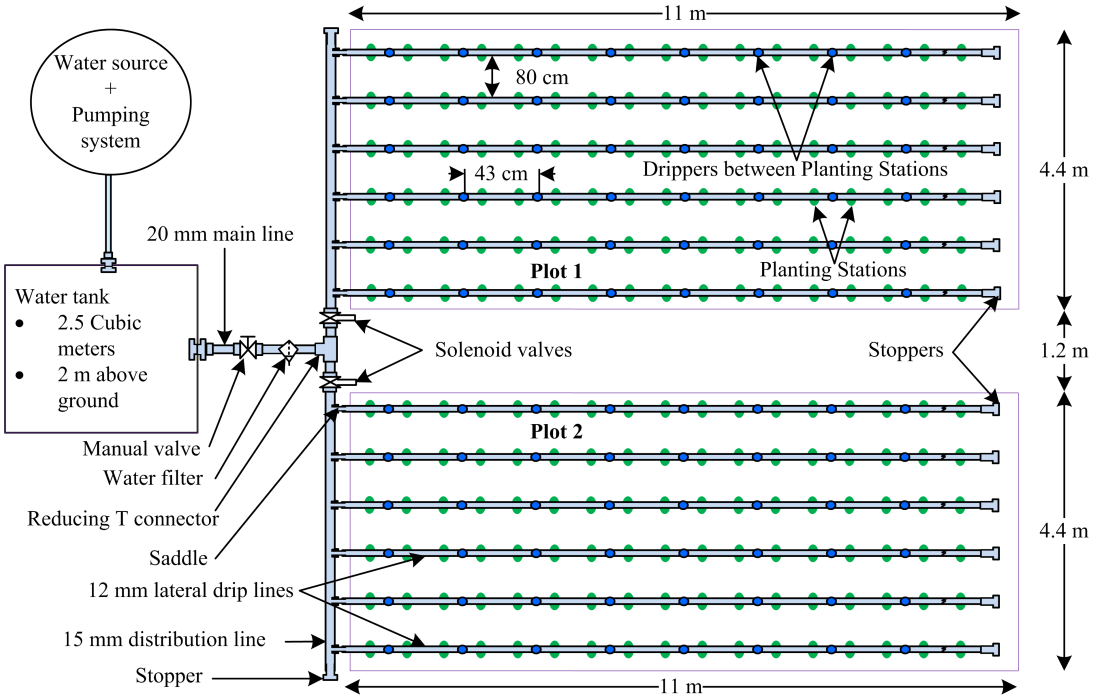

Fig. 3.8: *Drip irrigation system design*

Dripper flow rate depends on the number of drippers and the field application rate (water flow rate of the system). The maximum field application rate is obtained by multiplying the field area by the infiltration rate of the soil as shown by equation 3.1.

$$Maximum\ field\ application\ rate = R_i * A_f \tag{3.1}$$

where R_i and A_f are the infiltration rate and the areas of the field, respectively, as defined in section 4.5and have values of 34.2 mm/h and 48.4 m^2. Substituting these values into equation 3.1 yields a maximum field application rate of $1.65528\,m^3/hour$. However, in order to avoid surface run-off, the actual application rate must be less than the maximum rate. Therefore, a value of 0.69108 $m^3/hour$ as determined in section 4.5 was appropriate.

Now $dripper\ flow\ rate = field\ flow\ rate/number\ of\ drippers.$

That is $dripper\ flow\ rate = (0.69108\,m^3/hour)/156 = 0.00443\,m^3/hour$

3.4.5.2 Water Pipes (Lines)

As shown in the schematic diagram for the drip irrigation system (refer to Fig. 3.8), there are three categories of pipes in this design: *main line* that carries water from the tank; *distribution line* that gets water from the main line and feeds each respective plot; and the *lateral drip lines* where drippers are attached. All these pipes were flexible since they were made of Polyethylene (PE) .

Each lateral line must be able to operate at a flow rate as demanded by the drippers. Since each dripper can handle a flow rate of $0.00443 m^3/hour$ and that there are 26 drippers per lateral drip line, then each lateral line must handle a flow rate of at least $0.115 m^3/hour$ (i.e. 26*$0.00443 m^3/hour$). Using PE specification chart, a PE drip line with 12 mm diameter can easily handle this flow rate with a small friction loss. Since each distribution line has six lateral lines, then the distribution line must be able to handle a flow rate of $0.69 m^3/hour$ (6*0.115). This requires a PE pipe with 15 mm diameter. Finally, the main pipe feeds two distribution pipes. As such, the flow rate must be $1.38 m^3/hour$ which requires a 20 mm PE pipe.

3.4.5.3 Valves and Other Accessories

As shown in the drip system design (Fig. 3.8), there is a manual ball valve just after the tank which can be used to manually open and close water flow in order to allow maintenance work to the rest of the irrigation system.

Along the main line there is a water filter which is a very crucial component of any drip system regardless of water source. Its function is to prevent clogging of drippers and hence reduces the task of regular manual flushing of the entire drip system. For the system to operate effectively the filter must be cleaned regularly.

Along the distribution lines there are solenoid valves which are used to control each field independently. These valves open and close in response to the command received from the irrigation controller through latching circuits. There was a high motivation to use L182D01-ZB10A (SIRAI®) solenoid valves because of the low cost ($76.43), low

power consumption (5.5 W when latched); and the possibility of using a DC power supply. The two latter features allowed the use a single 14 W, 12V solar panel to power both the solenoid valves and the latching circuit. This was more appealing for deployments in rural areas of developing countries where grid power supply is either scarce or unstable.

There were also other accessories and fittings employed to fully develop a working and effective drip irrigation system. These included stoppers, saddles, couplers, tees, elbows, clamps and barbed fittings which were mainly used to join drip pipes. Fig. 3.9 shows some of the major components and accessories which were used in the design of drip irrigation system for this study.

Fig. 3.9: *Some of the components and accessories used in the drip irrigation system*

3.4.5.4 Water Tank

The parameters that must be considered when sizing the water tank are Available Soil Water (ASW), area of the field, depth of the root zone and Management Allowable Depletion (MAD). All these parameters were discussed in chapter 2. It will be shown through an experiment in section 4.3 that the soil under study has an ASW of 13% (or 130 mm/m) and as such the water tank must be designed to satisfy its watering requirements as follows:

Firstly, following the discussion in section 4.5 it is clear that the deepest irrigation event would be required to push the soil moisture level from a 50% MAD to 10%

MAD. Employing equation 2.1 means that $RAW = ASW * MAD = (130\,mm/m) * (50 - 10)/100 = 52\,mm/m$.

Secondly, in order to find Total Available Water (TAW), the root depth (Rd) must be used and for this study the effective root zone of maize was set at a maximum of 40 cm (see section 4.2.2). Employing equation 2.2 means that $TAW = RAW * Rd = 52 * 0.4 = 20.8\,mm$. TAW is the effective depth of an irrigation event.

Thirdly, the effective area of the field is needed in computing the volume of water that must effectively be applied in the soil. Specifically, $V_e = TAW * A_f$, where V_e is the effective water volume and A_f is the effective area of the field as previously defined. In this case, $V_e = (20.8\,mm/1000) * 48.4\,m^2 = 1.007\,m^3$.

Finally, in order to evaluate the tank capacity the irrigation system efficiency is required. That is $volume\ of\ the\ tank = effective\ water\ volume\ /\ system\ efficiency$. Assuming an efficiency of a drip irrigation system to be 90% means that $volume\ of\ the\ tank = 1.007\,m^3/0.9 = 1.119\,m^3$. However, considering the fact that the two plots may be irrigated simultaneously, the total capacity of the tank required was 2.238 m^3. A general rule of thumb is to employ a tank that can hold water for at least three full irrigation events. Therefore, a $7m^3$ tank may be ideal.

3.4.5.5 Water Source and Pumping System

The development of a Solar Photovoltaic Water Pumping (SPVWP) system requires the knowledge of the geographical location of the area as well as the water demand. It was discussed in section 2.5 that direct coupling of PV array to a brushless DC motor with centrifugal pump and a water tank is a more plausible configuration of an SPVWP (refer to Fig. 2.8). Therefore, the design for this study is based on this configuration and is broken into the following five steps:

(1) Determining the solar resource for the location: As stated in section 3.1, the site is 1045 m above sea level and its coordinates are: latitude 15º 48’ 28.41” S; and

longitude 35º 00' 24.04" E. The average minimum annual temperature ranges from 13 °C to 24 °C during the cold season (May to July) while the maximum annual temperature ranges from 21 °C to 32 °C during the hot season (September to November). Furthermore, the site receives an average annual insolation of $5.6 kWh/m^2/day$, and the monthly average solar radiation is 8 hours per day with least sunny days experiencing 6 hours of radiation. These levels of insolation and solar radiation are high enough to make this location suitable for solar water pumping system.

(2) Determining watering needs: Irrigation interval (time taken before irrigation is needed) is useful in determining the watering needs. When water is applied, evapotranspiration (ET) depletes it from the soil. The rate at which the water is depleted is dependent on the weather and growth stage of the plant. In a sunny, hot and windy climate the value for the ET can be at around $8 mm/day$ when maize plant is fully grown. This means that, when 20.8 mm of water (as discussed in section 3.4.5.4) is applied, it will take 2.6 (20.8/8) days before the next irrigation.

The daily water need is then evaluated by using the following equation:

$$daily\ water\ need = \frac{(water\ for\ full\ irrigation\ event) * (cushion\ factor)}{irrigation\ interval} \tag{3.2}$$

The cushion factor in necessary in case of water pumping system failure or to cater for cloudy weather conditions in the case of solar water pumping system. Consequently, a cushion factor assumed is 3. This means that the pumping system should be able to provide water for three full irrigation events before the next irrigation is initiated.

Therefore, using equation 3.2 means that

$$daily\ water\ need = \frac{(2.238 m^3) * 3}{2.6 days} = 2.582 m^3/day$$

(3) Determining water source: There are various sources of water suitable for irrigation including subsurface (e.g. borehole) and surface (e.g. stream, pond, etc). The type of water source determines the configuration of the water pumping system. Al-

though a borehole is expensive to drill, especially in an area where water table is deep, this study chose this type of water source for advantages it offers. In addition to water level consistency, generally, water from a well drilled and constructed borehole is of high quality. At the site where this study was conducted water is typically found at around 15 m distance below the surface.

(4) Determining total dynamic head: Total Dynamic Head (TDH) is a very important parameter in designing SPVWP system. This is a measure of how much pressure the pump must exert in order to deliver water to the required level and, hence, determines the size of both the pump and PV array. It is expressed in meters and must take into account the following four factors: (1) static lift of the water; (2) dynamic lift of water; (3) static height of the storage tank; and (4) the losses from friction. That is

$$TDH = static\ lift\ of\ water + dynamic\ lift\ of\ water + static\ height\ of\ storage\ tank + frictional\ losses \quad (3.3)$$

Fig. 3.10 shows the measurements which are used in computing TDH. The static lift of water is the distance from the mouth of the borehole to the surface of water in the borehole before the commencement of pumping. When pumping starts the water level drops down until when a lower steady level is reached. The difference between the previous level and the current level represents dynamic lift of the borehole. A fast flowing borehole will have a small value of dynamic lift. Here we assume a combined static and dynamic lift to be 14 m for a borehole whose total depth is 15 m. The static height of the storage tank is the total height from the mouth of the borehole to the top of the tank as shown in Fig. 3.10. Again in this study the value for the tank static height is taken to be 3 m.

Finally, the losses from friction account for the resistance of water as it travels through the pipe. A number of factors determine the value of frictional losses including flow rate, type and internal diameter of the pipe, and type and number of connectors. The losses are expressed in terms of equivalent head (metres) and can be computed by

using Pipe Sizing Charts or employing Hazen-Williums equation which is expressed as follows:

$$H_f = \frac{7.925 * 10^{-12}(1000 * Q)^{1.85} L}{C^{1.85} d^{4.87}} \tag{3.4}$$

where

- H_f is a head loss over the length of the pipe (m);
- Q is a flow rate (m^3/hour);
- L is a length of the pipe (m);
- C is a roughness coefficient; and
- d is the inside diameter of the pipe.

A typical roughness coefficient C of a PE pipe is 140 while that of a Polyvinyl chloride (PVC) pipe is 150.

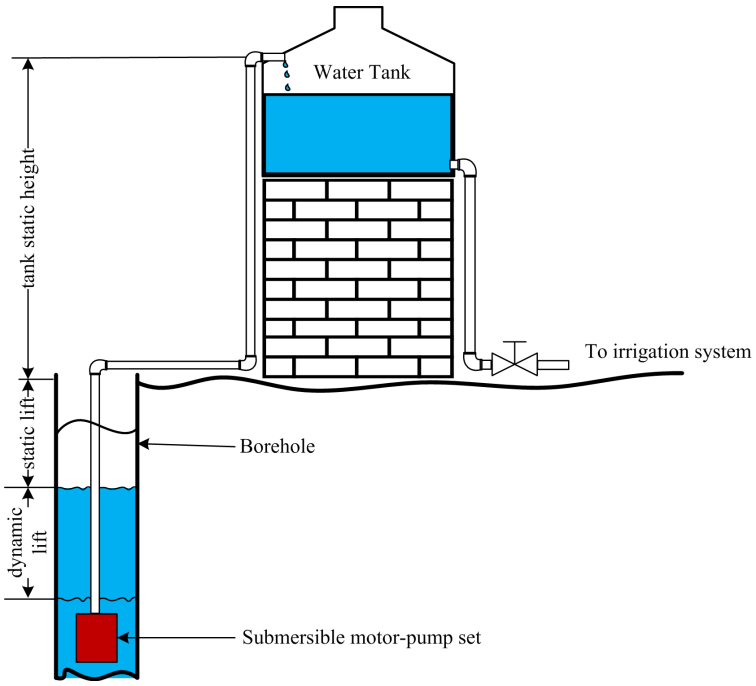

Fig. 3.10: *Water pumping system showing measurements used in computing Total Dynamic Head*

In order to determine flow rate (Q in m^3/hour) which represents the pumping rate of the water pump, information on peak sun hours per day is required. The following equation can then be used to compute pumping rate:

$$Q = \frac{daily\ water\ need\ (m^3/day)}{Peak\ sun\ hours\ per\ day} \tag{3.5}$$

As evaluated earlier on in this section, the minimum peak sun hours at this site is 6 hours/day while daily water need was computed as 2.582 m^3/day. Therefore,

$$Q = \frac{2.582 m^3/day}{6 hours/day} = 0.43 m^3/hour$$

Now employing equation 3.4 in which total pipe length is 23 m, pipe internal diameter is 20 mm (3/4 inch), roughness coefficient is 140 (PE pipe), we get the following head loss:

$$H_f = \frac{7.925 * 10^{-12} * (1000 * 0.43)^{1.85} * 23}{140^{1.85} * 0.0254^{4.87}} = 0.085 m$$

In addition, a 90°standard elbow connector loses 0.6 m of head. Considering three such connectors means that the total head loss of the system is $0.085 + 0.6 * 3 = 1.885 m$

Therefore, using equation 3.3 we get TDH as follows:

$$TDH = 14 + 3 + 1.885 = 19 m$$

(5) Determining pump size and PV array: Information on pumping rate, and TDH is crucial in the determination of the size of both the pump and the PV array. This is done by referring to the charts provided by the manufacturer. The pump that satisfied all the design requirements was *25 SQF-7* (GRUNDFOS Holding A/S). The pump is centrifugal and is coupled to a motor which can operate at a terminal voltage range of 30 - 300 VDC. The motor-pump set has built-in protection features that include dry-running, over voltage and under voltage, overload, over temperature, sand shield, and MPPT. These features are in line with the objective of this study to minimize external controllers that otherwise increase running costs for the system. As such there is a direct connection between the PV array and the motor-pump set as it was discussed in section 2.5.

Referring to the performance chart (see Appendix A), this pump can deliver the required flow rate (0.43 m^3/hour) at the desired TDH (19 m - approximately 65 ft) when a 156 Watt-peak (Wp) is provided by the PV array. Since the minimum voltage supply

to the motor is 30 VDC, then a series combination of three panels with 12 V terminal voltage each is required. This will provide the motor with a voltage supply of 36 VDC. Since a total of 156 Wp is required, then each panel should be rated at 52 Wp.

The manufacturer of this pump developed the performance chart (Appendix A) at an insolation of $6 kWh/m^2/day$. This translates into a PV Generation Factor (PGF) of 3.72 Wh/day/Wp. Assuming negligible cable and connector losses between the PV array and the motor, at this insolation the total estimated PV energy provided by the array to the motor = 156* 3.72 = *580.3 Wh/day.* The amount of energy required to pump a given volume of water, known as Water Energy Use (WEU) , in an SPVWP system is evaluated by the following equation:

$$WEU = \frac{PV\ energy\ used\ per\ day}{Amount\ of\ water\ pumped\ per\ day} \tag{3.6}$$

Therefore, considering the designed SPVWP system which requires 580.3 Wh/day of solar PV energy to deliver 2.582 m^3 of water per day, the WEU is evaluated as

$$WEU = \frac{580.3 Wh/day}{2.582 m^3/day} = 224.7 Wh/m^3 \tag{3.7}$$

Although the water pumping system was theoretically designed, it was not practically implemented due to financial constraints. Instead, tap water from a water utility company was used. However, the SPVWP system was designed and used to quantify the amount of solar PV energy that would be saved by the proposed irrigation system controller.

3.5 Chapter Summary

This chapter discussed the components of an IMS. Specifically, it defined an experimental field layout and discussed the functional components of the IMS which are the IS and RMS. The chapter further developed various components of the IS. The next

chapter has been dedicated to the development of an efficient irrigation scheduling strategy upon which the controller discussed above was based.

Chapter 4

Irrigation Scheduling Strategy Development

4.1 Overview

In order to save irrigation water and energy used in water pumping, the irrigation controller developed in section 3.4.3 had to be based on an efficient irrigation scheduling strategy. The aim of this chapter is to develop such an efficient scheduling strategy to foster water and energy conservation.

Irrigation scheduling strategy relies heavily on the soil moisture sensing mechanism and the physical characteristics of the soil in the field. It is therefore important to investigate these characteristics before developing any scheduling strategy. The intent of this task is to establish water-holding capacity of the soil under study so that the irrigation system can apply the correct amount of water to satisfy crop water needs in the field without over-irrigating.

4.2 Developing Soil Moisture Sensing Mechanism

The soil moisture sensor is one of the most important components upon which the efficiency of the irrigation activity heavily relies. The suitability for a soil moisture sensing device depends on the cost, reliability, ease of interfacing to a signal processing device, accuracy and soil texture. Although it is impossible to single out a sensor that satisfies all of the above selection criteria, Watermark 200SS (Irrometer Company, Inc., Riverside, CA) was opted for because it scores highly on low cost, durability, maintenance-free operation and suitability for soil texture variability since it has a wide measuring range (0 to -200 kPa). The fact that this sensor monitors water potential makes it superior to other water content based sensors; knowledge of soil water content is not as important as that of the level of tension crop roots must exert to extract such water.

The manufacturer of this GMS sensor further stated that it has the following features:

(a) proven stable calibration;
(b) range of measurement from 0 to 200 kPa;
(c) fully solid state;
(d) will not dissolve in soil;
(e) not affected by freezing temperatures;
(f) internally compensated for commonly found salinity levels;
(g) inexpensive, easy to install and use;
(h) compatible with AC or DC reading devices (specialized circuit required); and
(i) no maintenance required.

However, the downside of this sensor is that its resistance can only be read by an AC meter. A special circuit is required if a DC meter is going to be used. Using this sensor, Miranda *et al.* (2005) successfully implemented a wireless sensor network for irrigation scheduling by designing a resistor-capacitor circuit and a program to read the moisture. Nevertheless, this study used an agriculture board (Libelium Co,) on top of a Waspmote node that has an MCU. This board has a built-in interface for Watermark

200SS sensor to enable reading of the AC signal frequency which is a function of the amount of water in the soil.

Section 4.2.1 gives a detailed analysis of how the Watermark 200SS sensor was used to read SMP by using a calibration equation that also requires soil temperature measurements. The soil temperature sensor chosen for its suitability in a harsh environment is TP1000 (Omega Engineering Ltd.) costing $52 and it can be coupled directly to the agriculture board. Its temperature measuring range is between -30 ºC to 300 ºC with 1 kΩ resistance at 0 ºC. Descriptions of how sensors were positioned and installed in the field are presented in sections 4.2.2 and 4.2.3, respectively.

4.2.1 Measuring Soil Moisture Potential

The measurement of the SMP using Watermark 200SS sensor is done in two stages: (1) reading the frequency of the AC signal pushed into the sensor which is then converted to resistance; and (2) using a nonlinear calibration equation to convert the Watermark electrical resistance (in kΩ) into SMP (in kPa).

Using the agriculture board as an interface of the Watermark sensor and a Waspmote MCU, it is possible to measure the frequency directly. The frequency generated from the Watermark sensor circuit is related to the resistance as shown in Fig. 4.1. The following equation was developed by Libelium (n.d.), the manufacturer of the agriculture board, and is used to convert the measured frequency into the sensor's resistance:

$$R = \frac{150390 - 8.19f}{1000(0.021f - 1)} \tag{4.1}$$

where f is the measured frequency in Hz and R is the sensor resistance in kΩ.

Since the frequency generated from the Watermark sensor circuit ranges approximately from 50 Hz (for very dry soil) to 10,000 Hz (for saturated soil), then the resistance ranges from 3 MΩ to 330 Ω, respectively.

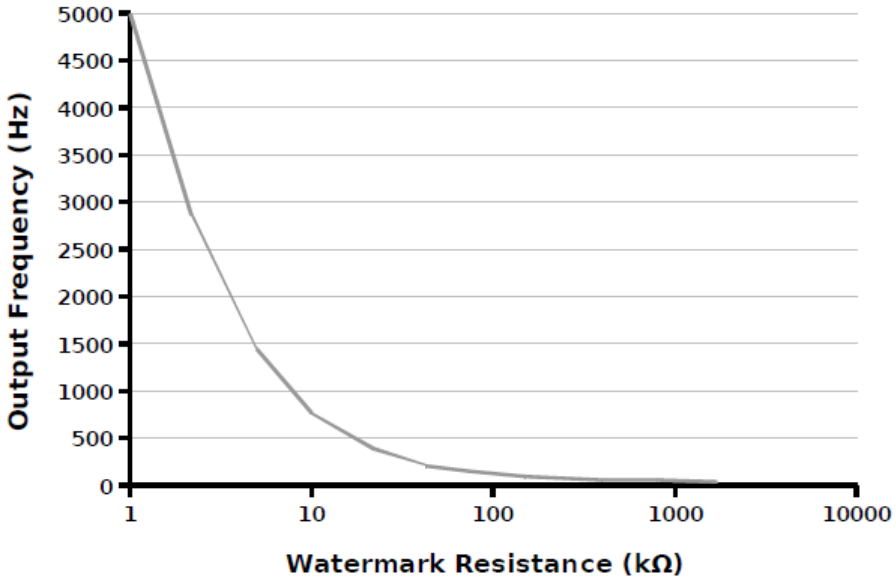

Fig. 4.1: *Relationship between the output frequency of the Watermark sensor circuit and the resistance of the sensor (Libelium Co.)*

Fig. 4.2 shows the characteristics of the TP1000 soil temperature sensor in terms of output voltage as a function of temperature. However, the agriculture board and the Waspmote MCU allow direct measurement of soil temperature (in ºC) from the TP1000 sensor.

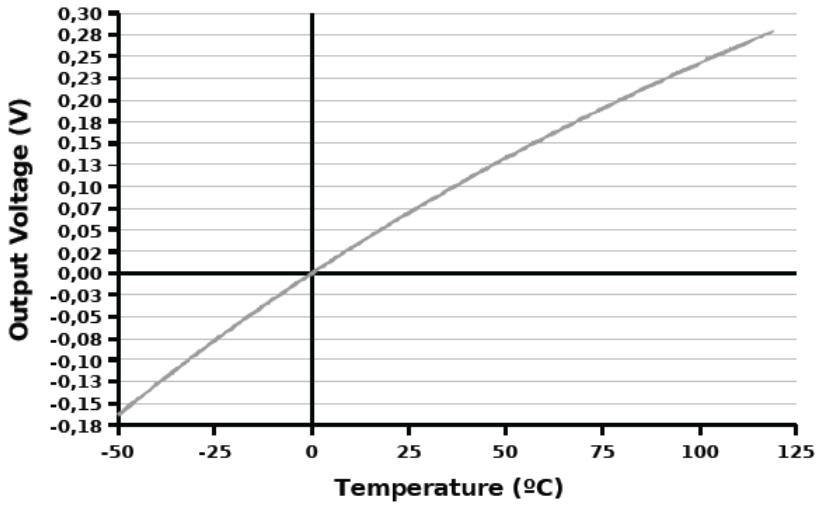

Fig. 4.2: *Output voltage of the PT1000 sensor with respect to temperature (Libelium Co.)*

Once the measurement of the soil resistance and temperature is done then an appropriate calibration equation (discussed below) is used to derive SMP. Various equations

have been proposed in literature (Thomson and Armstrong, 1987; cited in Thompson *et al.*, 2006; Shock *et al.*, 1998; Allen, 2000). The accuracy of most of these equations depends on the measurement range of SMP (drier soil conditions or moist soil conditions) as well as on the environment. As such, soil specific calibration may be paramount regardless of whichever equation is used.

The equation developed by Shock *et al.* (1998) is expressed as follows:

$$SMP = -\frac{4.093 + 3.213R}{1 - 0.009733R - 0.01205T} \tag{4.2}$$

where

- SMP is soil moisture potential (in kPa);
- R is soil resistance (in kΩ) as measured by Watermark sensor; and
- T is soil temperature (in ºC) in the vicinity of the sensor.

On the other hand Allen (2000) developed a composite equation comprising of the Shock *et al.* (1998) equation and two other equations which were generated from a standard calibration table (Watermark calibration table no.3; Irrometer Co. USA). The resistance was divided into three sections and each section has its own equation applied as follows:

- For $0 \leq \mathrm{R} \leq 1$ kΩ:

$$SMP = -20[(1 + 0.018(T - 24))R - 0.55] \tag{4.3}$$

- For 1 kΩ < R $\leq$ 8 kΩ: the Shock *et al.* (1998) equation is used (see equation 4.2).
- For R > 8 kΩ:

$$SMP = -2.246 - 5.239R[1 + 0.018(T - 24)] - 0.06756R^2[1 + 0.018(T - 24)]^2 \tag{4.4}$$

where SMP, R and T have the same definitions as stated in equation 4.2.

Fig. 4.3 shows four different calibration equations assuming constant soil temperature of 24 ºC. The graphs show that Thomson and Armstrong (1987) method underestimates SMP in dry conditions (< -45 kPa). On the other hand Thompson *et al.* (2006)

overestimates SMP in moist soil conditions and underestimates it in dry conditions. Although Allen (2000) equation overestimates SMP in very wet conditions (> -10 kPa), it compares very well with Shock *et al.* (1998).

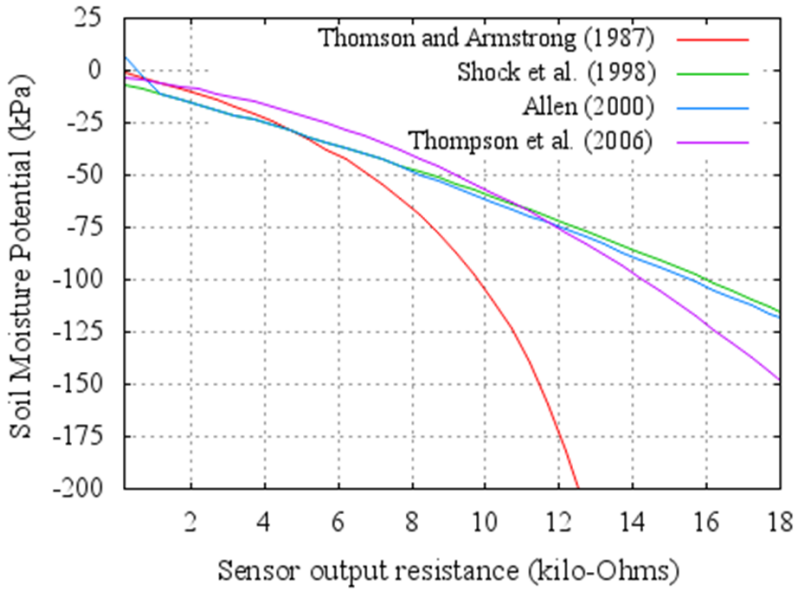

Fig. 4.3: *The relationship between soil moisture potential (kPa) and the Watermark output resistance (kΩ) at 24 ºC using four calibration equations*

Nonetheless, this study chose the Shock *et al.* (1998) equation which is also used in many Watermark digital meters and dataloggers (Chard, 2002; Johnstone *et al.*, 2005). Moreover, the manufacturer of the Watermark 200SS sensor uses this equation as a default calibration (Thompson *et al.*, 2006).

4.2.2 Positioning Sensors in the Field

Sensor positioning in the root zone of the plant is crucial, because it determines the amount of water to be applied during each irrigation event. A sensor placed very deep into the soil allows the irrigation system to apply more water up to that depth beyond plant roots; the water below plant roots is lost through deep percolation. On the other hand, a very shallow sensor promotes light irrigation with a consequence of the system failing to apply water into the root zone, and plants may therefore be stressed.

Maize is a deep rooted crop with approximate maximum rooting depth ranging from

75 cm to 120 cm (Texas Water Development Board, 2004) depending on the characteristics of the soils like presence of restrictive soil layers. Fandika (2006) estimated the maximum rooting depth as 120 cm for soils in Malawi. However, according to Evans *et al.* (1996) and Morris (2006), 70% of soil-water uptake activity by roots is within the top half of the rooting depth (above 60 cm for maize crop) where most of the roots are located (refer to Fig. 4.4). This means that water will be lost to deep percolation if the bottom half of the rooting depth is filled to FC. As such this study considered a depth of 60 cm as an effective root zone for maize.

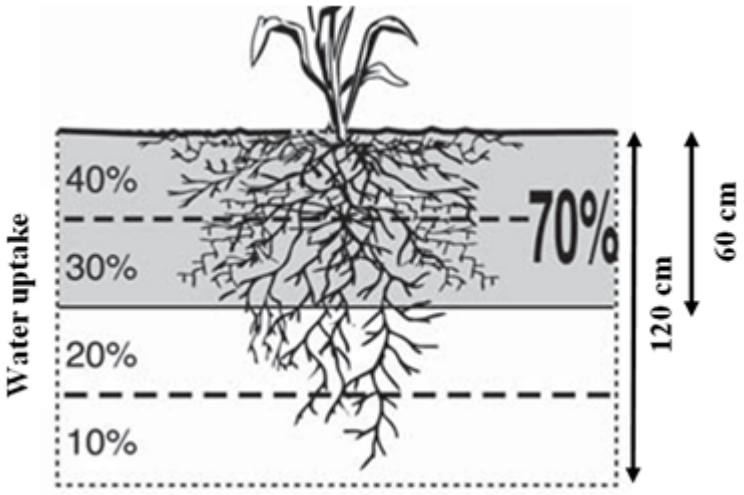

Fig. 4.4: *Effective root zone for maize adapted from Morris (2006)*

However, the effective root zone discussed above is for a fully grown maize crop. Crop roots are shallow during early growth stages and grow deeper with the growth stage. In North Carolina, Evans *et al.* (1996) showed how the stage of crop development influences the effective root depth of a maize plant. Their results (refer to Fig. 4.5) show that the maximum root depth for maize in North Carolina is 60 cm, and hence the effective root depth for a fully grown plant (about 70 days after planting) is 30 cm. Evans *et al.* (1996) further observed that irrigation scheduling should be based on the effective root depth rather than the maximum root depth.

Considering the variability of the water uptake activity in the root zone it is prudent to vary the position of the sensors with the growth stage of maize plants. However, this is not practical and may damage plant roots during subsequent sensor installations in the field. Alternatively, many sensors may be placed at different depths in the root zone.

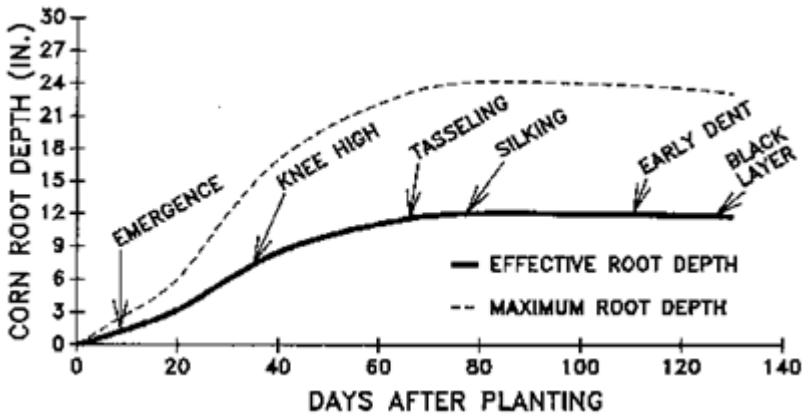

Fig. 4.5: *Maize rooting depth in North Carolina at various growth stages (Evans* et al.*, 1996)*

According to Alam and Rogers (2001) three-sensor stations are common with the third sensor placed between the upper and the lower sensors. The upper sensor is used when crops are at their early growth stage. Nevertheless, this approach is obviously expensive.

Therefore, this study opted for a two-sensor scenario - upper and lower positions. Alam and Rogers (2001) recommended placing a shallow sensor at a depth between 1/4 and 1/3 and a deep sensor at a depth between 2/3 and 3/4 of the effective root zone. This means that for the effective root zone of 60 cm which this research adopted, 15 – 20 cm and 40 – 45 cm are the respective optimum positions for shallow and deep sensors for maize. Accordingly, the depths that were preferred were 20 cm and 40 cm for shallow and deep sensors, respectively.

The ideal case was to use the upper sensor during the early growth stages and progressively adjust the role of the upper and lower sensors with the growth until when the lower sensor only is used. This was possible at software level of the controller. However, the agriculture board failed to provide connections to two or more Watermark sensors despite having three ports for the same. Although the board allows reading from one of the three sensors at a time, it has a single power switch to all the Watermark sensors. In this case sensors were interfering with each other and, hence, producing false readings. Although two sensors were installed, the shallow sensor was used during early growth stages (41 days) while the deep sensor was used afterwards.

Finally, it was of great importance to install sensors at appropriate locations to take into account the variability of spatial distribution of water in the field. While it is judicious to place sensors in the mostly dry locations of the field to avoid stressing crops in those areas, caution should also be exercised to avoid over-irrigation of the other parts of the field. Consequently, based on the topography, it may be necessary to divide a large field into smaller zones which must be levelled irrigated independently. This study used drip irrigation system and as shown in Fig. 4.6 one sensor was located almost at the center of the field and the other almost at the edge of the field in each of the two zones.

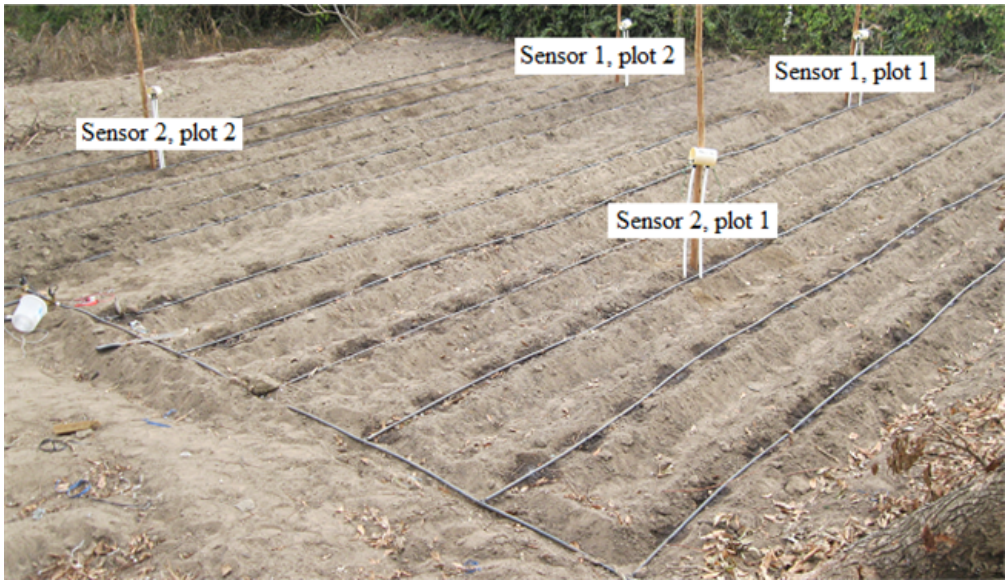

Fig. 4.6: *Sensor positions in two plots*

4.2.3 Installing Sensors in the Field

Sensor installation is another aspect upon which the effectiveness of an irrigation system depends. Poorly installed sensors will result in false readings and hence wrong scheduling of irrigation event. Therefore, it is very important to follow all fundamental procedures when installing sensors in the field.

For ease of installation of the Watermark sensor into the soil it is recommended (Spectrum Technologies, Inc., n.d.; Irmak *et al.*, 2006; IRROMETER Company, Inc., 2010) to use a 12.7 mm (1/2 inch), Class 2172 kPa, thin wall PVC pipe. This will give a good

snug fit of the sensor on its collar and will allow the sensor to be pushed easily into an access hole during installation (Irmak *et al.*, 2006). Two different lengths of PVC pipes were used in this set-up to allow sensors to be installed at different depths. The shallow sensor which was installed at 20 cm depth required a 80 cm pipe so that the sensor board could be placed at a height of 60 cm from the ground. On the other hand, a 100 cm pipe was used for a deep sensor (at 40 cm depth) for the same height of the sensor board. In order to have a good wireless link with a good Fresnel zone, radio transceivers must be raised as high as possible from the ground. However, the 60 cm height of the sensor board was chosen due to the limitation of the sensor cable which was 150 cm. A sensor depth of 40 cm means that a total of 100 cm cable length was used. This gave a 50 cm clearance cable length for ease of connecting to the processing board inside the housing.

Fig. 4.7 shows Watermark sensors fitted to PVC pipes. A 0.3 cm (1/8 inch) diameter hole was made in the PVC pipe and aligned with the sensor's slot as shown in Fig. 4.7. The hole permits the pipe to exchange the air with the soil. Along the PVC pipe near the Watermark sensor a hole was also made where a temperature sensor cable was slipped in to the other end of the pipe (refer to Fig. 4.7). The other end of the PVC pipe was inserted into a sensor board housing made of a 23 cm PVC pipe. At this end a 1.9 cm drip tubing was used as a connector of the PVC pipe and the housing. This connector was folded back over itself inside the housing (refer to Fig. 4.8). The folding of the drip tubing for the connector was carefully done to avoid damaging sensor cables coming from the other end of the PVC pipe.

After attaching sensors to the PVC pipes it was important to precondition them by following wet-dry cycles. Sensors were soaked in irrigation water (refer to Fig. 4.7) for 1 hour then air dried for 24 hours. Three wet-dry cycles were conducted before installing sensors. In addition, sensors were soaked in water for 24 hours just before installation. The wet-dry process is necessary in order to remove air from sensors (Irmak *et al.*, 2006) which, consequently, improves the response of sensors during the first few irrigation events (Spectrum Technologies, Inc., n.d.).

After selecting appropriate sensor stations in the field two access holes per station were

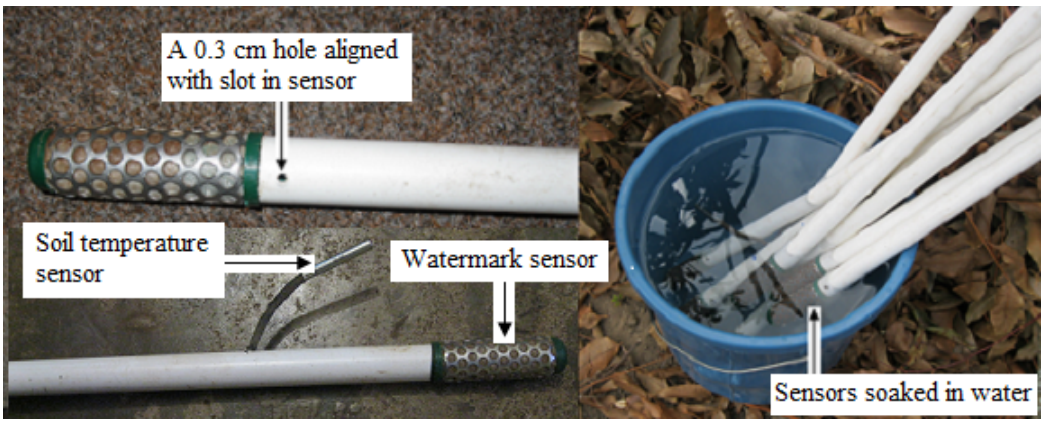

Fig. 4.7: *Watermark and soil temperature sensors fitted to PVC pipes and soaked in irrigation water*

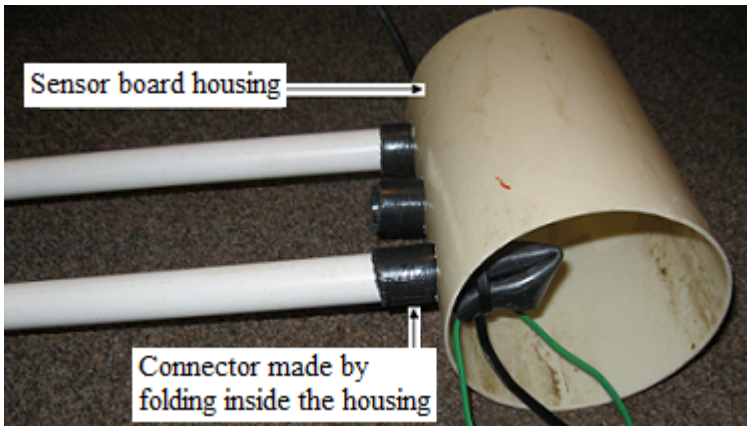

Fig. 4.8: *Sensor PVC pipes attached to a sensor board housing*

drilled. The depths of access holes were 23 cm and 43 cm in depth so as to position the centers of sensors at 20 cm and 40 cm depths, respectively. A 2.54 cm PVC pipe reinforced by a metal rod was used to drill these holes. Although a smaller access hole (2.22 cm) gives a good contact between the sensor and the soil, it was necessary to make a slightly bigger hole than the diameter of the sensor so as not to damage sensor membrane through abrasion when pushing the sensor down. Therefore, to permit good contact the hole was half-filled with water, sensor slipped in, then the access hole was backfilled using a rough slurry made from the same soil sample (see Fig. 4.9). This process also removes any air pockets from the hole.

Finally, sensor acclimatization was necessary before the intelligent irrigation management system could commence. After the installation of sensors a full manual irrigation event was conducted and maize planted. The irrigation controller was connected on

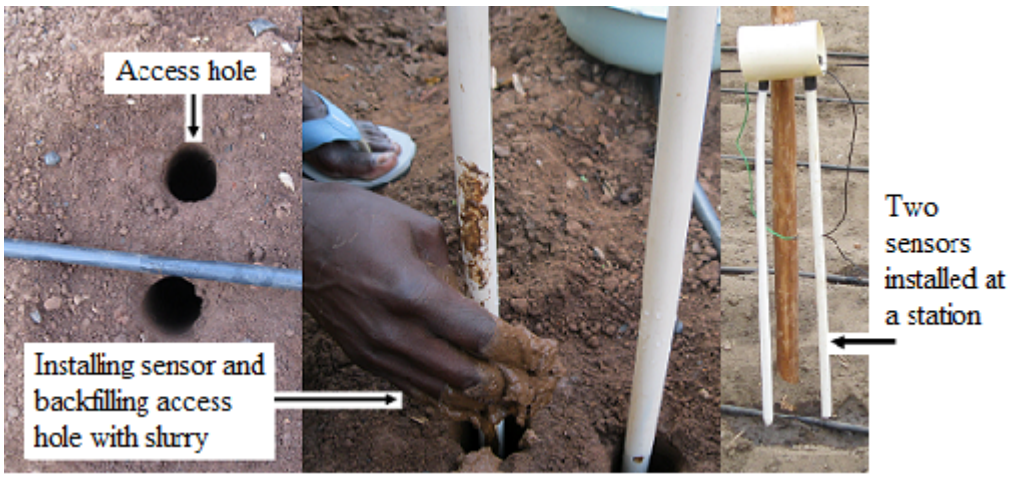

Fig. 4.9: *Installation of sensors in the field*

the fifth day when the irrigation water and that applied in the sensor hole during installation had diffused and established equilibrium. The sensor acclimatization process allowed the system to capture a true moisture representation of the field and not just around the sensor.

4.3 Establishing Soil Water Characteristics

Soil is a physical composition of four major parts: soil particles; organic matter; air spaces and living organisms. There are various textural classes of soils depending on the size of particles. The major classes are clay, silt and sand. Clay particles are smallest with a diameter of less than 0.002 mm; while silt particles are relatively larger (0.002–0.05 mm) than clay particles; sand particles are the largest with a diameter of 0.05–2.0 mm. The percentage composition of these major particles yields other soil textural classes which include loamy sand, loam, sandy loam, clay loam, silty clay loam, silty clay, sandy clay, and sandy clay loam. The percentage composition of each of these soil textures can be read from a triangle as shown in Fig. 4.10. For example, a soil with 10% clay, 30% silt and 60% sand is classified as sandy loam.

A specialized equipment in the soil testing laboratory is required for determination of soil texture under study. Although the accuracy of this method is high, it is expensive.

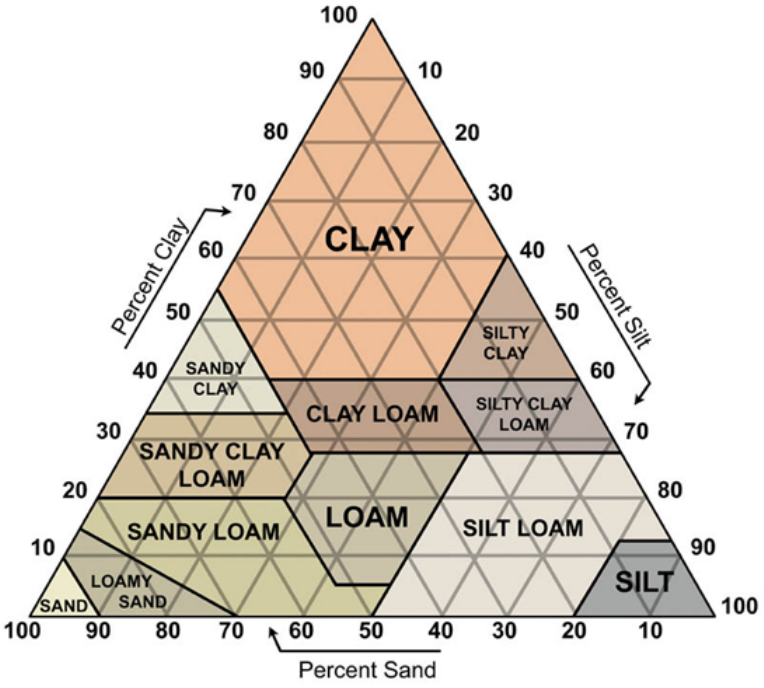

Fig. 4.10: *Soil textural classes based on the percentage of sand, silt, and clay (Bellingham, 2009)*

This study used a very simple but relatively accurate method to establish soil textural composition as outlined below.

(a) Four soil samples were taken from two stations in the field. At each station two samples were taken with the first from the top 20 cm and the other from within the next 20 cm. These depths were according to the sensor placement of 20 cm and 40 cm as discussed in subsection 4.2.2

(b) The soil samples were thoroughly air dried and lumps crushed, and then sifted using a wire-mesh sieve to remove small rocks, roots and trash.

(c) Each of the four soil samples was placed into a straight-sided transparent bottle up to 1/3 of the straight part.

(d) A tablespoonful of powered dishwasher detergent was added to each bottle. This helps in separating soil particles.

(e) The bottles were then filled to 3/4 of the straight part with water, and the top of the bottles were tightly covered by a hard plastic paper and a rubber band.

(f) Each bottle was vigorously shaken for 15 minutes so as to combine the soil, detergent, and water thoroughly. The shaking also helps in crushing and hence separating soil particles as well as ensuring that no soil is stuck to the sides or bottom of the bottle.

(g) The bottles were set on a flat table for sedimentation to take place. The separated soil particles settle down according to their sizes - larger particles settle faster than smaller particles. In this case sand particles will settle faster (1-2 minutes) followed by silt (2 hours) then clay will settle afterwards (2 or more days or when the water clears). Fig. 4.11 shows how the experiment was set-up.

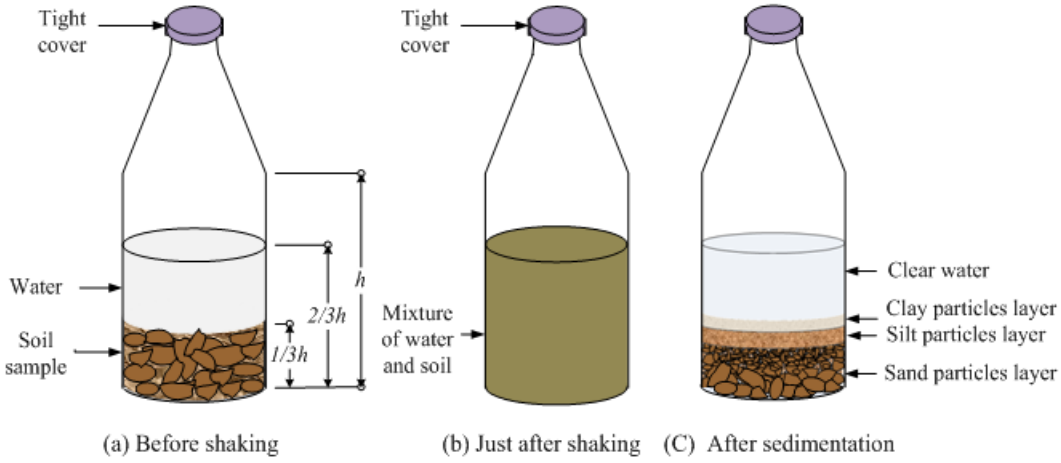

Fig. 4.11: *Experimental set-up for determining soil textural composition*

(h) At the stated time intervals in (vii) thickness measurements (in mm) were taken and table 4.1 shows the results for all the four soil samples. The table also shows the percentage composition of the three major soil textures.

(i) After computing the percentage composition of the soil samples reference was made to Fig. 4.10 to establish the soil textures in the field. Samples 1 and 3 were found to be loamy sand while samples 2 and 4 were sandy loam.

These results show that the top 20 cm soil layer was predominated by loamy sand while the 20 cm - 40 cm layer was dominated by sandy loam. Overall, the soil under the study was a mixture of the two stated soil textures.

Table 4.1: *Soil textural composition experimental results*

Soil Texture	Station 1				Station 2			
	Sample1 (20 cm depth)		**Sample 2** (40 cm depth)		**Sample 3** (20 cm depth)		**Sample 4** (40 cm depth)	
	Thickness		Thickness		Thickness		Thickness	
	(mm)	(%)	(mm)	(%)	(mm)	(%)	(mm)	(%)
Sand	24.8	80	25.1	76	28.4	79	23.1	68
Silt	3.7	12	4.6	14	6.1	17	6.8	20
Clay	2.5	8	3.3	10	1.5	4	4.1	12
Total soil thickness	31	100	33	100	36	100	34	100

The water-holding capacity for the soil structure in this field was established by referring to Fig. 4.12 in which soil textural classes are related to hydrological thresholds. According to this figure the soil that is somewhat between loamy sand and sandy loam has a FC of 0.2 water fraction by volume (wfv), PWP of about 0.07 wfv, a 50% MAD of 0.14 wfv and ASW of 0.13 wfv. These threshold levels can also be expressed as percentages by volume/weight/depth as 20%, 7%, 14% and 13%, respectively.

Using these threshold levels the following equation is derived to relate Percentage Soil Water Content (PSWC) and MAD (expressed as a fraction):

$$PSWC = 100(0.2 - 0.13MAD) \tag{4.5}$$

Since MAD can range from 0 (i.e. when the soil is at FC) to 1 (i.e. the soil is at PWP), then using equation 4.5 means that PSWC can indeed range from 20% to 7% for this particular soil type.

4.4 Calibrating Sensors for Soil-Specific and Environmental Conditions

Section 2.6 discussed two forms of measurements for soil water as water content and water potential. The water content measure gives the actual amount of water that is present in the soil. However, crop roots must exert a force in order to extract that

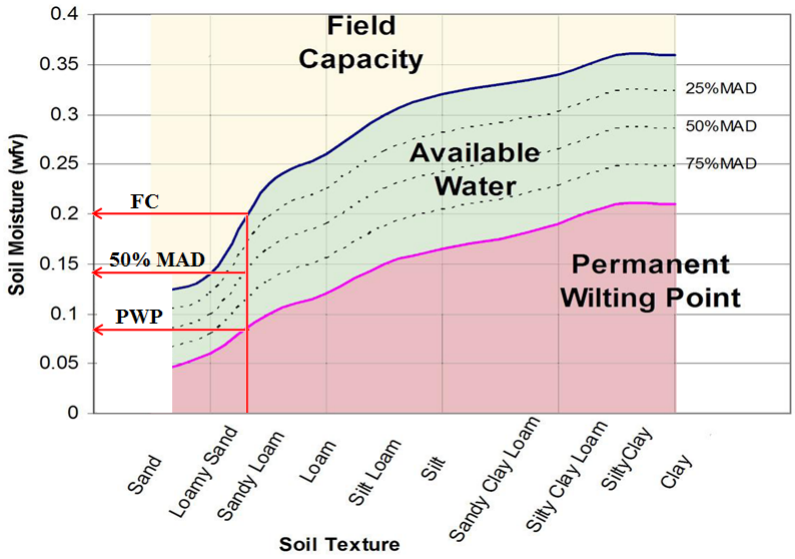

Fig. 4.12: *Water holding capacities of various soil textural classes modified from Bellingham (2009)*

water. As previously discussed, this force is known as SMP. Soil moisture sensors used in this study were based on SMP which is the important parameter to monitor as it indicates how hard it is for plant roots to absorb water from the soil.

The irrigation system however has to know how much water (by volume) is needed in order to satisfy the crop water needs. It is therefore important to convert SMP as read by sensors in the soil to water content required from the water source. Specific soil characteristic curves are used to relate SMP to water content. In order to establish such curves, a soil-specific sensor calibration experiment must be conducted. This will also take into account the environmental condition of the area under study through soil temperature measurements. The procedure was as discussed below.

(a) Four soil samples were taken from two stations in the field. At each station two samples were taken with the first from the top 20 cm and the other from within the next 20 cm. This is also where the four samples in the previous experiment (section 4.3) were taken.

(b) Four-five litre tins were opened at both ends and the bottom end was tightly covered by a piece of cloth that could allow easy flow of water (a piece of hessian sack can be a good material for this exercise). The combined weight of the

covering cloth, tin, Watermark sensor and soil temperature sensor was recorded as *"tare"*.

(c) Each tin was half-filled with dry soil in which Watermark and soil temperature sensors were buried. The tins were then soaked in water for 2 hours so that the soil is completely saturated with water.

(d) The tins were then placed on a wire mesh which was suspended in the air at a height of 30 cm from the ground to allow dripping of water. The tins were left in this arrangement until when gravitational drainage ceased.

(e) The weight of each tin and its contents was recorded every day at 7:00 AM. This weight was recorded as *(wet soil + tare)*. At the same time SMP was read using Waspmote node which was connected to the sensors buried in the soil sample.

(f) After 15 days of recording, when the soil was very dry, sensors were carefully removed from the soil sample.

(g) The soil samples were placed in metallic pots which were put into an oven. The soil dried for 24 hours at 110 ºC.

(h) The dry soil and sensors were put back into the original tins and the weight was recorded as *(dry soil + tare)*.

(i) The PSWC was computed using the following formula:

$$PSWC = 100\frac{(wet\ soil + tare) - (dry\ soil + tare)}{(dry\ soil + tare) - tare} \tag{4.6}$$

Table 4.2 presents the results for the sensor calibration discussed above. The table also shows how PSWC is related to SMP.

Fig 4.13 shows graphs that relate PSWC to SMP. Regressed functions for all the experiments are also shown.

The following equation expresses SMP (kPa) as a function of PSWC (%) and was developed by regressing the average results of all the four calibration experiments as

Table 4.2: *Sensor calibration results - showing how percentage water content is related to soil moisture potential*

Experiment 1 ($tare = 325g$; $dry soil + tare = 3775g$)			**Experiment 2** ($tare = 400g$; $dry soil + tare = 3725g$)			**Experiment 3** ($tare = 400g$; $dry soil + tare = 3750g$)			**Experiment 4** ($tare = 340g$; $dry soil + tare = 3790g$)		
wet soil + tare (g)	*water content (%)*	*SMP (kPa)*	*wet soil + tare (g)*	*water content (%)*	*SMP (kPa)*	*wet soil + tare (g)*	*water content (%)*	*SMP (kPa)*	*wet soil + tare (g)*	*water content (%)*	*SMP (kPa)*
4825	30.4	-8.5	4985	37.9	-8.3	4825	32.1	-10.2	4865	31.2	-9.9
4800	29.7	-8.7	4870	34.4	-8.6	4809	31.6	-10.9	4645	24.8	-11.8
4713	27.2	-9.1	4770	31.4	-9.3	4525	32.1	-14.5	4520	21.2	-14.4
4563	22.8	-11.5	4510	23.6	-11.0	4363	18.3	-20.7	4465	19.6	-18.7
4450	19.6	-12.2	4413	20.7	-15.5	4293	16.2	-21.7	4415	18.1	-23.0
4413	18.5	-13.1	4388	19.9	-15.7	4275	15.7	-23.9	4328	15.6	-29.7
4375	17.4	-14.8	4350	18.8	-17.2	4240	14.6	-26.6	4215	12.3	-34.0
4355	16.8	-14.9	4290	17.0	-19.8	4225	14.2	-27.1	4165	10.9	-37.1
4300	15.2	-19.4	4250	15.8	-20.8	4213	13.8	-36.0	4153	10.5	-40.7
4275	14.5	-21.7	4188	13.9	-25.9	4190	13.1	-39.4	4115	9.4	-56.9
4215	12.8	-23.8	4090	11.0	-29.9	4138	11.6	-45.1	4100	9.0	-59.1
4150	10.9	-31.6	3990	8.0	-39.5	4075	9.7	-55.2	3990	5.8	-86.1
4063	8.3	-42.9	3920	5.9	-50.3	3950	6.0	-68.6	3932	4.1	-95.4
3950	5.1	-61.1	3851	3.8	-63.6	3850	3.0	-88.4	3920	3.8	-99.6
3835	1.7	-90.3	3750	0.8	-84.8	3837	2.6	-97.8	3904	3.3	-106.1

depicted in Fig. 4.14:

$$SMP = -106.1916 * 0.911645^{PSWC} \tag{4.7}$$

Alternatively, PSWC can be expressed in terms of SMP by the following equation:

$$PSWC = 50.43 - 10.81 ln|SMP| \tag{4.8}$$

Substituting equation 4.5 into equation 4.7 yields an equation which expresses SMP in terms of MAD as follows:

$$SMP = -106.1916 * 0.911645^{100(0.2-0.13MAD)} \tag{4.9}$$

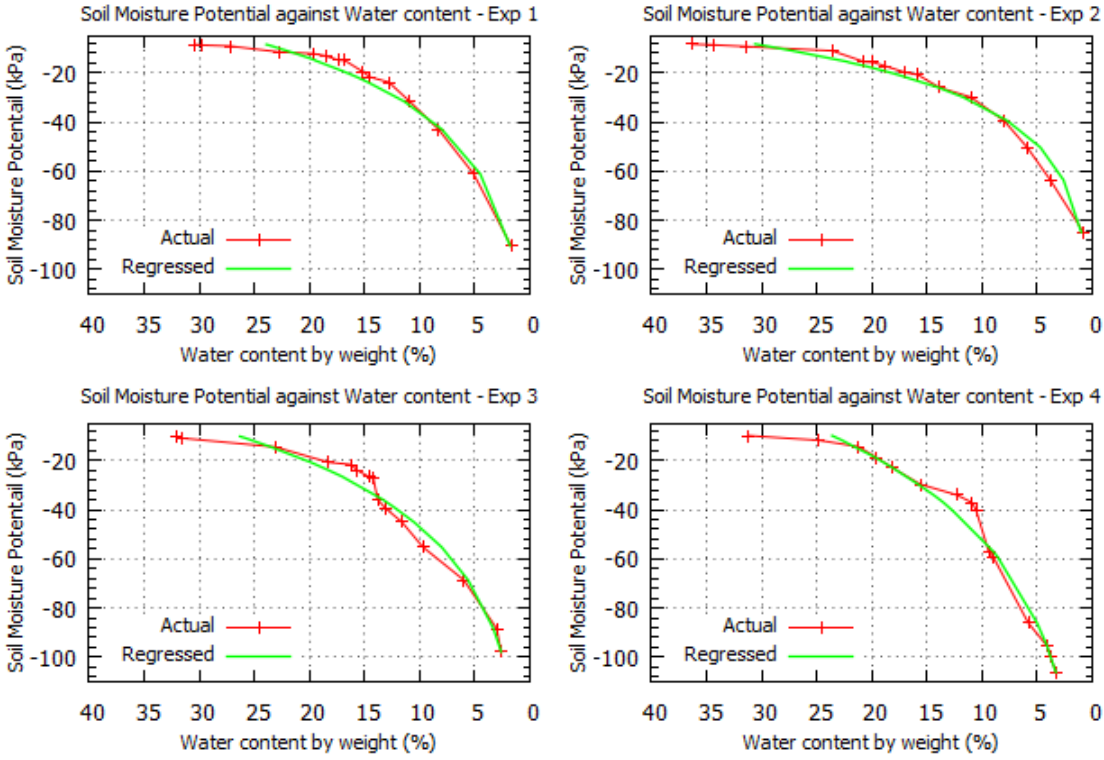

Fig. 4.13: *Sensor calibration results - showing how percentage water content is related to soil moisture potential*

This equation is used in irrigation scheduling as discussed in section 4.5. For example, if the moisture is to be maintained within a MAD of 0 (soil is at FC) to 50% then using equation 4.9 we see that SMP should range from -16.7 kPa to -30.46 kPa.

4.5 Irrigation Scheduling Strategy

Irrigation scheduling basically sets two threshold levels within which soil moisture must be maintained. These levels can be static or dynamic depending on the requirement.

Since the objective of this study was to investigate the effect of dynamic threshold levels on the amount of water used in the irrigation and on crop yield, then there was a need to adopt both strategies in order to compare their results. As stated in section 3.1 CT was irrigated based on static preset threshold levels. In order to avoid over-irrigation as a result of late termination of the irrigation event due to the slow flow of

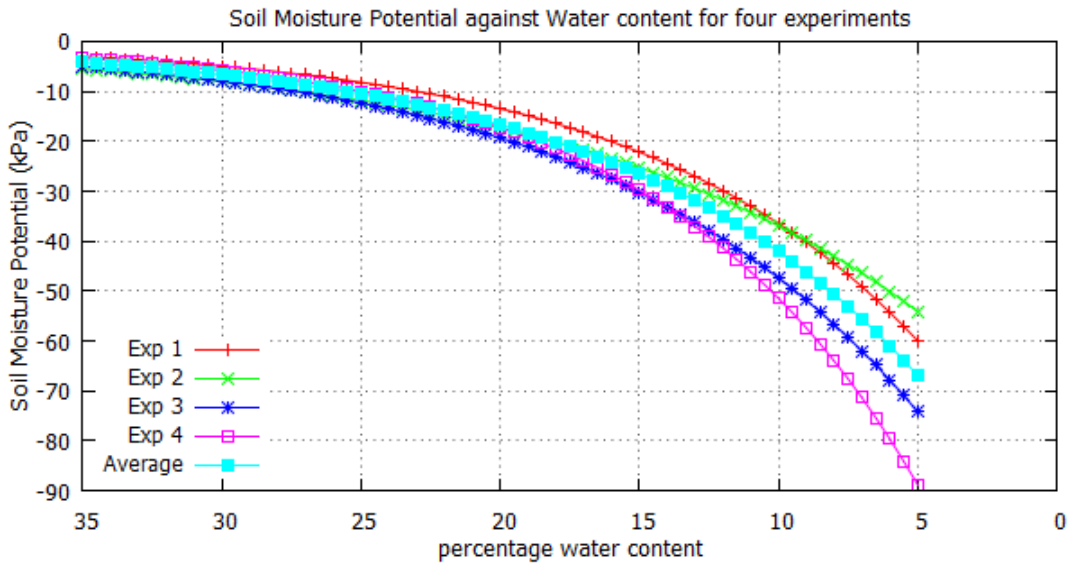

Fig. 4.14: *The relationship between the percentage water content and soil moisture potential derived from four experimental results*

water in the soil, this study used an upper threshold of 10% MAD. This allowed the controller to terminate the irrigation at 90% FC. Using equation 4.9 a MAD of 10% translates into a SMP of -18.83 kPa. In this treatment irrigation was initiated when the moisture dropped to a MAD of 50% (i.e. when ASW was 50%). This gives a lower threshold level of -30.46 kPa. These threshold levels are shown graphically as "CT threshold" in Fig. 4.15 which is a plot of equation 4.9. For this treatment soil moisture was kept within these threshold levels throughout the growing period of the maize crop.

On the other hand, the advanced controller which was deployed in the ExT was based on variable threshold levels to mimic the crop coefficient pattern of the water requirements by the maize crop. During the initial development stage of the maize crop, the upper threshold was set at 40% MAD (refer to Fig. 4.15) and was allowed to increase to 10% MAD at the middle stage (during tussling and cob formation). Thereafter the upper threshold was again lowered to 40% MAD. Similarly, the lower moisture threshold was initially set at 70% MAD (refer to Fig. 4.15) and was increased to 50% MAD, then lowered again to 70% MAD. The lower thresholds were opted for as a way of applying deficit irrigation during the early stages when crop water needs are low. A little stress to the maize crop during early stages can be beneficial as it encourages the

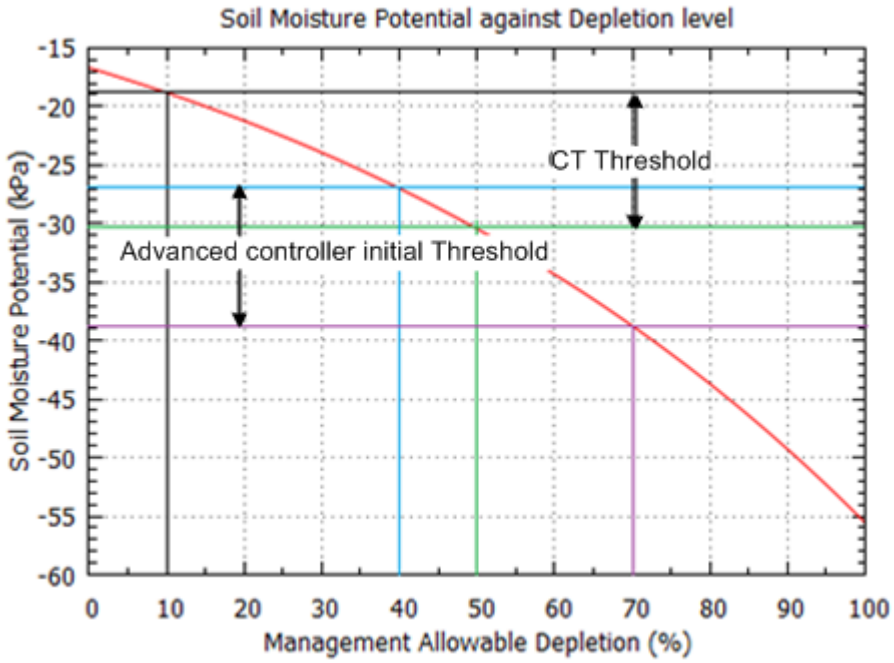

Fig. 4.15: *The relationship between Soil Moisture Potential and Management Allowable Depletion*

crop roots to go deeper and hence use water at that depth which otherwise could be lost through deep percolation.

For the advanced controller the following equations were developed to allow the upper and lower threshold levels vary with the crop growth stage:

$$SMP_{LT} = -0.0000755d^3 + 0.008773d^2 - 0.0892577d - 41.488 \tag{4.10}$$

$$SMP_{UT} = -0.0000700d^3 + 0.008129d^2 - 0.0827045d - 28.692 \tag{4.11}$$

where d is the number of days elapsed when about 10% of maize germinates, SMP_{LT} is the lower moisture threshold level (kPa) used to initiate irrigation, and SMP_{UP} is the upper moisture threshold level (kPa) used to terminate irrigation.

The threshold levels are shown graphically in Fig. 4.16 and are based on a maize crop with a maturity period of 100 days. The figure also shows constant threshold levels used in CT.

Since controllers terminate irrigation only when the upper moisture threshold is sensed,

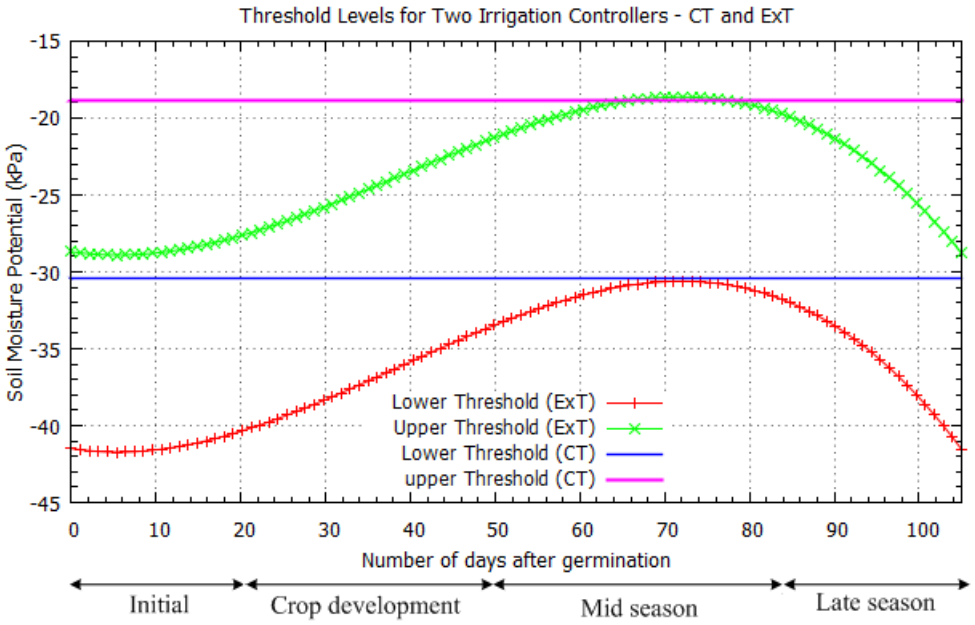

Fig. 4.16: *Soil Moisture threshold levels for two irrigation controllers - the control treatment and the experimental treatment*

then they may over-irrigate because they detect the threshold after a long time due to slow movement of water in the soil. In order to avoid this kind of phenomenon both treatments adopted an adaptive irrigation scheduling strategy - the *water-budget.* In this strategy the controller estimates the amount of water to be applied in order to bring the current moisture level to the upper threshold. Based on the water flow rate and application efficiency of the irrigation system, the controller computes the *irrigation duration*. When this duration elapses the system pauses for a predetermined time called *blackout time*. The blackout time is necessary to allow the applied water to infiltrate into the soil. After the blackout time the controller measures the level of moisture to check whether the correct amount of water was applied or not. Based on this analysis, the irrigation controller adjusts the water application efficiency and irrigates again if the level is less than the upper threshold. After a few irrigation events, it is expected that the controller will determine the correct efficiency of its irrigation system and eventually precise irrigation duration will ensue. The flowchart shown in Fig. 4.17 summarizes the water-budget scheduling strategy which was implemented in the study.

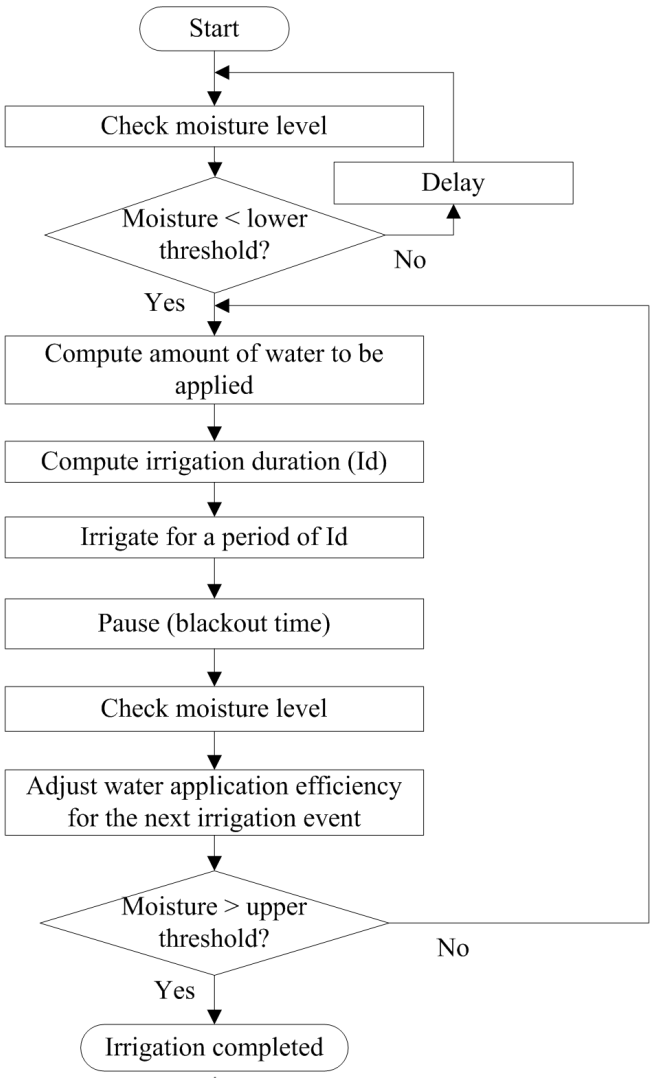

Fig. 4.17: *Flow chart for an adaptive irrigation controller based on water-budget scheduling strategy*

The amount of water to be applied is computed by using the following formula:

$$w_{ap} = \frac{(w_u - w_c)}{100} S_d A_f \tag{4.12}$$

where w_{ap} is the total amount of water (m^3) to be applied, w_u and w_c are respectively the upper threshold and current moisture levels as percentage water content, S_d is the sensor depth (m), and A_f is the area of the field (m^2). Note that w_u and w_c are evaluated from SMP by employing equation 4.8.

Water application efficiency accounts for the losses in the system as a result of evaporation, runoff, wind, and leakage in the pipes. It is the percentage of total amount of

water drawn from the source that is successfully delivered into the soil and is available to plants. Its value depends on the type of irrigation system employed. For example the efficiency of a sprinkler system is around 75% while that of a drip system is about 90%. Therefore, taking into account the efficiency of the irrigation system, the controller must compute the actual amount of water that it must draw from the supply.

However, the application efficiency may vary with time. As such, the adaptive irrigation controller proposed in this study was designed to compute the efficiency for each irrigation event. After the blackout time the controller compares, through sensor measurements, the estimated amount of water with the actual amount which has been applied. This information is then used to adjust the efficiency.

In order to evaluate irrigation duration the controller must know the water flow rate of the irrigation system. In this study, the flow rate was estimated by measuring the level of water in the tank before and after a timed irrigation event and a value of 0.69108 $m^3/hour$ was established. Flow rate can also be measured using flow meters which unfortunately attract an extra cost.

Once the flow rate, application efficiency and amount of water to be applied have been estimated the controller computes the irrigation duration by using the following formula:

$$T_i = \frac{w_{ap}}{A_e Q} \tag{4.13}$$

where T_i is the irrigation duration (minutes), w_{ap} is the estimated amount of water (m^3) to be applied as computed from equation 4.12, A_e is the application efficiency, and Q is the flow rate (m^3/minute).

For example, if the current level of moisture as measured by a 0.4 m deep sensor is at 13% and is required to be raised to a full capacity of 20% by an irrigation system whose flow rate and efficiency are 0.69108 $m^3/hour$ and 90%, respectively, then the controller will prompt the irrigation system installed in a 48.4 m^2 field to irrigate for *131 minutes*. This can be computed in two steps as follows:

Firstly, estimate the amount of water to be applied by using equation 4.12

$$w_{ap} = \frac{(20-13)}{100} * 0.4 * 48.4 = 1.355 m^3$$

Then, compute the irrigation duration using equation 4.13 as follows:

$$T_i = \frac{1.355}{0.9 * 0.69108/60} = 131 minutes$$

Finally, the adaptive irrigation scheduling discussed in this section requires evaluation of blackout time. This is the time during which irrigation is paused to allow the applied water to diffuse into the root zone on the plant. As shown in equation 4.14, the blackout time is directly proportional to the depth of the sensor and inversely proportional to the water infiltration rate of the soil; the proportionality constant being one.

$$T_b = \frac{S_d}{R_i} \tag{4.14}$$

where T_b is the blackout time (hours), S_d is the sensor depth (mm), and R_i is the infiltration rate (mm/hour).

The infiltration rate for the soil under study was experimentally evaluated as follows:

(a) A metal ring (380 mm tall, 150 mm diameter) was gently and evenly driven into the soil using a wooded hammer to a depth of 257 mm - leaving 123 mm above ground.

(b) A sheet of plastic paper was placed in the ring so as not to disturb the soil sample when pouring water.

(c) Water was then poured into the ring and the level recorded.

(d) A count down timer was started immediately the plastic paper was removed from the ring.

(e) At the expiry of a count down timer the level of water in the ring was recorded.

(f) The ring was then refilled with water to a new level and a count down timer restarted immediately.

(g) Steps (e) and (f) were repeated until the same level of water drop was recorded in two or more consecutive measurements.

Two such experiments were conducted at two locations in the field and the results are presented in table 4.3.

Table 4.3: *Infiltration rate - experimental results*

Time difference (min)	Cumulative time (min)	**Experiment 1**					**Experiment 2**					**Average infiltration rate**
		Water level reading (mm)		Infiltration (mm)	Infiltration rate		Water level reading (mm)		Infiltration (mm)	Infiltration rate		
		After filling	Before filling		mm/min	mm/hr	After filling	Before filling		mm/min	mm/hr	
start - 0	start - 0	118.0	-	-	-	-	117.8	-	-	-	-	-
5	5	117.5	70.5	47.5	9.5	570.0	115.2	73.6	44.2	8.84	530.4	550.2
5	10	118.4	106.6	10.9	2.18	130.8	114.5	105.7	9.5	1.90	114.0	122.4
10	20	117.1	109.2	9.2	0.92	55.2	115.7	103.9	10.6	1.06	63.6	59.4
10	30	117.2	110.3	6.8	0.68	40.8	116.0	107.8	7.9	0.79	47.4	44.1
10	40	116.8	111.1	6.1	0.61	36.6	116.3	109.0	7.0	0.70	42.0	39.3
10	50	117.5	110.9	5.9	0.59	35.4	115.8	110.6	5.7	0.57	34.2	34.8
20	70	118.4	105.9	11.6	0.58	34.8	118.1	104.6	11.2	0.56	33.6	**34.2***
20	90	-	106.8	11.6	0.58	34.8	-	106.9	11.2	0.56	33.6	**34.2***

***Basic infiltration rate**

The results show that the water infiltrated rapidly in the dry soil (550.2 mm/hour in the first 5 minutes), but as water replaced the pore spaces in the soil, the rate reduced until when a steady value was reached. This steady value is called the *basic infiltration rate* and is used in the calculation of blackout time. The results show that the soil under study had a basic infiltration rate of 34.2 mm/hour.

Therefore, if soil moisture sensor is placed at a depth of 0.4 m (as the case with the deep sensor in this study) then a blackout time of not less than *11.7 hours* should be observed. This was evaluated by using equation 4.14 as follows:

$$T_b = \frac{S_d}{R_i} = \frac{0.4 * 1000}{34.2} = 11.7\,hours$$

So a 12 hour blackout time was necessary.

4.6 Chapter Summary

This chapter has developed two irrigation scheduling strategies: one for the basic irrigation controller and another one for an advanced controller. In order to do this, the chapter developed the soil moisture sensing mechanism and experimentally established soil water characteristics for the site where the maize production was conducted. The chapter demonstrated how sensors were positioned and installed in the field. It further discussed how moisture sensors were experimentally calibrated in order to adapt to the soil and environmental conditions for the site. The next chapter will design the remote monitoring system which is the second part of the irrigation management system having already developed the other part (irrigation station) in chapters 3 and 4.

Chapter 5

Remote Monitoring System (RMS) Design

The IMS was divided into two parts, namely, IS and RMS which were then linked via the cellular network. While the IS was developed in chapter 3, this chapter is devoted to designing the RMS.

Balendonck *et al.* (2008) and Fazackerley and Lawrence (2009) reported that IMSs based on WSNs were efficient, cost-effective and flexible enough to adapt any environment. However, WSNs are still under developmental stage; as such, they are at times unreliable, fragile, power hungry and can easily lose communication (Balendonck *et al.*, 2008) especially when deployed in a harsh environment such as an agricultural field. It is therefore imperative to remotely monitor the status of WSN particularly when the ISs are located at a rural site where frequent physical visits may become inevitable but costly and time consuming. The RMS for IMSs helps in (1) accessing status of irrigation valves in real-time so that if, for example, the system fails to terminate irrigation, then the personnel should rush to the field and rectify the problem; (2) identifying wireless link failures between sensor nodes in the field in order to quickly fix the fault and have a more robust IMS; and (3) accessing the level of batteries for the solar powered sensor nodes to guard against total system failure in case of extended solar power absence.

Fig. 5.1 shows two architectural parts of RMS comprising the monitoring personnel and the server. The monitoring personnel receives valve status and fault alarms directly onto their mobile phone for prompt reaction to the IS. The fault alarms included low battery levels for sensor nodes and wireless communication link failures. The server is a computer equipped with a broadband dongle and was used to store and graphically display both current and historical IS data. The data stored in the server included SMP, soil temperature, battery voltage levels, valve status, sensor board temperature, and RSSI.

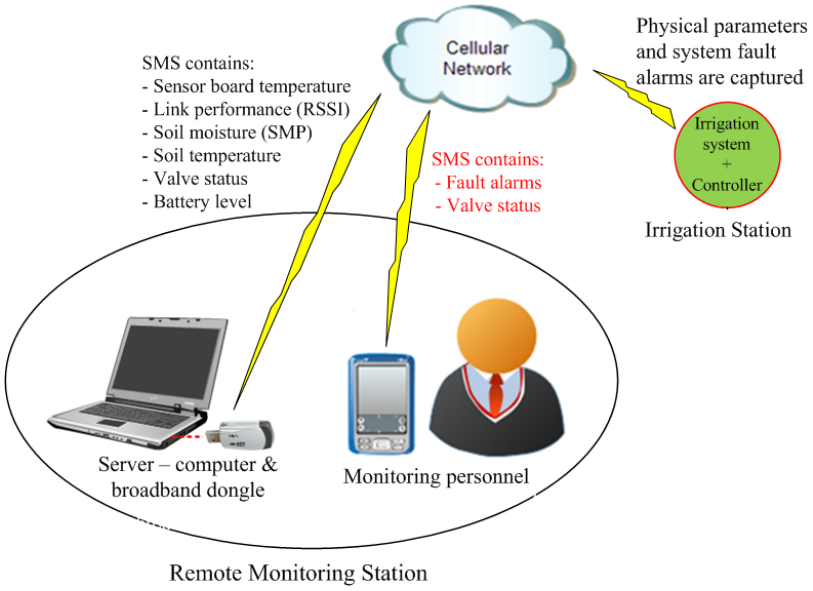

Fig. 5.1: *The architecture of the Remote Monitoring Station showing two parts and the type of information sent to each part*

Fig. 5.2 presents a conceptual model of the server depicting how data emanating from the broadband dongle was processed and analysed graphically. Firstly, the data from IS was received directly by the broadband dongle housed in the RMS. It was vital to delegate the data storing capabilities of the dongle to the first MySQL database using FrontlineSMS, a free open source software tool licensed under GNU Lesser General Public License (LGPL) . This tool enables users to connect a range of mobile devices to a computer to send and receive SMS text messages and works without an Internet connection by connecting a device such as a cell phone or GPRS modem with a local phone number. FrontlineSMS was chosen because it offers a more user-friendly front-end browser based on Java FrontlineSMS back-end. Additionally, it has functionalities

such as group forwarding, auto replying and message forwarding.

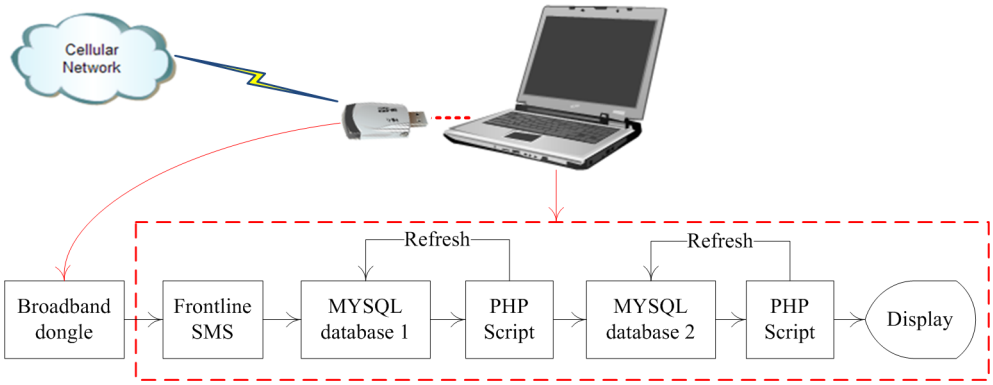

Fig. 5.2: *A conceptual model of the server for Remote Monitoring Station*

Apparently, the raw data stored in the first MySQL database, as depicted in Fig. 5.3 (a), were not in the right format and syntax for display because the coordinator node housed in the IS prepared the data to suit the SMS transmission system (with character limitation of 90). Consequently, a Hypertext Preprocessor (PHP) script was prompted to create a new database, as shown in Fig. 5.3 (b), where processed data was stored ready to be graphed and uploaded onto the Internet. A separate PHP script was then interfaced with PHPlot library to plot the data from the new database.

MySQL was installed using Windows Apache MySQL Package (WAMP) server, a Windows web development environment that allows creation of web applications with Apache2, PHP and a MySQL database. With the integration of PHP and HyperText Markup Language (HTML), dynamic pages were created and graphical analysis was easily achieved using PHPlot library. The web pages were automatically refreshed at some predetermined time intervals and each time a refresh was initiated, PHPlot library crosschecked any new data in MySQL database. The data was thus monitored in real-time and, hence, any mishap was quickly noted and acted upon.

5.1 Chapter Summary

In this chapter, an efficient, cost-effective and real-time wireless based remote monitoring mechanism has been developed for a WSN based irrigation system at a remote

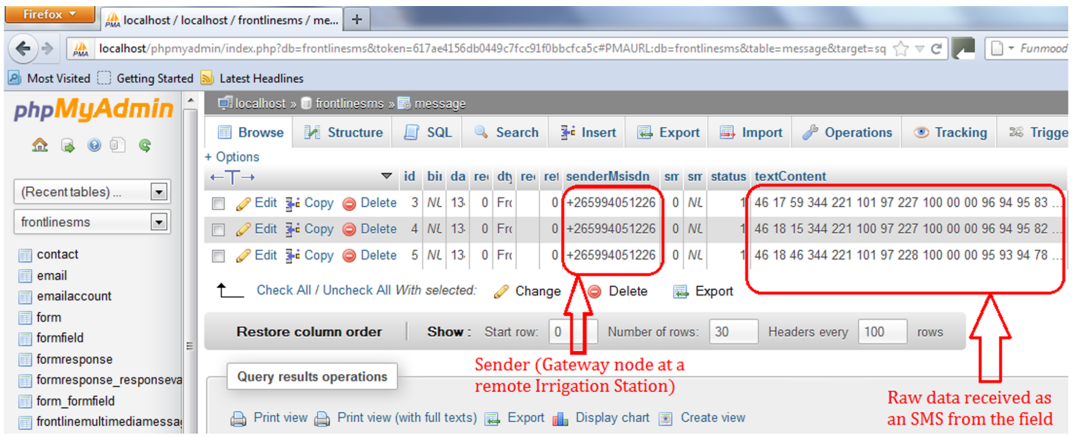

(a) Raw data in MYSQL database 1

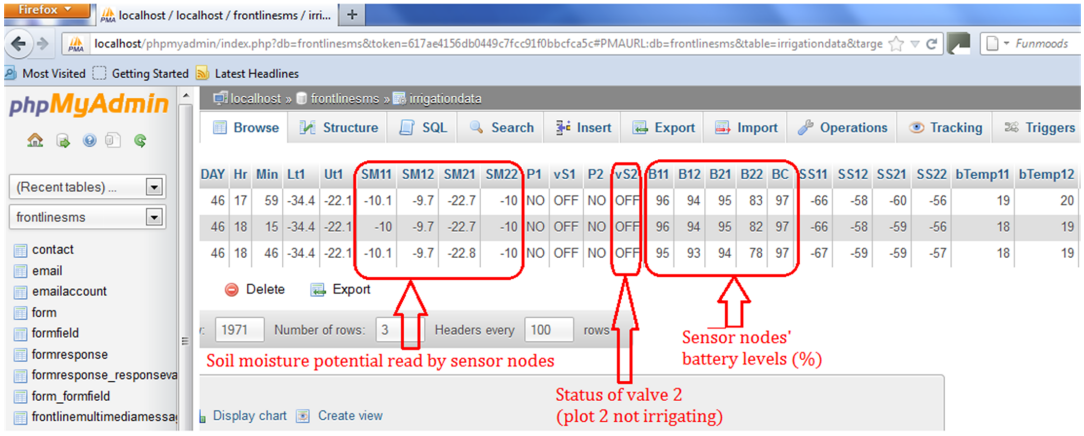

(b) Processed data in MYSQL database 2

Fig. 5.3: *Snapshots from MySQL database*

site. The chapter demonstrated how the WSN was used to archive the soil moisture potential, link performance, electrical power levels, valve statuses, and fault alarms and how this information was sent as a text message over a cellular network to a server or management personnel at a monitoring site.

The following chapter presents and discusses the results obtained from the study. Firstly, it discusses the effectiveness of the developed irrigation scheduling strategy. Secondly, it evaluates the level of water and solar PV energy used in both CT and ExT fields. Thirdly, it evaluates the water use efficiency and its impact on the level of crop yield. Finally, the chapter assesses the robustness of the deployed WSN irrigation controller.

Chapter 6

Results and Discussion

6.1 Soil Moisture Profile and Effectiveness of the Irrigation Scheduling

Fig. 6.1 shows the soil moisture profile in terms of SMP for the experimental and control fields. The results show that the crop coefficient pattern, as depicted by the threshold levels, was followed in the scheduling of irrigation events for the ExT. On the other hand, CT scheduling allowed a constant threshold level of moisture. This means that the controller was able to schedule irrigation events according to the design - constant level for CT and variable for ExT. Specifically, the controller initiated irrigation when any of the two sensors reported low moisture level. The irrigation event was considered completed only when both sensors read a moisture level to be above the upper threshold.

However, the results show that it was very difficult for the controller in both treatments to precisely terminate the irrigation event at the upper threshold. Despite the use of water budget and blackout concept in both treatments, the moisture was still rising above the upper threshold. A plausible explanation is that a smaller capacity locally available water tank was used. This tank was unable to hold enough water for an irrigation event. Furthermore, although the source of water was from a utility company

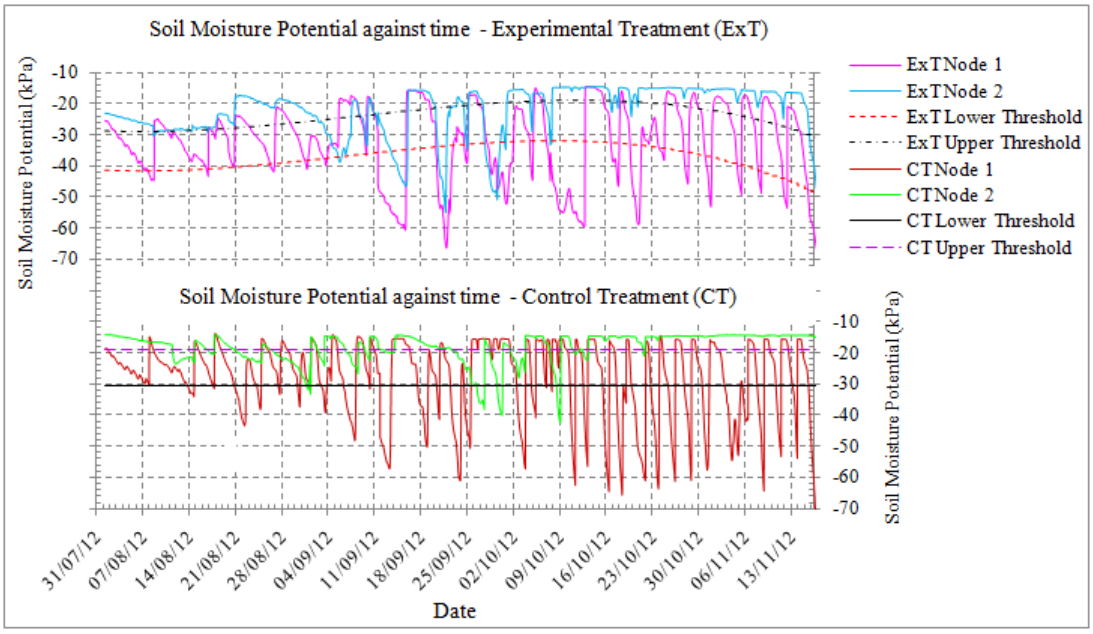

Fig. 6.1: *Soil moisture profile for experimental and control treatments*

which would, otherwise, satisfy the irrigation process since its flow rate was higher than the water application rate of the irrigation system, the supply was intermittent resulting in the controller wrongly and continuously varying its application efficiency and hence failing to safeguard both the upper and the lower thresholds.

The results further show that when a shallow sensor was being used, the controller managed to keep the lower threshold levels on check. However, when the deep sensor was employed (from 11 September 14:04:00 when more water was required in order to satisfy an irrigation event) it was really difficult for the controller to push the moisture above the lower threshold because of the tank capacity and water source challenges explained earlier.

Nonetheless, the irrigation scheduling process was generally effective since the moisture profile in the root zone of maize plants followed the desired pattern in both treatments - constant threshold for CT and variable for ExT.

6.2 Comparison of Irrigation Water and Energy Saved

In order to evaluate the effectiveness of the two treatments in terms of water and energy saving, it was imperative to estimate the total amount of water applied to both plots. This could be done by multiplying the irrigation duration by the water flow rate. However, it was erroneous to adopt this technique because the actual flow rate kept changing depending on the availability of water in the tank. As such, this task was done by recording the lowest level of moisture (before or during irrigation) and the highest level which was after an irrigation process. The difference between these two measurements was used to compute the amount of water effectively applied in the root zone of the plants.

Table 6.1 shows a sample of how the amount of water for each irrigation event for the two plots was estimated. Individual SMP readings from the two locations in each plot were first converted to PSWC using equation 4.8 before computing the average water content in each plot. Appendix F shows full results for the computation of irrigation water applied to both treatments. Plotting and regressing the cumulative water as shown in Fig. 6.2, reveals that a total of 27.1 m^3 and 42.6 m^3 of water was effectively applied to ExT and CT, respectively. Since each field was considered to be 48.4 m^2, then these readings translate to a total irrigation depth (and hence ET) of 560 mm and 880 mm for ExT and CT, respectively. Notably, these values are within a range of 500 mm to 1200 mm of total amount of irrigation water required by maize plants which was reported by Belfield and Brown (2008).

As a rule of thumb and as discussed earlier on, a drip irrigation system is approximately 90% efficient in delivering water from the source (tank) into the root zone of the plants. This means that the SPVWP system had to pump 30.1 m^3 (i.e. 27.1/0.9) of water for ExT and 47.3 m^3 (i.e. 42.6/0.9) for CT. Using these figures one would find the percentage water saved by ExT as follows:

$$percentage\ water\ saved\ by\ ExT = \frac{(water\ used\ in\ CT - water\ used\ in\ ExT)}{water\ used\ in\ CT} * 100\% \tag{6.1}$$

Table 6.1: *A sample of irrigation water computation in both Experimental and Control treatments*

(1) Date and Time of irrigation	SMP (kPa) reading from sensor node1		SMP (kPa) reading from sensor node2		Average *PSWC (%)*		(8) sensor depth (m)	(9) irrigation depth (mm) =(8)*[(7) - (6)]/100	(10) volume of water applied (m^3) = (9)*field area (i.e 48.4 m^2)	(11) Cumulative water applied (m^3)
	(2) before irrig.	(3) after irrig.	(4) before irrig.	(5) after irrig.	(6) before irrig.	(7) after irrig.				
Experimental Treatment										
01/08/12 09:45:00	-59.0	-25.5	-59.0	-23.0	6.35	15.98	200	19.25	0.93	0.93
08/08/12 19:15:00	-44.6	-25.0	-30.4	-28.8	11.45	14.87	200	6.84	0.33	1.26
16/08/12 19:00:00	-43.4	-24.6	-29.2	-23.2	11.81	16.13	200	8.62	0.42	1.68
...	...	...	...	...	...	...	...	...	...	...
12/11/12 06:33:00	-53.6	-21.0	-24.9	-16.3	11.53	18.89	400	29.42	1.42	28.15
Control Treatment										
01/08/12 09:45:00	-60.1	-18.8	-61.0	-14.2	6.07	20.23	200	28.32	1.37	1.37
08/08/12 01:45:00	-30.5	-14.8	-16.7	-16.5	16.74	20.71	200	7.95	0.38	1.76
14/08/12 19:00:00	-34.0	-16.0	-23.2	-16.0	14.38	20.46	200	12.16	0.59	2.34
...	...	...	...	...	...	...	...	...	...	...
13/11/12 18:21:00	-53.8	-15.5	-14.5	-14.4	14.44	21.20	400	27.05	1.31	43.58

That is

$$percentage\ water\ saved\ by\ ExT = \frac{(47.3 - 30.1)}{47.3} * 100\% = 36\%$$

The impact of this substantial water saving on crop yield is discussed in section 6.3.

The amount of solar PV energy required to pump a given volume of water for the designed SPVWP system based on equation 3.7 was *224.7 Wh/m^3*. This means that the SPVWP system would use *6,763 Wh* of energy to pump 30.1 m^3 of water and *10,628 Wh* to pump 47.3 m^3 of water in ExT and CT, respectively. Based on the concept used in equation 6.1, this represents a total energy saving by ExT of 36% also (each unit of water delivered equating to a unit of electrical energy expended for pumping). This means that if two equally-sized SPVWP systems are designed and implemented to serve irrigation systems that are based on the basic scheduling and the advanced

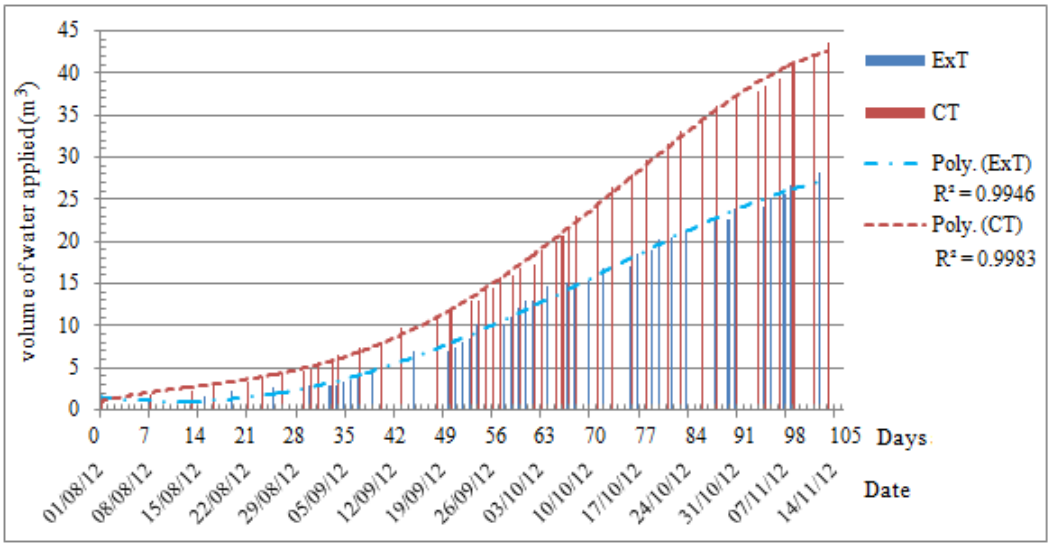

Fig. 6.2: *Cumulative water applied to Experimental and Control treatments*

scheduling strategies, the proposed advanced scheduling system would have a 36% energy saving which can be diverted to other activities such as household lighting, pumping of drinking water, and other income generating activities for instance cell phone charging and television shows. This could among other things boost the living standards of the people in the rural community. The generated income could also go a long away to sustaining the PV system. Alternatively, the capacity of the SPVWP for the advanced irrigation scheduling system could be set at a slightly lower level than that of a basic irrigation system. This could obviously lower the initial installation costs for the PV system.

Since solar PV systems are usually designed for the worst conditions, then in order to investigate the possibility of reducing the capacity of the SPVWP system, hence the cost, the peak water demand is used. In the maize irrigation system the highest water demand is generally at the middle growth stage. Notably, during this stage both treatments were set to use almost the same threshold levels when scheduling irrigation as previously presented in Fig. 4.16. Fourth order polynomial equations whose graphs are depicted in Fig. 6.2 closely represent the effective cumulative water applied to the

respective treatments at every point in time. These equations are given as follows:

$$CUW_{ExT} = -3.12952 * 10^{-7} d^4 + 2.85754 * 10^{-5} d^3 + 3.65071 * 10^{-3} d^2 - 0.0882971 d + 1.49728 \quad (6.2)$$

with $R^2 = 0.9946$; and

$$CUW_{CT} = -1.20508 * 10^{-6} d^4 + 2.14345 * 10^{-4} d^3 - 7.29688 * 10^{-3} d^2 + 0.195555 d + 1.00009 \quad (6.3)$$

with $R^2 = 0.9981$; where CUW_{ExT} and CUW_{CT} are effective cumulative water applied to ExT and CT, respectively, and d is the number of days elapsed since germination of maize plants.

For example, using these equations one would find that on day number 56 (i.e. on 26 September 2012) ExT had effectively applied 9.94 m^3 while CT had 14.86 m^3 of irrigation water applied in the root zone of the maize plants.

First derivatives of equations 6.2 and 6.3 represent effective irrigation water application rate (m^3/day) at any point in time. Fig. 6.3 shows the rate of effective irrigation water application and the corresponding water demand by maize plants in form of ET rate in both treatments. The results show that the maximum rate of water application was *0.415 m^3/day* and *0.685 m^3/day* which was on day 72 (i.e. on 12/10/2012) and 75 (i.e. on 15/10/2012) for ExT and CT, respectively. Examining Fig. 4.16 shows that these days are indeed within the middle growth stage which is between day 60 and day 84. The corresponding maximum ET rates were *8.57 mm/day* for ExT and *14.15 mm/day* for CT. These maximum ET rates are then used in the design of the SPVWP system.

Following the discussion in sections 3.4.5.4 and 3.4.5.5, in which case all other variables are kept constant but the ET rates, one would find the total PV energy required for the CT as *569.2 Wh/day* while that of ExT is *520.8 Wh/day*. These figures indicate that an SPVWP system implemented for the advanced scheduling irrigation system would save 8.5% of energy at its peak water demand. As shown in table 6.2, the sav-

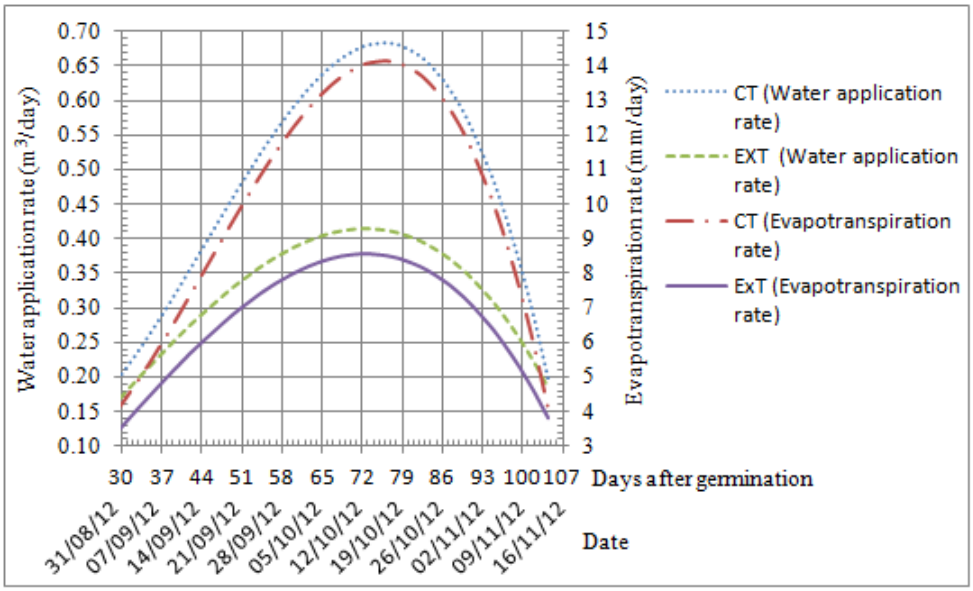

Fig. 6.3: *Effective irrigation water application rate and evapotranspiration rate in control and experimental treatments*

ing increases when the field area is increased. Specifically, doubling the field area for both treatments increases energy requirement from 569.2 Wh/day to *669.6 Wh/day* in CT and from 520.8 Wh/day to *587.8 Wh/day* for ExT. This results in an increase in energy saving by ExT from 8.5% to 12.2%. As such, in order to make a remarkable energy saving on the PV system the irrigated area should be increased. Unlike a high capacity SPVWP system which uses a basic irrigation controller that wastes water and hence energy used in water pumping, it is envisaged that the smaller capacity PV installation would be less costly and hence influence its diffusion into remote areas of the developing countries.

Table 6.2: *Solar PV Water Pumping system design procedure*

(1) Type of control strategy	(2) Total Available Water *[depth of irrigation]* (mm)	(3) Effective field area (m^2)	(4) Effective volume of water applied *[(3) * (2) / 1000]* (m^3)	(5) Volume of water to be pumped *[(4) / efficiency of drip - 90%]* (m^3)	(6) Maximum ET rate (mm/day)	(7) Irrigation Interval *[(2) / (6)]* (days)	(8) Daily water need *[(5) / (7) * cushion factor (=3)]* (m3/day)	(9) Water flow rate in borehole pipe *[(8) / (6hrs per day)]* (m3/hr)	(10) Total dynamic head *[water head]* (m)	(11) PV rating *[refer to pump performance chart - using (9) & (10)]* (Wp)	(12) Average daily PV energy required *[(11) * PGF]* (Wh/day)
Advanced	20.8	48.4	1.01	1.12	8.57	2.43	1.38	0.23	18.83	140	520.8
(ExT)	20.8	96.8	2.01	2.24	8.57	2.43	2.77	0.46	18.90	158	587.8
Basic	20.8	48.4	1.01	1.12	14.15	1.47	2.28	0.38	18.87	153	569.2
(CT)	20.8	96.8	2.01	2.24	14.15	1.47	4.56	0.76	19.04	180	669.6

6.3 Assessment of Crop Water Use Efficiency

While the first objective was to save irrigation water and hence energy used in water pumping by setting threshold levels in the ExT appropriately, the next was to evaluate the impact of applying less amount of water on crop yield. Fig. 6.4 shows the picture of the vegetating crop cover for the two treatments. Despite using equal spaces between planting stations, and ensuring that the same plant population was achieved, the crop cover in the Control Treatment was not as thick as in the Experimental Treatment. Consequently, a slightly lower crop yield was reported in the CT. Specifically, as shown in table 6.3, the grain yields obtained were 0.752 kg/m^2 and 0.812 kg/m^2 for CT and ExT, respectively. This means that the ExT improved the grain yield by 7.4%.

However, in order to assess crop water productivity, a quantitative terminology is used: crop Water Use Efficiency (WUE) . This is usually expressed as a ratio of the dry grain yield per unit land area (Y, kg/m^2) to the total amount of water used by crops per unit land area (ET, m^3/m^2, usually expressed as mm) (Ibragimov *et al.*, 2007):

$$WUE = \frac{Y}{ET} \quad kg/m^3 \tag{6.4}$$

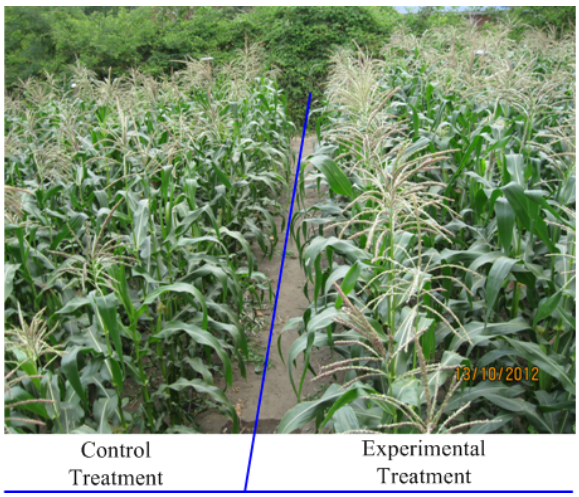

Fig. 6.4: *Vegetative crop cover for the Control and Experimental treatments*

Table 6.3 presents total irrigation depth expressed as ET, grain yield and WUE for the fully and deficit irrigated treatments. The results show an increase in WUE from 0.86 kg/m^3 for the fully irrigated treatment to 1.45 kg/m^3 for the deficit irrigated treatment, representing a 69% improvement. Although the results for the fully irrigated treatment obtained in this study strongly agree with those obtained by Igbadun *et al.* (2008) in Tanzania (0.85 kg/m^3), there is a significant difference in the deficit irrigated treatment. Igbadun *et al.* (2008) obtained WUE ranging from 0.42 kg/m^3 to 0.78 kg/m^3 depending on the growth stage where deficit irrigation was effected, suggesting that deficit irrigation lowers WUE. However, the results obtained in this study contradict this suggestion, and are consistent with the results obtained by Yenesew and Tilahun (2009) in Ethiopia and Payero *et al.* (2008) in Nebraska.

Table 6.3: *Maize grain yield, evapotranspiration (ET) and crop Water Use Efficiency (WUE) for Control (CT) and Experimental (ExT) treatments*

Treatment	Irrigation depth - ET (mm)	Grain yield (kg/m^2)	WUE (kg/m^3)
CT (fully irrigated)	880	0.752	0.86
ExT (deficit irrigated)	560	0.812	1.45

Yenesew and Tilahun (2009) and Payero *et al.* (2008) obtained WUE of 1.04 kg/m^3 and 0.98 kg/m^3, respectively, for the treatments which received full irrigation. These values are not significantly different from 0.86 kg/m^3 obtained in this study for the fully irrigated treatment. Furthermore, Yenesew and Tilahun (2009) and Payero *et al.* (2008) obtained WUE ranging from 1.09 kg/m^3 to 1.78 kg/m^3 and 1.32 kg/m^3 to 1.49 kg/m^3,

respectively, depending on the growth stage where deficit irrigation was applied. These results strongly agree with those obtained in this study (1.45 kg/m^3) for the deficit irrigated treatment.

These results suggest that applying deficit irrigation dynamically, following the crop coefficient pattern, improves WUE. This confirms the arguments of Jalota *et al.* (2006) and Tariq *et al.* (2003) that deficit irrigation can improve crop water productivity if it is employed at the right growth stage. Specifically, Jalota *et al.* (2006) reported that avoiding crop stress at the most sensitive crop growth stage is beneficial in terms of enhancing water productivity.

6.4 Assessment of the System Performance

This study assessed the WSN deployment field readiness in agricultural application by inspecting three aspects. Firstly, it investigated the ZigBee radio link performance through measurements of RSSI which varied with time and maize crop cover. Secondly, the study monitored battery performance for sensor nodes at night and during the day. Finally, the study monitored the board temperature for sensor nodes.

6.4.1 Received Signal Strength Indicator

The performance of the IMS was assessed in terms of RSSI as a function of time and maize crop cover. Zennaro *et al.* (2008) reported that RSSI is one of the three commonly used WSN link quality estimators which is a signal based indicator. The other indicators are the Link Quality Indicator and the Packet Reception Rate. In this experiment the performance of the network was analysed based on RSSI. Accordingly, the study used XBee-ZB modules at 2.4 GHz as radio transceivers whose sensitivity was -96 dBm (Libelium, 2010). This means that the communication link is bound to fail when RSSI goes below -96 dBm.

As stated before, sensor nodes were placed at a height of 60 cm above the ground. Monitoring of the link performance commenced immediately after planting the maize. At the end of the experiment the crops had grown to about 207 cm thereby covering in-field sensor nodes completely. Fig. 6.5 shows a scenario in which the sensor is fully covered by the maize plants.

Fig. 6.5: *Sensor node being covered by maize plants*

Fig. 6.6 depicts the variation of RSSI for individual nodes with time and crop height. The results show a dramatic decrement in the level of RSSI with crop height. Specifically, when the maize plants were about 57 cm tall and, consequently, started covering sensor nodes, the level of RSSI slumped heavily. The results mean that during the early stages of maize growth (before the height of 57 cm) it was essentially improbable for the network to fail since the level of RSSI was at an average of -61 dBm. On the other hand, the results mean that the communication links were bound to fail when the plants covered the nodes since the RSSI was at around -80 dBm with a minimum of -95 dBm. This is very close to the receiver sensitivity of -96 dBm. Nevertheless, the results indicate that the network was robust despite sensor nodes being covered by crops.

It should be noted that the experiments were conducted with a distance of 10 m be-

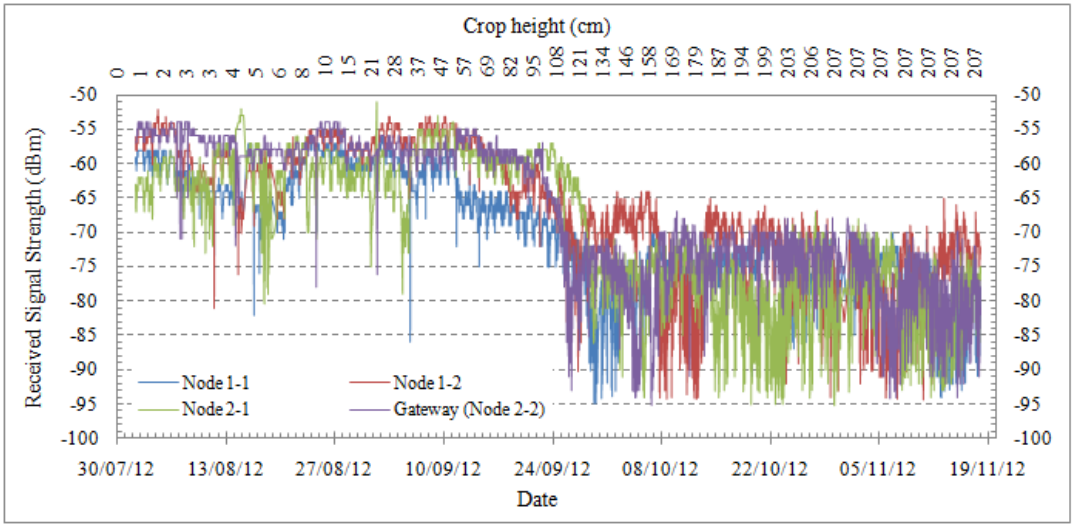

Fig. 6.6: *Variation of Received Signal Strength with crop height*

tween sensor nodes. Based on the Friis equation, which states that the level of the signal strength is inversely proportional to the square of the distance, is it likely that the level of RSSI would go down if the distance between sensor nodes exceeded 10 m. Consequently, this study recommends that in order to have a more resilient WSN deployment in the maize field where line-of-sight communication is impossible, distances between sensor nodes should not exceed 10 m when 2 dBi antennas are used for Waspmote nodes.

6.4.2 Sensor Node Battery Performance

As the system had to be self-sustained in terms of power, solar PV and rechargeable batteries were used to power all electronic devices in this system. After evaluating the performance of the system in terms of power usage (refer to Fig. 6.7), it was discovered that nodes 1-1, 1-2, and 2-1 were more resilient to power failure than the gateway (node 2-2). As generally expected, the gateway node had its battery level depleted heavily because most of its power was used to send SMSs to a remote monitoring site. Nevertheless, the study shows that the 2.5 W solar panels and 1, 150 mAh batteries sufficed the powering requirements of the gateway and the other three in-field sensor nodes.

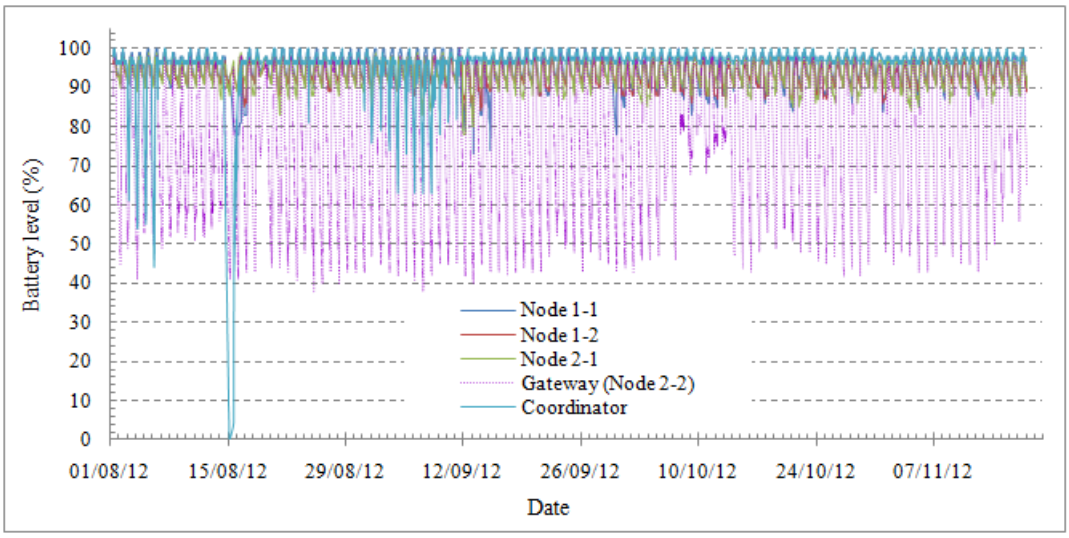

Fig. 6.7: *Sensor node battery level varying with time*

Although sleeping mode was not used as a method for conserving energy, the coordinator node was also robust in terms of power because it employed a bigger capacity solar panel and battery (14 W and 7, 000 mAh, respectively). This was also used to power solenoid valves. However, as seen from the graphs in Fig. 6.7, there was a power failure for the coordinator node on 15^{th} August due to a loose connection. This behaviour was reported to the management personnel who rectified the problem without undue impact on the crops or the research.

6.4.3 Sensor Node Board Temperature

The operation of WSN nodes depends on the environment in which they have been deployed. An agricultural field is described as one of the harshest environments since sensors are left in an open air where they are exposed to high levels of temperature. Therefore, measuring the level of internal temperature of the sensor board is critical in order to assess the performance of the system.

Fig. 6.8 shows the level of sensor board temperature for all the five nodes, showing a day-night and a seasonal trend of temperature variation. Specifically, the results show that the board temperature rose during the day when the sun struck the sensor board and slumped drastically at night. On the other hand, there was a slight overall increment

of board temperature in the long run as portrayed by the trend lines of the sensor nodes in Fig. 6.8. The rising trend of the sensor board temperatures corresponds to the rising ambient temperature which is generally expected in Malawi between August and November.

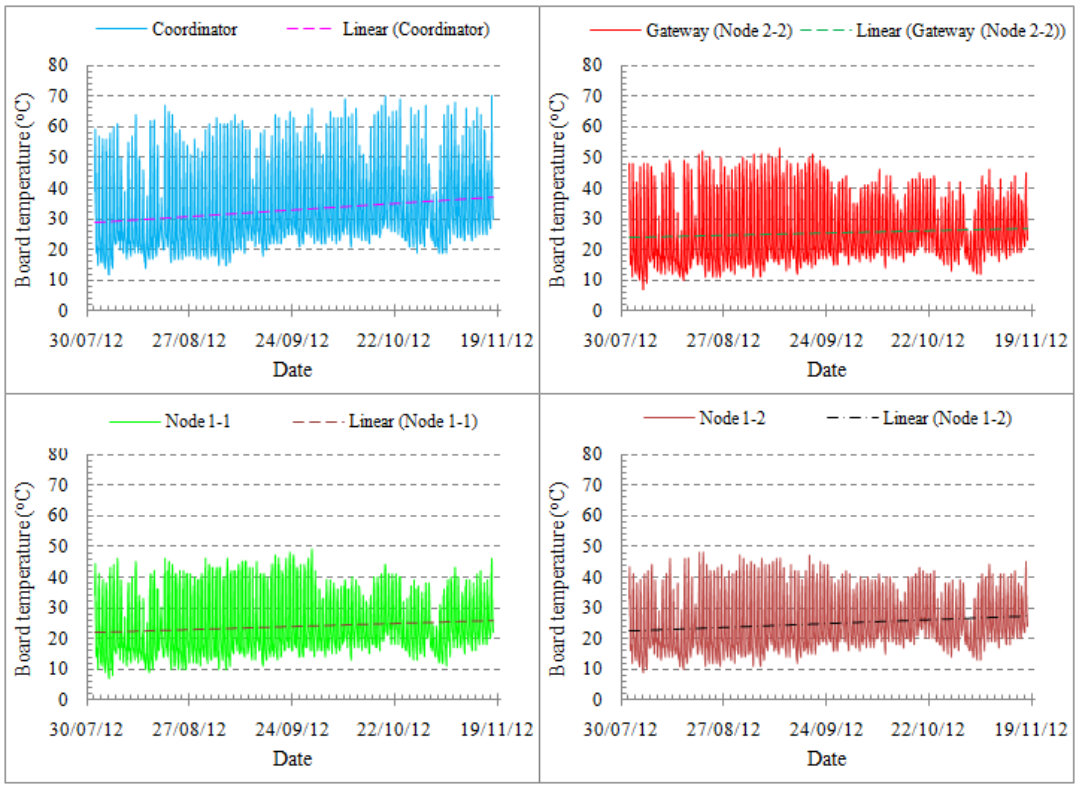

Fig. 6.8: *Sensor node board temperature varying with time*

Furthermore, the results show that there was a high correlation between the function of the node and the board temperature. A node handling more functions had generally high board temperature. Specifically, the average board temperature for the coordinator node which ranged from 28 °C to 37 °C was the highest commensurate with its functions. This node was never put into sleeping mode and was used to receive and process data from all the in-field nodes. As such, it was the busiest node in this network. This trend was followed by the gateway node which was capturing and sending moisture data to the coordinator in addition to sending SMSs to the RMS. Its average board temperature ranged from 24 °C to 29 °C. The other three in-field sensor nodes were least loaded since they were performing basic functions of capturing and sending the moisture data to the coordinator, thereafter going to sleep. Consequently, their av-

erage board temperatures were the lowest and ranged from 21 °C to 25.5 °C, 22.5 °C to 27 °C and 22 °C to 25 °C for nodes 1-1, 1-2 and 2-1, respectively, which were not significantly different.

Additionally, the crop cover also played a very crucial role on the performance of the nodes in terms of board temperature fluctuations. The results depicted in Fig. 6.8 show that the maximum board temperature decreased when the crops covered the in-field nodes. This took place from about 24^{th} September for the gateway and node 1-2 and on 30^{th} September for node 1-1. A similar trend was noted on node 2-1 whose graph is not shown. The coordinator node never experienced this phenomenon since it was never covered by the crops. Consequently, on several occasions (for instance on 19^{th}October and 17^{th}November) the board temperature of this node shot above the permitted level of 65 °C as specified by the manufacturer (Libelium, 2010). This posed a serious threat on its performance. Nonetheless, the electronic boards were robust enough not to fail under these conditions (although longer term failure might still be made more likely by these conditions). As generally expected, it is recommended that sensor nodes should have a well-ventilated cover to protect them from the direct sunlight.

6.5 Chapter Summary

This chapter has discussed the results of the experimental deployment of the IMS. It has assessed the effectiveness of the developed irrigation scheduling strategy. The chapter has further evaluated the level of water and energy saving and the impact of such savings on the crop yield. Finally, the chapter has analyzed the robustness of the WSN irrigation controller and outlined areas of improvements to enhance the resilience of the deployment.

Chapter 7

Conclusions and Recommendations

7.1 Overview

An integral part of sustainable development of irrigation farming is the availability and management of water resource. This resource is becoming scarce as it faces high demand from agricultural, industrial, commercial and domestic use. Efficient irrigation scheduling is the key parameter to sustainable water management systems. It provides knowledge about how much water is to be applied and when; in order to satisfy crop water requirements. This does not only avoid over-irrigation which wastes water and energy but also avoids under-irrigation which reduces crop yield.

Most of the advanced irrigation controllers currently on the market use constant preset threshold levels when scheduling irrigation unless intervened by the user. This method is laborious and prone to errors from the user. Therefore the principle aim of this study was to investigate whether a fully automated irrigation controller that uses the crop coefficient pattern to adjust moisture threshold levels when scheduling irrigation could improve both crop water use efficiency and solar PV energy used in water pumping and optimise crop yield.

This thesis has successfully developed and implemented an efficient solar powered irrigation management system for drip irrigated maize field based on wireless sen-

sor networks. The results have shown that the implementation of this system saved 36% of both water and solar PV energy used in pumping. Furthermore, the results have shown that the developed irrigation controller improved the grain yield by 7.4%. The water use efficiency was also increased from 0.86 kg/m^3 for the basic irrigation scheduling strategy to 1.45 kg/m^3 for the advanced scheduling strategy, representing a 69% improvement. Sections 7.2 through 7.5 summarize the key findings for this study and present recommendations accordingly, while section 7.6 discusses proposed future work.

7.2 Water and Energy Saving versus Crop Yield

This thesis has shown that automatic variation of deficit irrigation, following the crop coefficient pattern of the maize crop, saves a substantial amount of water. Specifically, a total of 880 mm of water was applied to the control treatment field which used constant preset moisture threshold levels while 560 mm of water was applied to the experimental treatment field which adopted dynamic moisture threshold levels. This translates to a water saving of 36% in the experimental treatment field.

The impact of the water saving on the maize yield was investigated. The results have shown that the dry grain yield in the control treatment field and the experimental treatment field was 0.752 kg/m^2 and 0.812 kg/m^2, respectively. This means that the controller deployed in the experimental treatment field improved the grain yield by 7.4%, while applying less amount of water. Accordingly, the water use efficiency was higher in the experimental treatment field (1.45 kg/m^3) than in the control treatment field (0.86 kg/m^3).

The study also computed the level of solar PV energy that would be saved by improving the efficiency of the irrigation scheduling. It was discussed is section 6.2 that a total of 36% of solar PV energy would be saved by implementing a solar PV water pumping system for the advanced irrigation scheduling strategy. However, when sizing a solar PV water pumping system the peak water demand is used. This study established that

at peak-water-demand stage, which was at the middle growth stage of the maize plant, the control treatment field would require 569.2 Wh/day of solar PV energy while the experimental treatment field would need a total of 520.8 Wh/day. This represents an 8.5% PV energy saving. Consequently, the total cost of the solar PV water pumping system would be reduced by 8.5%. Nevertheless, the study has demonstrated that the level of energy saving increases with the size of the field. Specifically, it was shown that doubling the size of the field from 48.4 m^2 to 96.8 m^2 results in a 12.2% improvement in the efficiency of the solar PV water pumping system hence its cost would be reduced by the same margin.

These results indicate that the developed scheduling strategy has a potential of saving water and energy used in water pumping, more so when deployed at a larger scale. Consequently, fully automated irrigation systems would be implemented where initially it was impossible due to limited water and power supplies. Moreover, the crop yield has been improved by the proposed scheduling strategy.

7.3 System Performance

This study has demonstrated how an irrigation management system can practically be implemented based on wireless sensor network. It has further evaluated the performance of the design in order to develop a more robust and sustainable system considering the challenges that any practical wireless sensor network deployment would face. Firstly, the study explored the ZigBee radio link performance through measurements of received signal strength indicator. Secondly, it evaluated battery performance for sensor nodes. Finally, the study assessed the board temperature for sensor nodes.

7.3.1 Radio Link Performance

The results have shown that maize crop cover has a very serious repercussion on the performance of the radio link. For wireless sensor network radio transceivers having

sensitivities of -96 dBm, employing 2 dBi antennas, placed at a height of 60 cm from the ground and at a distance of 10 m between them, the study has shown that the performance of the link is fairly compromised (received signal strength indicator was at around -80 dBm with a minimum of -95 dBm) when the maize plants covered them. Based on the Friis equation, which states that the level of the signal strength is inversely proportional to the square of the distance, increasing the distance between the nodes beyond 10 m would further compromise the performance of the wireless sensor network deployment in the maize field. Therefore, despite the manufacturer (Libelium, 2010) specifying a distance of 500 m based on the line-of-sight communication and the use of a 5 dBi antenna, this study recommends a maximum of 10 m distance between sensor nodes in the maize field in order to improve the resilience of the system remarkably.

7.3.2 Sensor Nodes Battery Performance

The results have further shown that in order to have a self-sustained wireless sensor network deployment in terms of power, sleeping mode must be employed whenever it is possible. Sensor nodes which used this mode were more robust to power failure than those that did not. Precisely, the study showed that the 2.5 W solar panels and 1,150 mAh batteries sufficed the powering requirements of the gateway and the other three in-field sensor nodes. However, where it is impossible to use the sleeping mode, like the case of the coordinator node in this study, the power capacity must be commensurate with the duties of such a node. Specifically, the deployment under this study used a 7,000 mAh battery and a 14 W solar panel to power the coordinator node. Notably, this power option was also used for the solenoid valves.

7.3.3 Sensor Nodes Board temperature

In order to have a more robust wireless sensor network deployment, sensor nodes should not be exposed to high levels of temperature. In an agricultural field, nodes

are left in an open air where ambient temperature exacerbates the electronic board temperature of the nodes. If left unchecked, the nodes will likely crash. The results have shown that the nodes that handle more duties have higher board temperatures than those with less functions. For instance, the gateway node which was under the same environment as the other three in-field nodes had more functions and therefore its average board temperature was the highest. The average temperature ranged from 24 °C to 29 °C as compared to the other nodes whose minimum and maximum average board temperatures ranged from 21 °C to 22.5 °C and 25 °C to 27 °C, respectively.

Furthermore, the results have shown that crop cover helps to reduce the board temperature of the nodes. All the in-field nodes and the gateway node had their maximum board temperatures lowered when the maize crop covered them. The coordinator node never experienced this phenomenon since it was never covered by the crops. As such, on several occasions the board temperature of this node shot above the permitted level of 65 °C as specified by the manufacturer (Libelium, 2010). This posed a serious threat on the board performance. Nonetheless, the electronic boards were robust enough not to fail under these conditions (although longer term failure might still be made more likely by these conditions). As generally expected, it is recommended that sensor nodes should have a well-ventilated enclosure to protect them from the direct sunlight.

7.4 Cost Analysis of the Irrigation Management System

As articulated in section 2.3.3, commercial irrigation controllers which are based on on-demand soil moisture sensing stratergy are efficient in the water application when there is an extensive user involvement. Otherwise, with the set-and-forget mentality it is more likely that users choose higher levels of moisture threshold than required as it is easier to notice signs of stressed maize crop than those from over-irrigation to a small extent. Consequently, water and pumping energy are wasted, soil nutrients are washed away and crop yield is reduced. Additionally, these commercial controllers

are expensive, hence, not suitable for medium and small scale farmers. For instance, Fazackerley and Lawrence (2009) reported $3,000 as the cost of such on-demand soil moisture sensing controllers. This is the cost of one completed node excluding the cost of the soil moisture sensor and data transmission components.

This study assumes that dividing a hectare into 10 zones which can be irrigated independently can fully and evenly distribute water in the field. This requires 10 wireless sensor network nodes with each completed node in the current study costing $453. This includes the cost of a processing board, sensor interfacing board (agriculture board), radio transceiver, moisture and temperature sensors, and the cost of data transmission module for remote monitoring purposes.

Although this is a remarkable reduction in the cost as compared to the commercial controllers, this study recommends that future deployments should focus on reducing the cost of such deployments in order to make them a widespread commercial success. Here it is suggested that the agriculture board which costs $169 should be eliminated. This can be done in two ways: One way is to replace the Watermark 200SS moisture sensor which costs $53, but requires an agriculture board as an interface, with the Watermark 200SS-V sensor which incorporates an interfacing circuit and costs $88. This arrangement can reduce the cost of each completed node from $453 to $326. The other way is to develop cheaper sensor interfacing circuits.

Furthermore, this study has revealed that several performance parameters can be monitored cost effectively using a wireless sensor network node equipped with a General Packet Radio Service (GPRS) module and using open source tools that include FrontlineSMS, MYSQL, and PHP. The use of cellular network reduces the cost of the remote monitoring system since an SMS charge is extremely low as compared to satellite communication or Wi-Fi connectivity. Moreover, cellular network coverage is broad even in remote areas of the developing countries. Additionally, the use of Wi-Fi increases the cost of the remote monitoring system since a full computer costing over $600 is needed, while with a cellular network only a basic mobile phone costing $6 can be used to receive SMSs. This is ideal for small scale farmers.

Finally, by fully automating the irrigation controller and incorporating the remote monitoring facility in the irrigation management system, it means that the intervention of the user has been reduced tremendously. Therefore, it is now possible for the user to concentrate on other developmental and income generating activities. This can further uplift the socioeconomic status of farmers.

7.5 Challenges, Experiences Gained and Recommendations

This study has exposed a number of valuable experiences which can be used to speed up the process of designing new wireless sensor network deployments for precision agriculture. Firstly, the study revealed a practical challenge concerning the conflict between ZigBee and GPRS modules. When both ZigBee and GPRS modules were powered up, either of them would lose connection which required manual reset in order to restart the network. Nonetheless, using an appropriate software configuration in the gateway node, it was possible to turn off one module when the other was active. This was not possible at the coordinator node since its ZigBee module was always required to be on to avoid losing connection with the other network nodes. However, this conflict could be specific to Waspmote and probably dependent on the firmware. It could be solved in a future release of firmware and may not be a general problem.

Secondly, there was a challenge to connect two Watermark moisture sensors to the agriculture board. The idea was to connect the deep and shallow moisture sensors to the same board so that the two could be used simultaneously to report the soil moisture status. However, despite the board being capable of integrating three Watermark sensors, it was not possible to do this as there were false readings from the sensors, possibly due to the interference when placed in the same soil substrate. The board has a common switch to all the three possible Watermark moisture sensors such that it was impossible at the software level to switch off the other two sensors when reading from one. Consequently, this study connected the shallow sensor only during the early

stages and the deep sensor only at the later stages. This change in hardware configuration necessitated a slight modification in the controller program to reflect the change in the depth of the sensor.

Thirdly, a very crucial requirement of any wireless sensor network deployment is close monitoring. Rather than conducting physical site visits, which is time consuming and expensive, it was compelling to monitor the system performance remotely. This arrangement permitted the management personnel to timely identify system faults and conduct pre-emptive maintenance by visiting the field only when needed. The study recommends that any successful wireless sensor network deployment must employ remote monitoring through a cellular network which is broadly available even in rural areas of the developing countries.

Fourthly, it was also observed that there is a possibility of disturbing the sensors during field work, for example, weeding. This can give false readings from the sensor and unnecessary irrigation may ensue. Once sensors are disturbed, they may need reinstallation in order to make a good contact with the soil. However, it is not advisable to re-install sensors after the crops have germinated and developed as this may damage crop roots and hence lower the yield.

Finally, this study focused on the maize production under Malawi's weather conditions. However, the concept would easily be replicated in other crops and in other parts of the world with two modifications: firstly, sensor calibration must be done onsite; and secondly, the specific crop coefficient pattern must be used to develop the scheduling strategy.

7.6 Future Work

Although this study has remarkably reduced the cost of a completed wireless sensor node from a reported $3, 000 (Fazackerley and Lawrence, 2009) for commercial controllers to just about $453, the study still recommends that future deployments should

focus on reducing the cost further in order to make them a widespread commercial success. For instance, the study suggests that the agriculture board, used as an interface between the Watermark 200SS moisture sensor and the processing board, which costs $169 should be eliminated. This can be done in two ways: One way is to replace the Watermark 200SS moisture sensor which costs $53, but requires an agriculture board as an interface, with the Watermark 200SS-V sensor which incorporates an interfacing circuit and costs $88. This arrangement can reduce the cost of each completed node from $453 to $326. The other way is to develop cheaper sensor interfacing circuits. It is, however, worth noting that the price reduction of the completed wireless sensor from $3, 000 to $453 might also be due to component price reduction over the years.

The study further proposes the deployment of the developed wireless sensor based irrigation controller on a large scale to investigate the level of solar PV energy saving. The study has theoretically demonstrated that doubling the size of the field from 48.4 m^2 to 96.8 m^2 increases the level of PV energy saving from 8.5 % to 12.2 %. However, this finding needs to be investigated practically by designing and implementing a solar PV water pumping system for such a relatively large-scale deployment. Cost analysis for the solar PV water pumping system has also to be undertaken.

In addition, the proposed large-scale deployment would be a platform for assessing the ability of the wireless coordinator node in handling numerous queries from in-field wireless sensor nodes, as well as investigating the robustness of the entire wireless sensor network in an agricultural field.

Finally, this research proposes the deployment of the developed irrigation controller for other crops other than maize, for instance cotton, sugarcane, groundnuts, cassava, and a wide range of vegetables. In this case, one needs to establish crop coefficient patterns for such crops.

References

Abubaker, J. (2009). *Irrigation Scheduling for Efficient Water Use in Dry Climates*. M.Sc. thesis, Swedish University of Agricultural Sciences, Sweden.
URL http://stud.epsilon.slu.se/619/1/abubaker_j_091116.pdf

Alam, M., & Rogers, D. H. (2001). *Scheduling Irrigation by Electrical Resistance Blocks*. Kansas State University Agricultural Experiment Station and Cooperative Extension Service.
URL http://www.ksre.ksu.edu/library/ageng2/l901.pdf

Ali, G., Shaikh, A. W., & Shaikh, Z. A. (2010). A Framework for Development of Cost-effective Irrigation Control System Based on Wireless Sensor and Actuator Network (WSAN) for Efficient Water Management. In *2010 2nd International Conference on Mechanical and Electronics Engineering (ICMEE 2010)*, vol. 2, (pp. V2–378–V2–381).

Allen, R. (2000). *Calibration for the Watermark 200SS Soil Water Potential Sensor to fit the 7-19-96 "Calibration no.3" Table from Irrometer*. University of Idaho, Kimberley.
URL http://www.kimberly.uidaho.edu/water/swm/calibration_Watermark2.pdf

Allen, R., Walter, I., Elliot, R., Howell, T., Itenfisu, D., & Jensen, M. (2005). *The ASCE Standardized Reference Evapotranspiration Equation*. Asce-ewri task committee report, Environmental and Water Resources Institute (EWRI) of the American Society of Civil Engineers (ASCE).

Andrada, P., & Castro, J. (2007). Solar photovoltaic water pumping system using a new linear actuator. *Renewable Energy and Power Quality Journal*, *5*(321).

Balendonck, J., Hemming, J., van Tuijl, B., Incrocci, L., Pardossi, A., & Marzialetti, P. (2008). *Sensors and Wireless Sensor Networks for Irrigation Management under Deficit Conditions (FLOW-AID)*. FLOW - AID.
URL http://www.flow-aid.wur.nl/NR/rdonlyres/DA8B2ECC-9EEE-4A99-A1BA-E0F7EDCEB087/73978/2008BalendonckFLOWAIDAgEng.pdf

Belfield, S., & Brown, C. (2008). *Field Crop Manual: Maize - A Guide to Upland Production in Cambodia*. Tech. Rep. ISBN 978 0 7347 1882 2, The State of New South Wales, NSW Department of Primary Industries.

URL http://aciar.gov.au/files/node/8919/maize%20manual%2072dpi.pdf

Bellingham, B. K. (2009). Method for Irrigation Scheduling Based on Soil Moisture Data Acquisition. In *The 2009 Irrigation District Conference*, (pp. 1–17). United States Committee on Irrigation and Drainage.

Benson, T. (1999). *Area-specific fertilizer recommendations for hybrid maize grown by Malawian smallholders - A Manual for Field Assistants*. Maize Commodity Team - Chitedze Agricultural Research Station, Malawi.

Bernier, M. (2008). *Assessing On-Farm Water Use Efficiency in Southern Ontario*. PhD. thesis, McGill University, Montreal.

Cardenas-Lailhacar, B., & Dukes, M. D. (2007). Turfgrass Irrigation Controlled by Soil Moisture Sensor Systems. In *Proceedings of the 28th Annual International Irrigation Show, December 9-11*. San Diego, CA.
URL http://abe.ufl.edu/mdukes/pdf/publications/SMS/SMS%20performance-IA-2007.pdf

Chard, J. (2002). *Watermark Soil Moisture Sensors: Characteristics and Operating Instructions*. Utah State University.
URL http://www.usu.edu/cpl/PDF/WatermarkOperatingInstructions2.pdf

Chilimba, A. D. (1999). Conservation tillage in cotton and maize fields in Malawi. In P. Kaumbutho, A. Pearson, & T. Simalenga (Eds.) *Empowering farmers with animal traction. Proceedings of Animal Traction Network for Eastern and Southern Africa (ATNESA)*, (pp. 307–314). Mpumalanga, South Africa.
URL http://www.atnesa.org/Empowering99/Empowering99-CHILIMBA-MW-WWW.pdf

Comprehensive Assessment Secretariat (2006). *Insights from the Comprehensive Assessment of Water Management in Agriculture*. International Water Management Institute (IWMI) - World Water Week, Colombo, Sri Lanka, Stockholm.
URL http://news.bbc.co.uk/2/shared/bsp/hi/pdfs/21_08_06_world_water_week.pdf

Davis, S., Dukes, M. D., Vyapari, S., & Miller, G. L. (2007). Evaluation and Demonstration of Evapotranspiration-Based Irrigation Controllers. In *Proceedings ASCE EWRI World Environmental & Water Resources Congress, May 15-19*. Tampa, FL.

Dukes, M. (2012). *Smart Irrigation Controllers: What Makes an Irrigation Controller Smart?*. Institute of Food and Agricultural Sciences (IFAS) Extension, EDIS Document AE442, University of Florida.
URL http://edis.ifas.ufl.edu/pdffiles/AE/AE44200.pdf

Dukes, M., Shedd, M., & Cardenas-Lailhacar, B. (2009). *Smart Irrigation Controllers: How Do Soil Moisture Sensor (SMS) Irrigation Controllers Work?*. Institute of Food and Agricultural Sciences (IFAS) Extension, EDIS Document AE437, University of

Florida.
URL http://edis.ifas.ufl.edu/pdffiles/AE/AE43700.pdf

Dukes, M. D., Cardenas-lailhacar, B., & Miller, G. L. (2008). *Evaluation of Soil Moisture-Based on-demand Irrigation Controllers*. Final report, Resource Conservation and Development Department, Southwest Florida Water Management District, Brooksville, FL 34604-6899.
URL http://www.swfwmd.state.fl.us/files/database/site_file_sets/13/SMS_Phase_I_Final_Report-FINAL_8-5-08.pdf

Ellis, R. D., & Merry, R. E. (2007). *Sugarcane Agriculture*, (pp. 101–142). Blackwell Publishing Ltd.
URL http://dx.doi.org/10.1002/9780470995358.ch5

Evans, R., Cassel, D., & Sneed, R. (1996). *Soil, Water, and Crop Characteristics Important to Irrigation Scheduling*. North Carolina Cooperative Extension Service, Publication Number: AG 452-1.
URL http://www.bae.ncsu.edu/programs/extension/evans/ag452-1.html

Fandika, I. (2006). *Use of Water Budget Irrigation Scheduling Tool in Maize Irrigation Water Management*. Irrigation and Drainage Commodity Team, Kasinthula Research Station, Malawi.
URL http://bscw.ihe.nl/pub/bscw.cgi/d2607441/Fandika.pdf

FAO (2010). *Crop Water Information: Maize*. FAO (Food and Agriculture Organization) - Water Development and Management Unit.
URL http://www.fao.org/nr/water/cropinfo_maize.html

Fazackerley, S., & Lawrence, R. (2009). Reducing Turfgrass Water Consumption using Sensor Nodes and an Adaptive Irrigation Controller. *Sensors Applications Symposium (SAS), 23-25 Feb 2010 IEEE*, (pp. 90–94).

Ghinassi, G. (2006). *Guidelines for Crop Production under Water Limiting Conditions*. Working Group on water and Crop (Wg-Crop).
URL http://www.wg-crop.icidonline.org/graziano_2006.pdf

GoM (2003). *Malawi's Climate Technology Transfer and Needs Assessment*. Report, The Government of Malawi - Environmental Affairs Department, Ministry of Natural Resources and Environmental Affairs, Lilongwe, Malawi.
URL http://unfccc.int/ttclear/pdf/TNA/Malawi/TNAReportMalawi.pdf

GoM (2008). *2008 Population and Housing Census*. Tech. rep., The Government of Malawi - Ministry of Economic Planning and Development, National Statistical Office, Zomba.

Grabow, G. L., Vasanth, A., Bowman, D., Huffman, R. L., & Miller, G. (2008). *Evaluation of Evapotranspiration-Based and Soil-Moisture-Based Irrigation Control in Turf*. NC State University.

URL http://www.bae.ncsu.edu/topic/go_irrigation/docs/ewrri-database.pdf

Humphreys, L., Fawcett, B., Neill, C. O., & Muirhead, W. (2005). *Maize under sprinkler, drip & furrow irrigation*. IREC Farmers' Newsletter No 170.
URL http://www.irec.org.au/farmer_f/pdf_170/Maize%20under%20sprinkler,%20drip%20and%20furrow%20irrigation.pdf

Ibragimov, N., Evett, S. R., Esanbekov, Y., Kamilov, B. S., Mirzaev, L., & Lamers, J. P. (2007). Water use efficiency of irrigated cotton in Uzbekistan under drip and furrow irrigation. *Agricultural Water Management*, *90*(1-2), 112–120.
URL http://linkinghub.elsevier.com/retrieve/pii/S0378377407000467

Igbadun, H. E., Salim, B. a., Tarimo, A. K. P. R., & Mahoo, H. F. (2008). Effects of deficit irrigation scheduling on yields and soil water balance of irrigated maize. *Irrigation Science*, *27*(1), 11–23.
URL http://www.springerlink.com/index/10.1007/s00271-008-0117-0

India Electric Market (2000). *Solar Photovoltaic Water Pumping for Rural Development*.
URL http://www.indiaelectricmarket.com/cgi-bin/iemhome1/recentadvances/solar.asp

Irmak, S., & Harman, D. (2003). *Evapotranspiration: Potential or Reference?*. Institute of Food and Agricultural Sciences (IFAS) Extension, EDIS Document ABE 343, University of Florida.
URL http://edis.ifas.ufl.edu/pdffiles/AE/AE25600.pdf

Irmak, S., Payero, J., Eisenhauer, D., Kranz, W., Martin, D., Zoubek, G., Rees, J., van De Walle, B., Christiansen, A., & Leininger, D. (2006). *Watermark Granular Matrix Sensor to Measure Soil Matrix Potential for Irrigation Management*. University of Nebraska - Lincoln Extension.
URL http://lancaster.unl.edu/ag/crops/watermark_sensor.pdf

IRROMETER Company, Inc. (2010). *WATERMARK Soil Moisture Sensor - MODEL 200SS*. Riverside, California.
URL http://www.irrometer.com/pdf/sensors/403%20Sensor%20%20Web5.pdf

Jalota, S., Sood, A., Chahal, G., & Choudhury, B. (2006). Crop water productivity of cotton (gossypium hirsutum l.)-wheat (triticum aestivum l.) system as influenced by deficit irrigation, soil texture and precipitation. *Agricultural Water Management*, *84*(1-2), 137–146.
URL http://ideas.repec.org/a/eee/agiwat/v84y2006i1-2p137-146.html

Johnstone, P. R., Hartz, T. K., Lestrange, M., Nunez, J. J., & Miyao, E. M. (2005). Managing Fruit Soluble Solids with Late-season Deficit Irrigation in Drip-irrigated Processing Tomato Production. *HortScience*, *40*(6), 1857–1861.

Kalpana, S., Chander, J. R., & Ahmed, S. M. (2011). Wireless Sensor Network for Remote Monitoring of Crop Field. *International Journal Of Advanced Engineering Sciences and Technologies*, *8*(2), 210–213.

Libelium (2010). *Waspmote Datasheet, Vers. 0.8*. Libelium Comunicaciones Distribuidas S.L.
URL `http://www.libelium.com/waspmote`

Libelium (n.d.). *Watermark Sensors Interpretation Reference*. Libelium Comunicaciones Distribuidas S.L.
URL `http://www.libelium.com/forum/libelium_files/watermark_sensors_interpretation_reference.pdf`

Meah, K., Ula, S., & Barrett, S. (2008). Solar Photovoltaic Water Pumping - Opportunities and Challenges. *Renewable and Sustainable Energy Reviews*, *12*(4), 1162 – 1175.
URL `http://www.sciencedirect.com/science/article/pii/S1364032106001584`

Miranda, F., Yoder, R., Wilkerson, J., & Odhiambo, L. (2005). An Autonomous Controller for Site-Specific Management of Fixed Irrigation Systems. *Computers and Electronics in Agriculture*, *48*(3), 183–197.
URL `http://linkinghub.elsevier.com/retrieve/pii/S0168169905000815`

Mokeddem, A., Midoun, A., Ziani, N., Kadri, D., & Hiadsi, S. (2007). Test and analysis of a photovoltaic DC-motor pumping system. *2007 ICTON Mediterranean Winter Conference*, (pp. 1–7).
URL `http://ieeexplore.ieee.org/lpdocs/epic03/wrapper.htm?arnumber=4446963`

Morris, M. (2006). *Soil Moisture Monitoring : Low-Cost Tools and Methods*. National Center for Appropriate Technology (NCAT).
URL `http://attra.ncat.org/attra-pub/PDF/soil_moisture.pdf`

Mpaka, C. (2010). *MALAWI: Green Belt Initiative Taking Shape*. IPS (Inter Press Service)-Africa.
URL `http://www.ips.org/africa/2010/01/malawi-green-belt-initiative-taking-shape`

Muñoz-Carpena, R. (2009). *Field Devices For Monitoring Soil Water Content*. Institute of Food and Agricultural Sciences (IFAS) Extension, EDIS Document BUL343, University of Florida.
URL `http://edis.ifas.ufl.edu/pdffiles/AE/AE26600.pdf`

Nautiyal, M., Grabow, G., Miller, G., & Huffman, R. (2010). Evaluation of Two Smart Irrigation Technologies in Cary, North Carolina. In *American Society of Agricultural and Biological Engineers (ASABE) 2010 Annual International Meeting*. Michigan.

Oi, A. (2005). *Design and Simulation of Photovoltaic Water Pumping System*. M.Sc. thesis, California Polytechnic State University, San Luis Obispo.

Pardossi, A., Incrocci, L., Incrocci, G., Malorgio, F., Battista, P., Bacci, L., Rapi, B., Marzialetti, P., Hemming, J., & Balendonck, J. (2009). Root zone sensors for irrigation management in intensive agriculture. *Sensors (Basel)*, *9*(4), 2809–2835. URL http://dx.doi.org/10.3390/s90402809

Payero, J. O., Tarkalson, D. D., Irmak, S., Davison, D., & Petersen, J. L. (2008). Effect of irrigation amounts applied with subsurface drip irrigation on corn evapotranspiration, yield, water use efficiency, and dry matter production in a semiarid climate. *Agricultural Water Management*, *95*(8), 895–908. URL http://linkinghub.elsevier.com/retrieve/pii/S0378377408000619

Prince-Pike, A. (2009). *Power Characterisation of a Zigbee Wireless Network in a Real Time Monitoring Application*. M.Sc. thesis, Auckland University of Technology.

Shock, C. (2006). *Efficient Irrigation Scheduling*. Oregon State University, Malheur Agricultural Experiment Station, Information for Sustainable Agriculture. URL http://www.cropinfo.net/irrigschedule.php

Shock, C. C., Barnum, J. M., & Seddigh, M. (1998). Calibration of Watermark Soil Moisture Sensors for Irrigation Management. In *International Irrigation Show*, (pp. 139–146). San Diego, CA.: Irrigation Association.

Short, T., & Mueller, M. (2002). Solar Powered Water Pumps: Problems, Pitfalls and Potential. In *IEE International Conference on Power Electronics Machines and Drives*, (pp. 280–285).

Spectrum Technologies, Inc. (n.d.). *Watchdog, Watermark Soil Moisture Sensor - PRODUCT MANUAL- Item no. 6450WD*. Plainfield, Illinois. URL http://www.specmeters.com/assets/1/22/6450WD.pdf

Tariq, J. A., Khan, M. J., & Usman, K. (2003). Irrigation Scheduling of Maize Crop by Pan Evaporation Method. *Pakistan Journal of Water Resources*, *7*(2), 29–35.

Texas Water Development Board (2004). *Agricultural Water Conservation Practices*. URL http://www.twdb.state.tx.us/assistance/conservation/conservationpublications/agbrochure.pdf

Thompson, B., Gallardo, M., Agu, T., Valdez, C., & Ferna, D. (2006). Evaluation of the Watermark sensor for use with drip irrigated vegetable crops. *Irrigation Science*, *24*(3), 185–202.

Thomson, M. A. (2003). *Reverse-Osmosis Desalination of Seawater Powered by Photovoltaics Without Batteries*. PhD. thesis, Loughborough University.

Tichenor, J., Dukes, M. D., & Trenholm, L. E. (2004). *Using the Irrigation Controller for a Better Lawn on Less Water*. Institute of Food and Agricultural Sciences (IFAS)

Extension, EDIS Document ENH978, University of Florida.
URL http://edis.ifas.ufl.edu/pdffiles/EP/EP23500.pdf

Waddington, S., Palmer, A., & Edje, O. (Eds.) (1990). *Research Methods for Cereal/Legume Intercropping*, Proceedings of a Workshop on Research Methods for Cereal/Legume Intercropping in Eastern and Southern Africa. Mexico, D.F.: CIMMYT.

Yenesew, M., & Tilahun, K. (2009). Yield and water use efficiency of deficit-irrigated maize in a semi-arid region of Ethiopia. *African Journal of Food, Agriculture, Nutrition and Development*, *9*(8), 1635–1651.

Zennaro, M., Ntareme, H., & Bagula, A. (2008). Experimental Evaluation of Temporal and Energy Characteristics of an Outdoor Sensor Network. In *Proceedings of the International Conference on Mobile Technology, Applications, and Systems*, Mobility '08, (pp. 99:1–99:5). New York, NY, USA: ACM.
URL http://doi.acm.org/10.1145/1506270.1506391

Appendices

Appendix A: Performance Curves for ’25 SQF - 7’ Submersible Pump (GRUNDFOS Holding A/S)

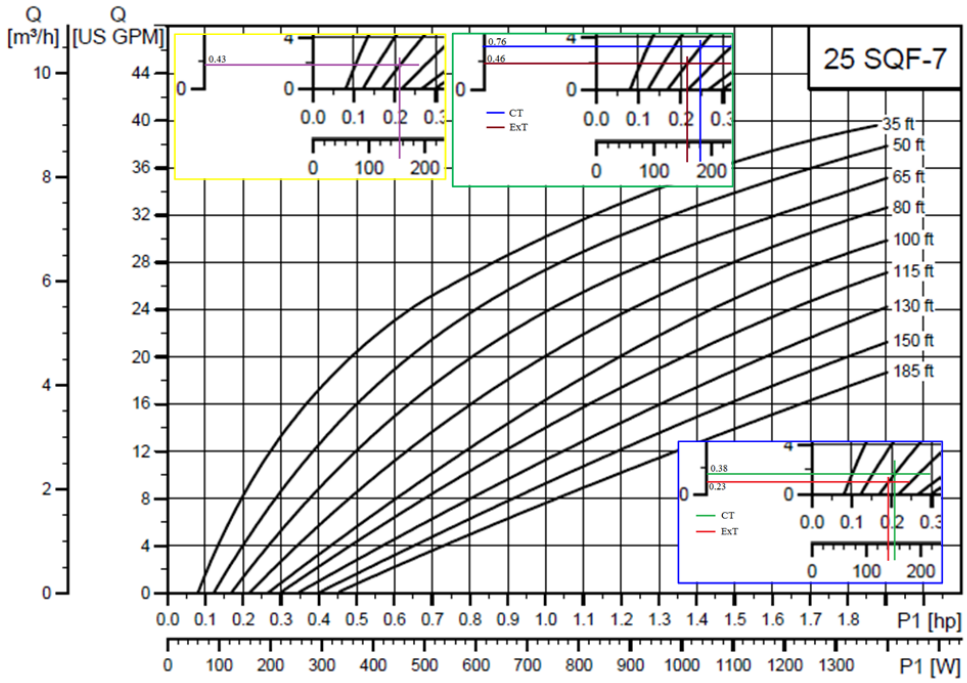

Note: Max. P1 (W) shown on curve represents max. motor RPM.

Appendix B: Software Programs for Creating a ZigBee PAN

```
//This code is loaded into a ZC node to create
//a PAN with ZEDs
uint8_t PANID[2]={0x20,0x12};
char*  NETKEY="Takondwa98765432"; // 16 byte key
char*  LINKKEY="Mafuta1234567890"; // 16 byte key
void setup()
{
  // Init. the XBee ZigBee library
  xbeeZB.init(ZIGBEE,FREQ2_4G,NORMAL);
  //Powers XBee
  xbeeZB.ON();
  createNetwork();
  delay(100);
}
void loop()
{
  // blink LEDs - indicating start of loop
  Utils.blinkLEDs(1000);
  delay(1000);
}
void createNetwork()
{
  // Getting Channel
  xbeeZB.getChannel();
  if( !xbeeZB.error_AT )
  {
    XBee.print("Channel obtained OK! -Channel is: ");
    XBee.println(xbeeZB.channel,HEX);
  }
  else XBee.println("Error getting channel");
  // Chosing a PANID : PANID=0x2012
  xbeeZB.setPAN(PANID);
  if( !xbeeZB.error_AT ) XBee.print("PANID set OK");
  else XBee.println("Error while changing PANID");
  // Enabling security
  xbeeZB.encryptionMode(1);
  if( !xbeeZB.error_AT )
  XBee.println("Security enabled");
  else XBee.println("Error while enabling security");
  // Configuring Trust Center
  xbeeZB.setEncryptionOptions(0x02);
  if( !xbeeZB.error_AT )
  XBee.println("Security options configured");
  else
  XBee.println("Error while configuring security");
  // Setting Link Key: LINKKEY="Mafuta1234567890"
  xbeeZB.setLinkKey(LINKKEY);
  if( !xbeeZB.error_AT )
  XBee.println("Link Key set OK");
  else XBee.println("Error while setting Link Key");
  // Setting Network Key (only in Coordinator)
  //-NETKEYY: Takondwa98765432
  xbeeZB.setNetworkKey(NETKEY);
  if( !xbeeZB.error_AT )
  XBee.println("Network Key set OK");
  else XBee.println("Error while setting Net Key");
  // Setting APS Encryption
  xbeeZB.setAPSencryption(XBEE_ON);
  if( !xbeeZB.error_AT )
  XBee.println("APS Encryption set OK");
  else
  XBee.println("Error while setting APS Encryption");
  xbeeZB.writeValues();   // Keep values
  if( !xbeeZB.error_AT )
  XBee.println("Changes stored OK");
  else XBee.println("Error while storing values");
  delay(1000);
}
```

```
//This code is loaded into all ZEDs to create
//a PAN with the ZC
uint8_t PANID[2]={0x20,0x12};
// 16 byte key
char*  LINKKEY="Mafuta1234567890";
void setup()
{
  // Init. the XBee ZigBee library
  xbeeZB.init(ZIGBEE,FREQ2_4G,NORMAL);
  xbeeZB.ON();   //Powers XBee
  createNetwork();
  delay(100);
}
void loop()
{
  // blink LEDs - indicating start of loop
  Utils.blinkLEDs(1000);
  delay(1000);
}
void createNetwork()
{
  // Getting Channel
  xbeeZB.getChannel();
  if( !xbeeZB.error_AT )
  {
    XBee.print("Channel obtained OK! -Channel is: ");
    XBee.println(xbeeZB.channel,HEX);
  }
  else XBee.println("Error getting channel");
  // Chosing a PANID : PANID=0x2012
  xbeeZB.setPAN(PANID);
  if( !xbeeZB.error_AT ) XBee.print("PANID set OK");
  else XBee.println("Error while changing PANID");
  // Enabling security
  xbeeZB.encryptionMode(1);
  if( !xbeeZB.error_AT )
  XBee.println("Security enabled");
  else XBee.println("Error while enabling security");
  // Configuring Trust Center
  xbeeZB.setEncryptionOptions(0x02);
  if( !xbeeZB.error_AT )
  XBee.println("Security options configured");
  else
  XBee.println("Error while configuring security");
  // Setting Link Key: LINKKEY="Mafuta1234567890"
  xbeeZB.setLinkKey(LINKKEY);
  if( !xbeeZB.error_AT )
  XBee.println("Link Key set OK");
  else XBee.println("Error while setting Link Key");
  // Setting APS Encryption
  xbeeZB.setAPSencryption(XBEE_ON);
  if( !xbeeZB.error_AT )
  XBee.println("APS Encryption set OK");
  else
  XBee.println("Error while setting APS Encryption");
  // Keep values
  xbeeZB.writeValues();
  if( !xbeeZB.error_AT )
  XBee.println("Changes stored OK");
  else XBee.println("Error while storing values");
  delay(1000);
}
```

Appendix C: Flow Chart for in-Field Sensor Nodes

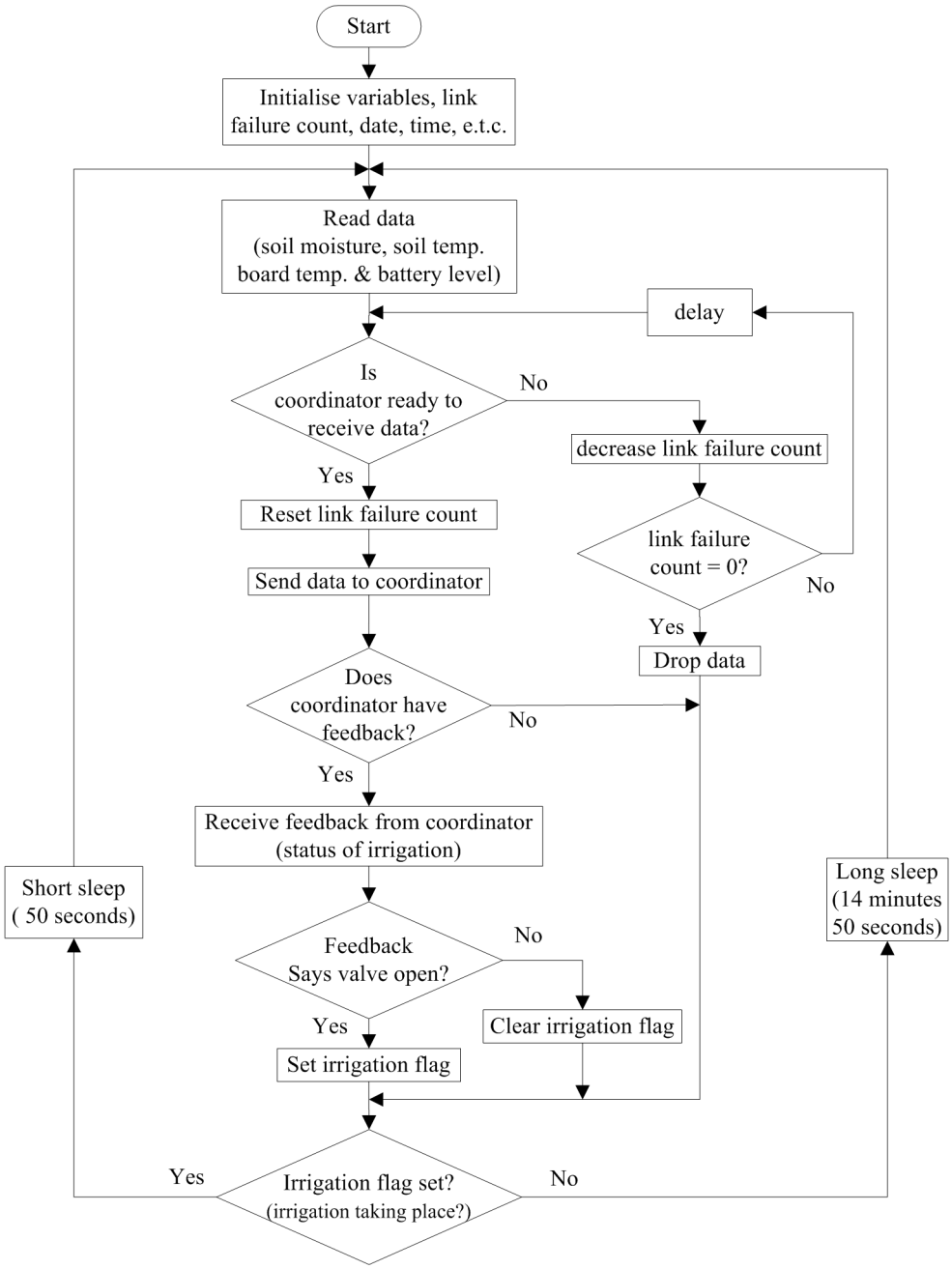

Appendix D: Flow Chart for Coordinator and Actuator Node

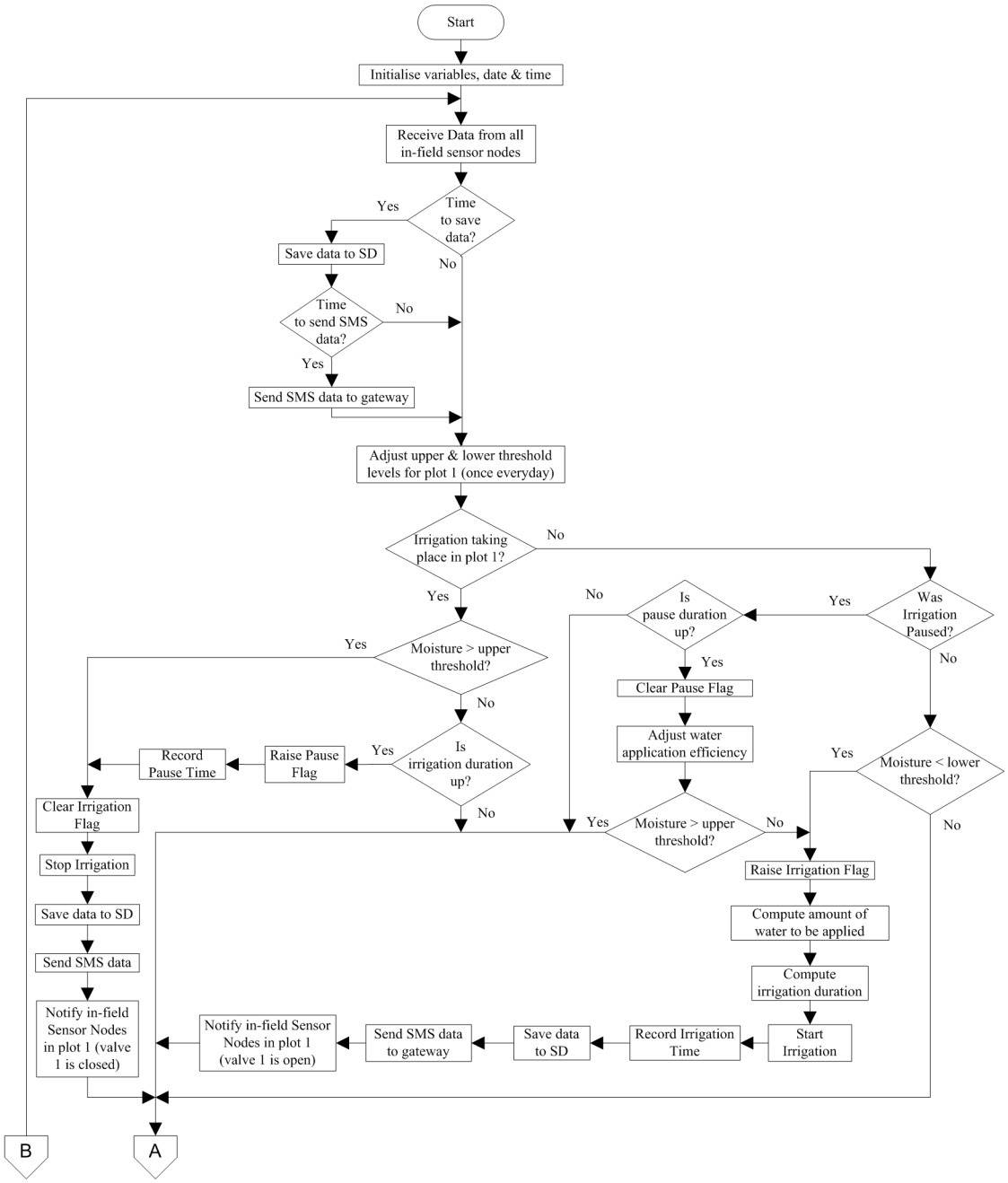

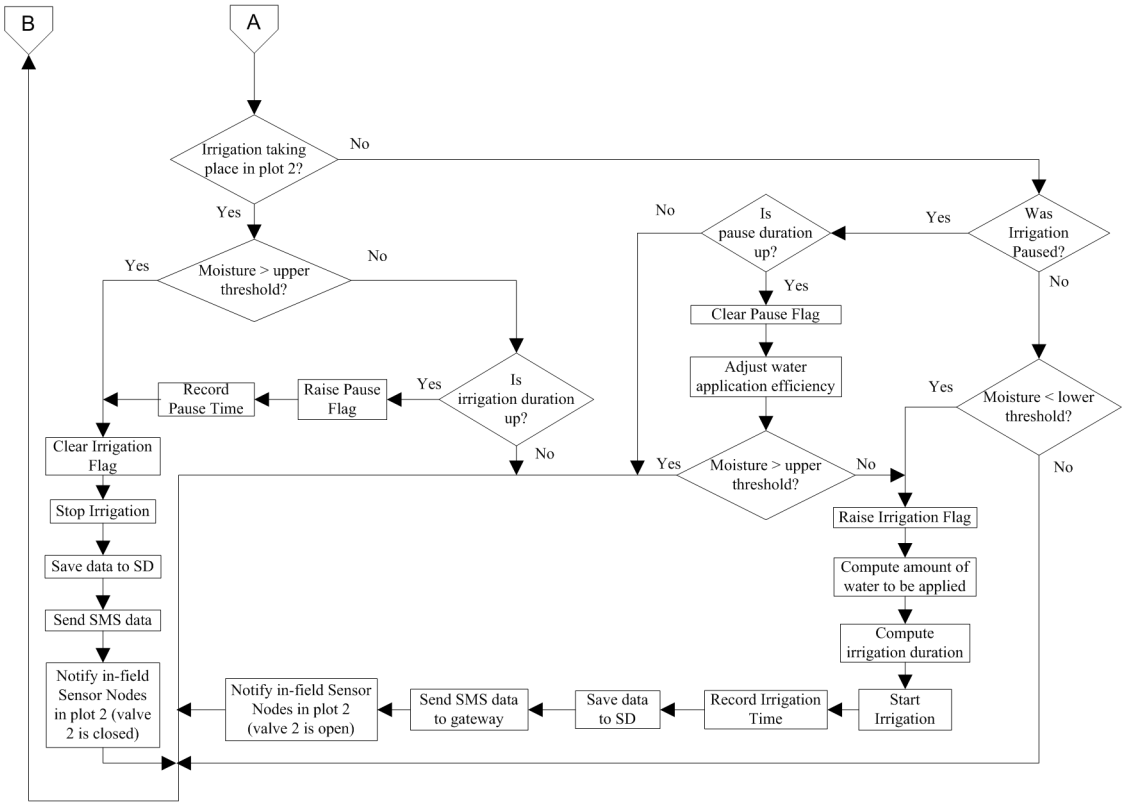
B
A
Irrigation taking place in plot 2?
No
Yes
Moisture > upper threshold?
Yes
No
Is pause duration up?
No
Yes
Was Irrigation Paused?
Yes
No
Clear Pause Flag
Adjust water application efficiency
Record Pause Time
Raise Pause Flag
Yes
Is irrigation duration up?
No
Yes
Moisture < lower threshold?
No
Clear Irrigation Flag
Stop Irrigation
Save data to SD
Send SMS data
Yes
Moisture > upper threshold?
No
Raise Irrigation Flag
Compute amount of water to be applied
Compute irrigation duration
Notify in-field Sensor Nodes in plot 2 (valve 2 is closed)
Notify in-field Sensor Nodes in plot 2 (valve 2 is open)
Send SMS data to gateway
Save data to SD
Record Irrigation Time
Start Irrigation

Appendix E: Flow Chart for the Gateway Node

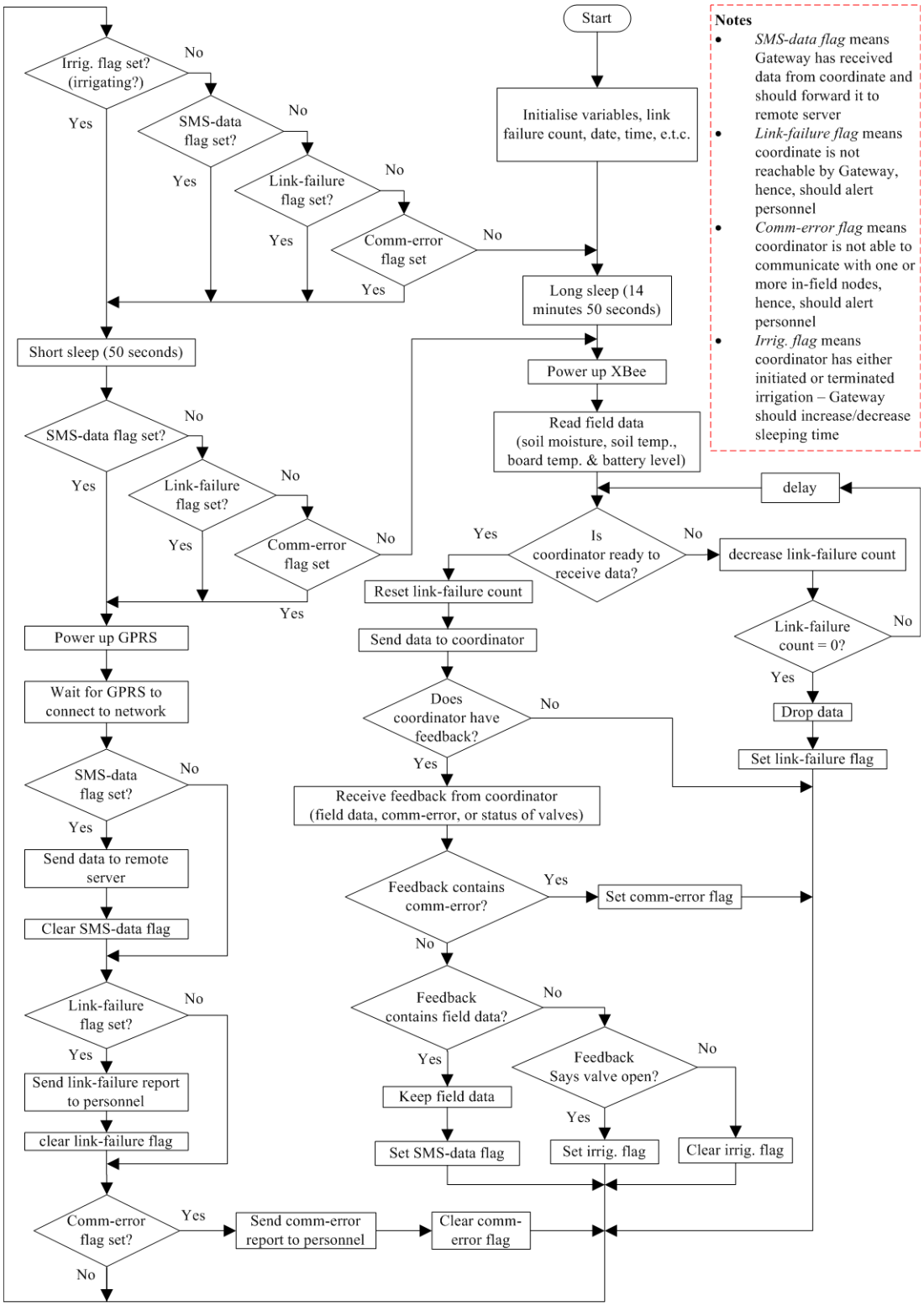

Appendix F: Applied Water Computation Tables

Experimental Treatment										
(1) Date and Time of irrigation	SMP (kPa) sensor node1		SMP (kPa) sensor node2		Average *PSWC (%)*		(8) sensor depth (mm)	(9) irrigation depth (mm) =(8)*[(7) - (6)]/100	(10) volume of water applied (m^3) = (9)*field area (i.e 48.4 m^2)	(11) Cumulative water applied (m^3)
	(2) before irrigation	(3) after irrigation	(4) before irrigation	(5) after irrigation	(6) before irrigation	(7) after irrigation				
01/08/2012 09:45	-59	-25.5	-59	-23	6.35	15.98	200	19.25	0.93	0.93
08/08/12 19:15:00	-44.6	-25.0	-30.4	-28.8	11.45	14.87	200	6.84	0.33	1.26
16/08/12 19:00:00	-43.4	-24.6	-29.2	-23.2	11.81	16.13	200	8.62	0.42	1.68
20/08/12 21:02:00	-40.6	-23.6	-27.1	-17.3	12.58	17.94	200	10.72	0.52	2.20
26/08/12 22:00:00	-41.9	-21.2	-21.4	-18.4	13.68	18.18	200	9.00	0.44	2.63
26/08/12 22:00:00	-41.9	-21.2	-21.4	-18.4	13.68	18.18	200	9.00	0.44	2.63
31/08/12 18:00:00	-41.0	-30.2	-24.0	-23.8	13.18	14.88	200	3.40	0.16	2.80
03/09/12 16:20:00	-39.9	-33.0	-29.8	-29.8	12.16	13.18	200	2.05	0.10	2.90
04/09/12 07:13:00	-33.3	-32.8	-34.4	-34.2	12.36	12.47	200	0.23	0.01	2.91
05/09/12 09:23:00	-34.1	-18.4	-38.7	-38.6	11.59	14.94	200	6.70	0.32	3.23
05/09/12 21:41:00	-19.2	-18.8	-38.7	-34.1	14.70	15.50	200	1.60	0.08	3.31
06/09/12 15:23:00	-20.3	-17.8	-36.3	-30.4	14.74	16.41	200	3.34	0.16	3.47
07/09/12 09:17:00	-18.1	-18.0	-30.6	-18.8	16.29	18.95	200	5.33	0.26	3.73
09/09/12 19:49:00	-36.8	-17.7	-33.5	-18.1	11.96	19.25	200	14.57	0.71	4.43
15/09/12 06:33:00	-60.6	-15.9	-46.5	-15.6	7.49	20.63	400	52.54	2.54	6.98
20/09/12 21:31:00	-53.8	-52.7	-43.5	-43.3	8.50	8.63	400	0.55	0.03	7.00
21/09/12 16:00:00	-66.3	-50.9	-24.1	-21.0	10.56	12.73	400	8.69	0.42	7.42
22/09/12 08:22:00	-55.3	-31.1	-21.3	-20.8	12.21	15.45	400	12.96	0.63	8.05
23/09/12 07:12:00	-32.4	-27.4	-21.0	-17.8	15.17	16.97	400	7.20	0.35	8.40
23/09/12 20:28:00	-30.1	-29.4	-19.5	-19.3	15.97	16.16	400	0.73	0.04	8.44
24/09/12 16:00:00	-39.2	-17.1	-34.3	-16.0	11.49	20.10	400	34.42	1.67	10.10
28/09/12 06:47:00	-42.7	-37.4	-48.1	-47.8	9.20	9.95	400	3.00	0.15	10.25
29/09/12 07:36:00	-48.4	-42.0	-50.8	-26.7	8.23	12.47	400	16.97	0.82	11.07
30/09/12 17:00:00	-52.3	-39.1	-34.6	-15.7	9.89	15.73	400	23.37	1.13	12.20
01/10/12 17:00:00	-39.4	-20.8	-15.8	-15.5	15.66	19.21	400	14.23	0.69	12.89
02/10/12 17:00:00	-21.9	-21.7	-15.5	-15.3	18.93	19.05	400	0.48	0.02	12.91
04/10/12 17:00:00	-44.7	-15.0	-28.9	-16.6	11.71	20.61	400	35.59	1.72	14.63
07/10/12 17:00:00	-44.8	-35.8	-33.2	-28.5	10.95	12.98	400	8.15	0.39	15.03
08/10/12 23:56:00	-54.8	-47.3	-14.8	-14.6	14.23	15.09	400	3.48	0.17	15.20
10/10/12 17:00:00	-55.2	-54.5	-16.0	-14.8	13.76	14.26	400	1.96	0.09	15.29
12/10/12 17:00:00	-59.5	-14.6	-15.4	-14.6	13.57	21.45	400	31.53	1.53	16.82
16/10/12 17:00:00	-38.8	-37.7	-22.8	-17.3	13.76	15.40	400	6.59	0.32	17.14
17/10/12 17:00:00	-46.6	-16.0	-21.5	-14.8	13.08	20.88	400	31.19	1.51	18.65
19/10/12 17:00:00	-37.0	-37.0	-24.0	-16.8	13.74	15.66	400	7.71	0.37	19.02
20/10/12 17:00:00	-58.9	-27.6	-21.0	-14.9	11.94	17.90	400	23.81	1.15	20.17
22/10/12 07:51:00	-33.0	-24.5	-15.0	-15.0	16.89	18.50	400	6.44	0.31	20.48
24/10/12 17:00:00	-38.2	-16.0	-15.0	-14.8	16.10	20.88	400	19.10	0.92	21.41
28/10/12 06:40:00	-45.8	-16.5	-15.1	-15.0	15.09	20.64	400	22.22	1.08	22.48
30/10/12 19:55:00	-32.0	-32.0	-18.2	-15.3	16.02	16.95	400	3.75	0.18	22.66
31/10/12 17:00:00	-53.0	-17.7	-16.0	-15.1	13.98	20.23	400	24.96	1.21	23.87
04/11/12 17:00:00	-38.0	-38.0	-19.5	-15.5	14.71	15.95	400	4.96	0.24	24.11
05/11/12 08:27:00	-49.3	-16.6	-15.6	-15.6	14.51	20.40	400	23.53	1.14	25.25
07/11/12 19:10:00	-36.0	-36.0	-21.1	-15.9	14.58	16.11	400	6.12	0.30	25.55
08/11/12 08:26:00	-48.8	-17.8	-18.0	-16.0	13.79	19.88	400	24.35	1.18	26.73
12/11/2012 06:33	-53.6	-21	-24.9	-16.3	11.53	18.89	400	29.42	1.42	**28.15**

Control Treatment										
(1) Date and Time of irrigation	SMP (kPa) sensor node1		SMP (kPa) sensor node2		Average *PSWC (%)*		(8) sensor depth (mm)	(9) irrigation depth (mm) =(8)*[(7) - (6)]/100	(10) volume of water applied (m^3) = (9)*field area (i.e 48.4 m^2)	(11) Cumulative water applied (m^3)
	(2) before irriga-tion	(3) after ir-rigation	(4) before irriga-tion	(5) after ir-rigation	(6) before irriga-tion	(7) after ir-rigation				
01/08/12 09:45:00	-60.1	-18.8	-61.0	-14.2	6.07	20.23	200	28.32	1.37	1.37
08/08/12 01:45:00	-30.5	-14.8	-16.7	-16.5	16.74	20.71	200	7.95	0.38	1.76
14/08/12 19:00:00	-34.0	-16.0	-23.2	-16.0	14.38	20.46	200	12.16	0.59	2.34
17/08/12 19:00:00	-31.4	-13.7	-20.6	-14.3	15.45	21.90	200	12.91	0.62	2.97
22/08/12 09:38:00	-43.2	-21.8	-21.5	-21.1	13.49	17.29	200	7.60	0.37	3.34
24/08/12 18:00:00	-38.0	-15.2	-23.2	-17.2	13.77	20.34	200	13.14	0.64	3.97
27/08/12 18:00:00	-33.3	-16.0	-22.2	-21.7	14.73	18.81	200	8.17	0.40	4.37
30/08/12 18:00:00	-37.3	-19.8	-26.0	-26.0	13.26	16.68	200	6.85	0.33	4.70
31/08/12 18:46:00	-29.0	-29.0	-31.8	-23.4	13.53	15.19	200	3.32	0.16	4.86
01/09/12 00:36:00	-32.8	-15.0	-33.2	-14.8	12.63	21.23	200	17.19	0.83	5.69
03/09/12 07:00:00	-32.0	-32.0	-24.2	-14.6	14.48	17.21	200	5.46	0.26	5.96
03/09/12 12:28:00	-39.2	-24.6	-14.6	-14.6	16.11	18.63	200	5.04	0.24	6.20
04/09/12 06:25:00	-29.0	-14.1	-15.7	-14.6	17.35	21.64	200	8.58	0.42	6.62
07/09/12 20:49:00	-48.2	-14.7	-26.8	-16.5	11.71	20.75	200	18.08	0.88	7.49
10/09/12 08:09:00	-31.5	-15.0	-22.5	-14.7	14.95	21.27	200	12.62	0.61	8.10
13/09/12 07:57:00	-57.2	-15.4	-20.0	-14.4	12.37	21.23	400	35.47	1.72	9.82
18/09/12 18:51:00	-50.2	-19.2	-18.0	-17.8	13.64	18.90	400	21.02	1.02	10.84
20/09/12 18:16:00	-41.3	-16.7	-18.7	-18.3	14.49	19.50	400	20.04	0.97	11.81
23/09/12 20:06:00	-61.0	-21.3	-22.1	-21.9	11.48	17.22	400	22.94	1.11	12.92
24/09/12 16:00:00	-36.0	-36.0	-25.5	-24.5	13.56	13.77	400	0.86	0.04	12.96
25/09/12 05:51:00	-50.6	-15.5	-30.5	-29.5	10.75	17.32	400	26.30	1.27	14.23
26/09/12 16:00:00	-19.0	-15.4	-36.2	-35.0	15.12	16.43	400	5.27	0.26	14.49
27/09/12 06:54:00	-22.1	-15.4	-38.2	-15.4	14.01	20.87	400	27.45	1.33	15.81
29/09/12 17:00:00	-18.8	-15.4	-33.0	-33.0	15.67	16.75	400	4.31	0.21	16.02
30/09/12 06:56:00	-15.5	-15.5	-40.0	-16.7	15.68	20.40	400	18.88	0.91	16.94
02/10/12 17:00:00	-36.0	-36.0	-28.0	-21.7	13.05	14.43	400	5.51	0.27	17.20
03/10/12 17:00:00	-50.2	-15.8	-26.2	-15.4	11.61	20.73	400	36.48	1.77	18.97
05/10/12 07:41:00	-40.8	-15.5	-15.5	-14.6	15.57	21.12	400	22.22	1.08	20.05
06/10/12 22:45:00	-31.2	-15.6	-17.0	-17.0	16.52	20.27	400	14.99	0.73	20.77
07/10/12 18:59:00	-32.4	-15.5	-22.0	-22.0	14.92	18.91	400	15.94	0.77	21.54
08/10/12 21:42:00	-24.8	-15.5	-42.5	-14.6	12.81	21.12	400	33.26	1.61	23.15
11/10/12 07:05:00	-62.5	-15.6	-20.5	-18.7	11.75	19.75	400	31.99	1.55	24.70
13/10/12 04:08:00	-56.4	-15.6	-22.3	-14.6	11.85	21.09	400	36.94	1.79	26.49
16/10/12 08:08:00	-64.6	-16.0	-16.2	-14.7	12.85	20.92	400	32.27	1.56	28.05
18/10/12 07:21:00	-65.6	-30.7	-15.2	-14.6	13.11	17.43	400	17.29	0.84	28.89
18/10/12 23:34:00	-36.0	-15.6	-14.8	-14.7	16.50	21.05	400	18.23	0.88	29.77
21/10/12 17:00:00	-61.0	-16.0	-21.0	-14.8	11.76	20.88	400	36.50	1.77	31.54
23/10/12 17:00:00	-63.5	-14.4	-16.0	-14.8	13.01	21.45	400	33.77	1.63	33.17
26/10/12 07:52:00	-61.2	-15.6	-14.8	-14.6	13.63	21.09	400	29.85	1.44	34.61
28/10/12 17:00:00	-60.9	-15.6	-14.8	-14.6	13.66	21.09	400	29.74	1.44	36.05
31/10/12 06:53:00	-57.5	-15.6	-14.8	-14.4	13.97	21.16	400	28.80	1.39	37.45
03/11/12 17:00:00	-54.5	-41.3	-14.4	-14.2	14.40	15.98	400	6.30	0.30	37.75
04/11/12 17:00:00	-53.0	-28.9	-14.4	-14.2	14.55	17.91	400	13.41	0.65	38.40
06/11/12 08:30:00	-42.0	-15.5	-14.4	-14.4	15.81	21.20	400	21.55	1.04	39.45
08/11/12 17:00:00	-64.3	-15.5	-14.8	-14.4	13.36	21.20	400	31.35	1.52	40.96
11/11/12 07:51:00	-53.1	-15.4	-14.6	-14.4	14.47	21.23	400	27.06	1.31	42.27
13/11/12 18:21:00	-53.8	-15.5	-14.5	-14.4	14.44	21.20	400	27.05	1.31	**43.58**